

**Proceeding
Of
4th International Conference on Electrical Electronics
Communication Robotics and Instrumentation
Engineering (ICEECIE 2015)
&
4th International Conference on Biotechnology, Civil and
Chemical Engineering (ICBCCE-2015)**

**Date: 1st March 2015
Chandigarh**

Editor-in-Chief

TEJINDER SINGH SAGGU,
Assistant Professor, Dept. of Electrical Engineering,
PEC University of University, Chandigarh

Organized by:



TECHNICAL RESEARCH ORGANISATION INDIA

Website: www.troindia.in

ISBN: 978-93-85225-06-2

About Conference

Technical Research Organisation India (TROI) is pleased to organize the 4th International Conference on Electrical Electronics Communication Robotics and Instrumentation Engineering (ICEECIE 2015) & 4th International Conference on Biotechnology, Civil And Chemical Engineering (ICBCCE-2015)

ICEECIE is a comprehensive conference covering the various topics of Electrical and Electronics Engineering. The aim of the conference is to gather scholars from all over the world to present advances in the aforementioned fields and to foster an environment conducive to exchanging ideas and information. This conference will also provide a golden opportunity to develop new collaborations and meet experts on the fundamentals, applications, and products of Electrical and Electronics Engineering. We believe inclusive and wide-ranging conferences such as ICEECIE can have Electrical and Electronics Engineering. It creating unique opportunities for collaborations and shaping new ideas for experts and researchers. This conference provide an opportunity for delegates to exchange new ideas and application experiences, we also publish their research achievements. ICBCCE shall provide a plat form to present the strong methodological approach and application focus on Biotechnology, Civil and Chemical Engineering that will concentrate on various techniques and applications. The ICBCCE conference cover all new theoretical and experimental findings in the fields of Biotechnology, Civil and Chemical Engineering or any closely related fields.

Topics of interest for submission include, but are not limited to:

Electrical Engineering
Electronics Engineering

Engineering Science
Network Engineering
Software Engineering
Structural Engineering
System Engineering
Telecommunication Engineering
And many more....

Organizing Committee

Editor-in-Chief:

TEJINDER SINGH SAGGU,

Assistant Professor, Dept. of Electrical Engineering,
PEC University of University, Chandigarh

Programme Committee Members:

Dr. Dariusz Jacek Jakóbczak

Assistant Professor , Computer Science & Management .
Technical University of Koszalin, Poland

Prof. (Dr.) Arjun P. Ghatule

Director, Sinhgad Institute of Computer Sciences (MCA),Solapur(MS)

Dr. S.P.ANANDARAJ.,

M.Tech(Hon's),Ph.D.,
Sr.Assistant Professor In Cse Dept,
Srec, Warangal

Prof O. V. Krishnaiah Chetty

Dean, Mechanical Engineering
Sri Venkateswara College of Engineering and Technology
Chittoor- Tirupati

Dr. D.J. Ravi

Professor & HOD, Department of ECE
Vidyavardhaka College of Engineering, Mysore

Prof. Roshan Lal

PEC University of Technology/Civil Engineering Department,
Chandigarh, India
rlal_pec@yahoo.co.in

Dr. Bhasker Gupta

Assistant Professor. Jaypee University of Information Technology, Himachal Pradesh

Dr. A. Lakshmi Devi,

Professor, department of electrical engineering,
SVU college of Engineering, Sri Venkateswara university, Tirupati

Prof. Shravani Badiganchala

Assistant professor, Shiridi sai institute of science and engineering

Prof. Surjan Balwinder Singh

Associate Professor in the Electrical Engineering Department,
PEC University of Technology, Chandigarh.

Dr. Shilpa Jindal ,

PEC University of Technology (Deemed University), Chandigarh
ji_shilpa@yahoo.co.in

Prof. S. V. Viraktamath

Dept. of E&CE S.D.M. College of Engg. & Technology Dhavalagiri, Dharwad

Subzar Ahmad Bhat

Assistant Professor, Gla University

Dr. G.Suresh Babu

Professor, Dept. of EEE, CBIT, Hyderabad

Prof .Ramesh

Associate Professor in Mechanical Engineering,
St. Joseph's Institute of Technology

Prof.Amit R. Wasnik

Sinhgad Institute of Technology, Pune, Maharashtra

IIT KHARAGPUR

Prof. Rajakumar R. V.

DEAN Academic, rkumar @ ece.iitkgp.ernet.in

Prof. Datta D., ddatta @ ece.iitkgp.ernet.in

Prof. Pathak S S,r,ssp @ ece.iitkgp.ernet.in

XIMB,BHUBANESWAR

Prof Dr. Subhajyoti Ray.M-Stat, (ISI); Fellow, IIM(A),
Dean academic,XIMB-subhajyoti@ximb.ac.in ,

Dr. Rajeev Agrawal ,

Assistant Professor, Department of Production Engineering
Birla Institute of Technology, Jharkhand

TABLE OF CONTENTS

SL NO	TOPIC	PAGE NO
Editor-in-Chief		
TEJINDER SINGH SAGGU		
1.	VOLTAGE STABILITY MARGIN ENHANCEMENT BY OPTIMAL CONTROL OF UPFC USING HYBRID ALGORITHM	
	- ¹ Elsa Prasad, ² Varaprasad Janamala	01-08
2.	OPTIMAL DESIGN ANALYSIS OF STANDALONE STREETLIGHT SYSTEM	
	- ¹ Anu Jacob, ² Prof.Devika Menon	09-12
3.	COMPARISON OF FUZZY LOGIC CONTROLLER AND THE PROPORTIONAL INTEGRAL CONTROLLER FOR THE APPLICATION OF SMES TO IMPROVE THE POWER QUALITY DURING VOLTAGE SAG	
	- ¹ Eldose valsalan, ² Haneesh K.M	13-16
4.	GENETICALLY OPTIMIZED LOAD SHEDDING: A CASE STUDY	
	- ¹ Vijaya Margaret, ² Geethu Thomas	17-23
5.	Application Of TVAC-PSO For Reactive Power Cost Minimization In Deregulated Electricity Markets	
	- ¹ K Rajitha Nair, ² Vara Prasad Janamala	24-30
6.	OPTIMIZATION IN ECONOMIC LOAD DISPATCH WITH SECURITY CONSTRAINTS	
	- ¹ Debi Sankar Roy, ² Venkataswamy R	31-36
7.	LOW POWER STAND-ALONE MICRO-GRID WITH WIND TURBINE	
	- ¹ Pooja Prasad, ² Prof. Manikandan.P	37-44
8.	RELIABLE OPERATION OF A HYBRID DC MICRO GRID FOR CRITICAL APPLICATIONS	
	- ¹ Sankeerth Sudhan, ² Prof. Manikandan.P	45-50
9.	CONTROL OF A FOUR LEG INVERTER FOR UNBALANCED POWER NETWORKS	
	- ¹ Jofey Simon	51-56
10.	SCREENING AND ANALYSIS OF RESPIRATORY SYSTEM USING CONTROLLER	

- ¹Ms. Dipti P. Kulkarni, ²Prof. S. S. Patil 57-61
- 11. FEATURE EXTRACTION OF MES (MYOELECTRIC SIGNAL TO DESIGN CALF STIMULATOR)**
 - ¹Ms. Rutuja U.Bachche, ²Prof. R.T.Patil 62-67
- 12. IMPLEMENTATION OF PERTURB AND OBSERVE MPPT OF PV SYSTEM USING BUCK-BOOST CONVERTER**
 - ¹Snehali Shankar Patil, ²Prof. M. S. Kumbhar 68-72
- 13. SECURE QUESTION PAPER TRANSFERRING USING LSB STEGANOGRAPHY TECHNIQUE**
 - ¹Tejashri Shivajirao Jadhav, ²Dr. S. A. Pardeshi 73-77
- 12. DESIGN OF A NOVEL PRESSURE SIGNAL BASED BIOMETRIC SYSTEM FOR AUTOMATED IDENTIFICATION OF COCKPIT PERSONNEL**
 - ¹Eswaran.R ²Rajatha, ³Viswanath Talasila 78-82
- 12. APPLICATION OF EXTENDED NERNST PLANCK MODEL IN NF200 MODELING FOR CHROMIUM REMOVAL**
 - ¹Manoj Kumaran, ²S. Bajpai 83-88
- 12. SEISMIC PERFORMANCE EVALUATION AND RETROFITTING OF RC MEMEBERS AND JOINTS**
 - ¹Dr. G.S Suresh, ²Mr. Sachin V 89-101
- 12. BUDGET MONITORING OF RESIDENTIAL BUILDING**
 - ¹Ingle Prachi Vinod 102-106
- 12. PRODUCTION OF BIOACTIVE COMPOUNDS USING MARINE ISOLATES IN CO-CULTURING SYSTEMS**
 - ¹Panjwani R, ²Deshpande A, ³Mahajani S, ⁴Joshi K 107-111
- 12. A HYBRID APPROACH FOR IPFC LOCATION AND PARAMETERS OPTIMIZATION FOR CONGESTION RELIEF IN COMPETITIVE ELECTRICITY MARKET ENVIRONMENT**
 - ¹Konduru VM ManoharVarma, ²J. Vara Prasad 112-119

Editorial

The conference is designed to stimulate the young minds including Research Scholars, Academicians, and Practitioners to contribute their ideas, thoughts and nobility in these two integrated disciplines. Even a fraction of active participation deeply influences the magnanimity of this international event. I must acknowledge your response to this conference. I ought to convey that this conference is only a little step towards knowledge, network and relationship.

The conference is first of its kind and gets granted with lot of blessings. I wish all success to the paper presenters.

I congratulate the participants for getting selected at this conference. I extend heart full thanks to members of faculty from different institutions, research scholars, delegates, TROI Family members, members of the technical and organizing committee. Above all I note the salutation towards the almighty.

Editor-in-Chief:

TEJINDER SINGH SAGGU,

Assistant Professor, Dept. of Electrical Engineering,

PEC University of University, Chandigarh



VOLTAGE STABILITY MARGIN ENHANCEMENT BY OPTIMAL CONTROL OF UPFC USING HYBRID ALGORITHM

¹Elsa Prasad, ²Varaprasad Janamala

¹Student, ²Asst. Professor,

Dept of Electrical Engg. Christ University, Bangalore, Karnataka,

Abstract— In the present scenario of the power system the main issue is the voltage stability enhancement which plays an important role in the complex network. This paper introduces the forthcoming technology employing the integration of Flexible AC transmission System (FACTS) device in to the system. Betwixt of all the FACTS devices this paper mainly rivet on Unified Power Flow Controller (UPFC). This is because UPFC has the aid to manage voltage, phase, and reactive power. A hybrid algorithm is developed for the improvement of voltage stability of the power system and to optimize the FACTS controller. The hybrid algorithm abide combination of Particle Swarm Optimization (PSO) and Gravitational Search Algorithm (GSA). PSO is performed to pinpoint the location of the UPFC device in the power system network. Whereas GSA is implemented to optimize UPFC device rating in a sequence. This method proposed was done for IEEE-14 bus system and IEEE-30 bus system using MATLAB platform. The results were impressive by the prospective method for practical applications.

Keywords—Voltage Stability, UPFC, FACTS, PSO, GSA

I. INTRODUCTION

Nowadays secure operation of power system has always been a challenge to system operators. With increasing interconnection and growing load demand, a power system, sometimes, may go into the insecure operation especially after severe contingencies. A complex network was obtained as a result of interconnection of transmission lines this strategy was done to reduce the fuel and generation plant costs[1].

Voltage stability is defined as the ability of a power system to maintain steady voltages at all the buses in the system after being subjected to a disturbances from a given initial operating condition it depends on the ability to maintain or restore equilibrium between the load demand and load supply from the power system[2]. The two types of voltage instability based on the time frame simulation are: static voltage stability and dynamic voltage stability. A system is said to be voltage stable if at a given operating condition for every bus in the system the bus voltage magnitude increases as the reactive power injection at the same bus is increased[3]. Thus voltage instability is mainly

due to imbalance in reactive power flow. The main factors considered for voltage analysis are real power, voltage magnitude and angle. enhance voltage stability margin of the selected operating system[5]. Therefore for the secure and economic operation Flexible AC Transmission System (FACTS) devices are installed into the system[6].

The FACTS devices have been used during the last three decades and provide better utilization of existing systems. The primary function of the FACTS is to control the transmission line power flow; the secondary function of FACTS can be voltage control, transient stability improvement and oscillation damping[7]. Depending on the power electronic devices used in the control, the FACTS controllers are classified as: variable impedance type and voltage source-based[8]. Among all the devices UPFC is the most versatile FACTS controller with three control variables. The FACTS controllers provide voltage support at critical buses in the system (shunt connected controllers) and regulate power flow in critical lines(series connected controllers). Whereas UPFC can control both voltage and power flow as its combination of series and shunt controllers[9]. The major advantage of integrating UPFC in power system is not only improves the power handling capability or installing new generations plant but also reduces the generations cost through utilizations of excess power available[10]

II. VOLTAGE STABILITY ANALYSIS

Voltage stability in a system is defined as the ability of a system to maintain the steady voltages at all buses even after the disturbances in the system. Voltage instability is mainly due to imbalance in reactive power flow in the network. The main factors to be considered for voltage stability analysis are real power, voltage

Where P_{Gi} , Q_{Gi} , P_{Di} and Q_{Di} are the real and reactive power injected at i^{th} bus and the corresponding load demands respectively. Y_{ij} and θ_{ij} are the admittance matrix and voltage angle between i^{th} and j^{th} buses. V_i, V_j ,

Voltage instability problem can be addressed in two different ways [4]. The first approach is to mitigate the problem and the second to magnitude and voltage angle. In order to maintain the voltage stability of the system these are the parameters that are to be controlled. This paper is emphasised on FACTS controllers which plays a vital role in the maintenance voltage to a secure level[11]. Among these FACTS devices this paper concentrates on UPFC as it injects real and reactive power to maintain the voltage stability of the system. Contingency analysis is done in order to determine the best outage condition using Newton-Raphson method[12][13]. PSO is used to determine the location of UPFC in power system[14][15]. GSA is used to determine the capacity of UPFC[16]. The problem can be formulated as multi-objective problem with objectives and constraints as follows:

$$\text{Min } F(x, u) \quad (1)$$

$$\text{Subject to } h(x, u) = 0 \quad (2)$$

$$p(x, u) \leq 0 \quad (3)$$

Where, F is the objective function, h is the equality constraints and p is the inequality constraints which depends on the control variables x and u .

A. Equality Constraints

The balance condition of the power system depends on principle of equilibrium between total generation and total load of the system. The power balance equation is represented in terms of nonlinear power flow equations described as follows:

$$P_{Gi} - P_{Di} = \sum_{j=1}^N |V_i| |V_j| |Y_{ij}| \cos(\theta_{ij} - \delta_i + \delta_j) \quad (4)$$

$$Q_{Gi} - Q_{Di} = \sum_{j=1}^N |V_i| |V_j| |Y_{ij}| \sin(\theta_{ij} - \delta_i + \delta_j) \quad (5)$$

δ_i and δ_j are the magnitude and angle of bus i^{th} and j^{th} respectively.

B. Inequality Constraints

The generation limits of the generating units are divided in to upper and lower limits in which actual value lies. The limits of the real and reactive power and the upper and lower limits for voltage magnitude and angles can be mathematically described as follows:

$$P_n^{min} \leq P_n \leq P_n^{max} \quad (6)$$

$$Q_n^{min} \leq Q_n \leq Q_n^{max} \quad (7)$$

$$V_n^{min} \leq V_n \leq V_n^{max} \quad (8)$$

$$\delta_n^{min} \leq \delta_n \leq \delta_n^{max} \quad (9)$$

P_n^{min} and P_n^{max} are the real power limits of the n^{th} bus,

Q_n^{min} and Q_n^{max} are the reactive power limits of the n^{th} bus,

V_n^{min} and V_n^{max} are the voltage limits of the n^{th} bus,

δ_n^{min} and δ_n^{max} are the angle limits of the n^{th} bus

respectively.

III. CONTINUATION POWER FLOW

The continuation power flow is used to run in various loading conditions. Initially load parameter is one then plot P-V curve for all buses and the weakest bus can be found , then gradually increment the load parameter[18]. When the maximum loading point reaches power flow would stop. Slack bus is also used so all transmission losses distributed among all the buses. The main principle in this technique is simple it uses predictor-corrector scheme to locate a solution path. Mainly two modes are used in this method are local parameterized and perpendicular iteration. Continuation power flow searches for successive load flow solutions according to the load patterns. A Tangent predictor is used to estimate next solution for a specified load scenario, from the base solution. The corrector step uses Newton-Raphson technique to determine exact solution by conventional power flow. For a new load, a new prediction is made based which is depended upon a new tangent vector. At critical point, the tangent vector is zero indicating the critical loadability of the system[19].

The major application of continuation power flow in this paper is for IEEE-14 and IEEE-30 bus systems. In IEEE-14 bus system there are 4

generator buses, 10 load buses, 20 transmission lines and in IEEE-30 bus system there are 5 generator buses, 25 load buses, 41 transmission lines.

IV. PRINCIPLE OPERATION AND INJECTION MODELING OF UPFC

UPFC is one of the most versatile devices in the FACTS family. Depending on the mode of operation it can be used as series/parallel compensator, phase shifter and voltage regulator. UPFC is a generalized as synchronous voltage source (SVS), the UPFC consists of two voltage sourced converters, as these back-to-back converters, labeled "Converter 1" and "Converter 2" are operated from a common dc link provided by a dc storage capacitor. The basic function of Converter 1 is to supply or absorb the real power demanded by Converter 2 at the common dc link to support the real power exchange resulting from the series voltage injection. This dc link power demand of Converter 2 is converted back to ac by Converter 1 and coupled to the transmission line bus via a shunt connected transformer. In addition to the real power need of Converter 2, Converter 1 can also generate or absorb controllable reactive power, if it is desired, and thereby provide independent shunt reactive compensation for the line.

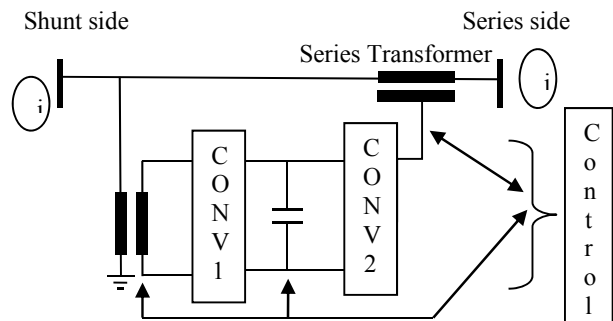


Fig. 1 UPFC device circuit arrangement

The real and reactive power flow model of UPFC is depended on the voltage magnitude, angle and series branch admittance values. In steady state condition the two voltage source converters represent the fundamental components of output voltage waveform and the two coupling transformers leakage reactance's. the injected

real and reactive power flow model of UPFC is described as follows:

$$P_{i,inj,upfc} = -rb_s V_i V_j \sin(\theta_{ij} + \gamma) \quad (10)$$

$$Q_{i,inj,upfc} = -rb_s V_i^2 \cos \gamma + Q_{conv1} \quad (11)$$

$$P_{j,inj,upfc} = rb_s V_i V_j \sin(\theta_{ij} + \gamma) \quad (12)$$

$$Q_{j,inj,upfc} = rb_s V_i V_j \cos(\theta_{ij} + \gamma) \quad (13)$$

Having the bus power injections of the UPFC obtained there is the UPFC injection model.

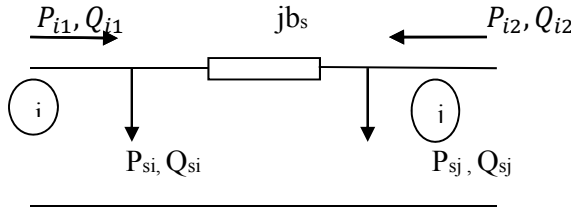


Fig. 2 The UPFC injection model

Besides the bus power injections it is very useful to have expressions for power flows from both sides of the UPFC injection model defined. At the UPFC shunt side, the active and reactive power flows are given as:

$$P_{i1} = -rb_s V_i V_j \sin(\theta_{ij} + \gamma) - b_s V_i V_j \sin \theta_{ij} \quad (14)$$

$$Q_{i1} = -rb_s V_i^2 \cos(\theta_{ij} + \gamma) - b_s V_j^2 + b_s V_i V_j \cos \theta_{ij} \quad (15)$$

Whereas at the series side they are

$$P_{i2} = +rb_s V_i V_j \sin(\theta_{ij} + \gamma) + b_s V_i V_j \sin \theta_{ij} \quad (16)$$

$$Q_{i1} = +rb_s V_i V_j \cos(\theta_{ij} + \gamma) - b_s V_j^2 + b_s V_i V_j \cos \theta_{ij} \quad (17)$$

The UPFC injection model is thereby defined by the constant series branch susceptance, b_s which is included in the system bus admittance matrix [B], and the bus power injections P_{si} , Q_{si} , P_{sj} and Q_{sj} .

V. LOCATION OF UPFC USING PSO

A. Overview of Particle Swarm Optimization

PSO plays an important role as it is a population based stochastic optimization technique. PSO shares similarities with evolutionary computation techniques such as Genetic Algorithms. In , PSO the potential solutions, called particles fly through the

problem space by following the current optimum particles.

Each particles keeps track of its coordinates in the problem space which are associated with the best solution (fitness) it has achieved so far. This value is called pbest. Another best value that is tracked by the particle swarm optimizer is the best value obtained so far by any particle in the neighbors of the particle. This location is called lbest when a particle takes all the population as its topological neighbors, the best value is a global best and is called gbest. The particle Swarm optimization concept consists of, at each time step, changing the velocity of each particle toward its pbest and lbest locations[20].

Here PSO is used to optimize the location of UPFC. The PSO steps are described below:

Step 1: Initialize a population array.

Step 2: for each particle, evaluate desired optimization

fitness function.

Step 3: Compare particle's fitness evaluation with its

pbesti. If current value is better than pbesti, then

pbesti = current value

p_i = current location x_i in D-dimensional space.

Step 4: Identify the particle with the best success so far,

and assign its index to variable g.

Step 5: Change the velocity and position of the particle.

Step 6: if the criteria is met then exit.

Step 7: If the criteria are not met then go to step 2.

VI. SIZING OF UPFC USING GSA

A GSA algorithm is based on the Newtonian laws and mass interaction. In the GSA technique, agents are considered to be objects and performances are their masses. Here the continuation power flow outcomes are used for the simulation of GSA algorithm. The bus voltages and the corresponding angles are the input. The input of GSA gives the minimized power loss for each outage condition in the network has been evaluated and the plots have been obtained; depending the evaluation the

optimal capacity of UPFC device is determined. The steps to determine the optimal capacity of UPFC can be described as follows:

Algorithm

Step 1: To determine the search space of proposed method and

initialize the voltage limits and the angle they are

considered as agents. Assume that the proposed system

consist of N agents and the position of the i^{th} agent is

given by:

$$X = (x_i^1, \dots, x_i^d, \dots, x_i^n)$$

for $i=1,2,\dots,n$

Where, n is the search space dimension of the problem, x_i^d is the position of the i^{th} agent in the d^{th} dimension.

Step 2: Random generation of input such as voltages and

corresponding angles. From the input the fitness value

is evaluated.

fitness function =

$$\text{Min} \left(\sum_{j=1}^N |V_i| |V_j| |Y_{ij}| \cos(\theta_{ij} - \delta_i + \delta_j) \right)$$

For $i=1,2,\dots,n$

Step 3: Evaluate the fitness of the agents and determine the

solution.

Step 4: Update the gravitational constant $G(t)$, best fitness

$F(B)$, worst fitness $F(W)$ and mass of the agents $M_i(t)$.

the gravitational search constant $G(t)$ is initialized at

beginning and will reduce the time to control the

search precision.

$$G(t) = G(G_0 + t) \quad (18)$$

$$F(B) = \text{Min}_{j \in \{1, \dots, N\}} \text{FITNESS}_j(t) \quad (19)$$

$$F(W) = \text{Max}_{j \in \{1, \dots, N\}} \text{FITNESS}_j(t) \quad (20)$$

$$M_i(t) = \frac{m_i(t)}{\sum_{j=1}^N m_j(t)} \quad (21)$$

$$\text{where } m_i(t) = \frac{F_i(t) - F(B)_t}{F(B)_t - F(W)_t}$$

with $F_i(t)$ represents the fitness values of the i^{th} agent at time t .

Step 5: To evaluate the total force of the agents at different

directions it can be described by the following:

$$TF_i^d(t) = \sum_{j \neq i} \text{random}_j \left(\text{force}_{ij}^d(t) \right) \quad (22)$$

Where,

$$\text{force}_{ij}^d(t) = G(t) \frac{M_{pi}(t) * M_{aj}(t)}{R_{ij} + \epsilon} * (y_i^d(t) - y_j^d(t))$$

$R_{ij} = \|X_i(t), X_j(t)\|_2$ is the Euclidian distance between two agents i and j , random_j is the random values, $[0,1]$. ϵ is a small constant M_{pi} and M_{aj} are the active and passive gravitational masses of the agents.

Step 6: the acceleration of the i^{th} agent,

$$a_i^d(t) = \frac{TF_i^d(t)}{M_i(t)} \quad (23)$$

Step 7: Updating agent's velocity and position using,

$$V_i^d(t + 1) = \text{random}_i V_i^d(t) + a_i^d(t) \quad (24)$$

$$X_i^d(t + 1) = x_i^d(t) + V_i^d(t + 1) \quad (25)$$

Step 8: Repeat the procedure from step 3 to 7 until it reaches the stop criteria.

Step 9: Terminate the process.

The GSA algorithm flowchart for the algorithm is:

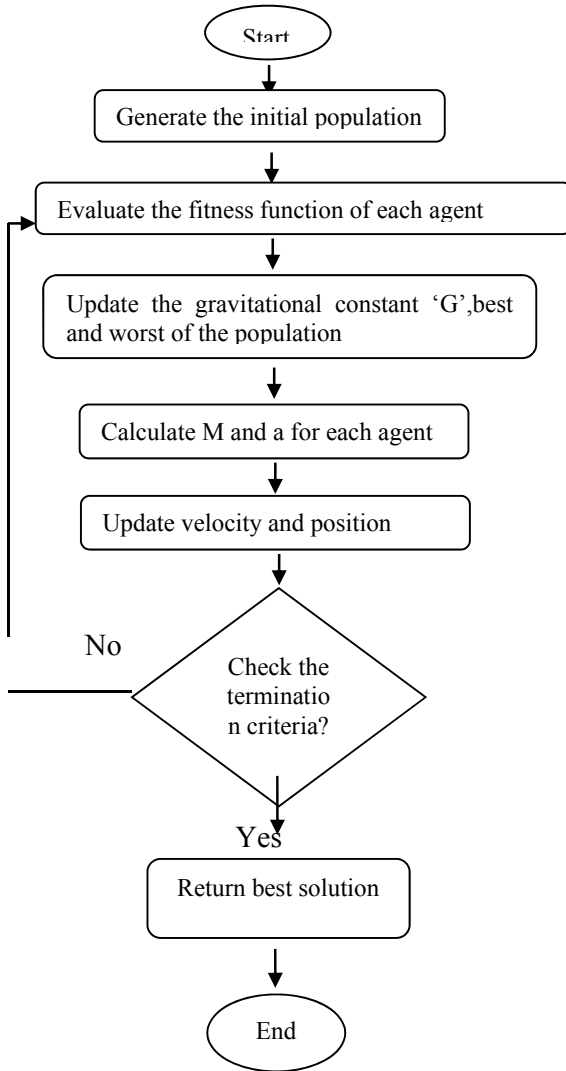


Fig. 3 Flow Chart for GSA Algorithm

VII. RESULTS AND DISCUSSIONS

In this paper PSO and GSA based hybrid algorithm is proposed for the voltage stability enhancement of the system. This was performed on MATLAB platform and output performance was evaluated for IEEE-14 bus system and IEEE-30 bus system. Firstly Newton-Raphson load flow analysis was used to analyze the system. Contingency analysis for the systems were performed and based on that performance indices were calculated at normal load and were ranked accordingly. Thus the optimal location for UPFC is decided determined based on the contingency analysis. The location of UPFC is optimized by PSO which depends on the fitness

value. Nextly the sizing of UPFC is optimized using GSA algorithm. After placing the UPFC in the system the results at the time of voltage collapse was analyzed. 1,2,3,6 and 8 are the generator buses excepted whereas UPFC is connected at all other buses.

TABLE I

BUS VOLTAGES PROFILES WITHOUT AND WITH UPFC

Bus No:	During Collapse	With UPFC
1	1.060	1.0600
2	1.0450	1.0380
3	1.0100	1.0100
4	1.0182	1.0100
5	1.0207	1.0100
6	1.0700	1.0700
7	1.0594	1.0590
8	1.0900	1.0900
9	1.0510	1.0500
10	1.0451	1.0450
11	1.0600	1.0580
12	1.0549	1.0549
13	1.0495	1.0490
14	1.0323	1.0320

The iteration performance of GSA is analysed for achieving an optimal voltage and minimum power loss when connecting UPFC. The performances are represented by in figures:2(a) and 2(b). Nextly the magnitudes of voltage of 14 buses are evaluated when connected to UPFC, when the load changes and without connecting UPFC when N-R method is applied. This performances are compared and is depicted in figure 3.

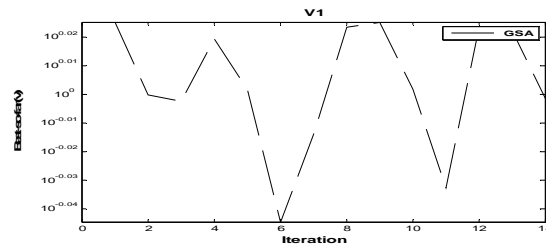


Fig.4(a) Iteration of GSA

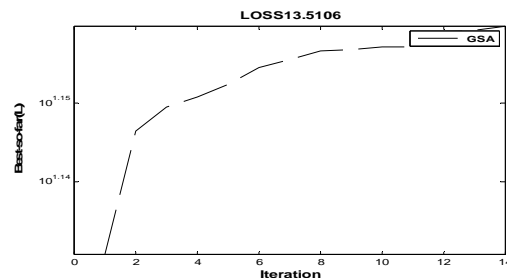


Fig. 4(b) Loss of GSA while connecting UPFC

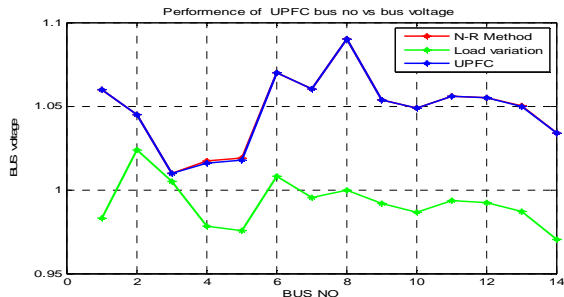


Fig. 5 Comparison performance of bus voltage after connecting UPFC

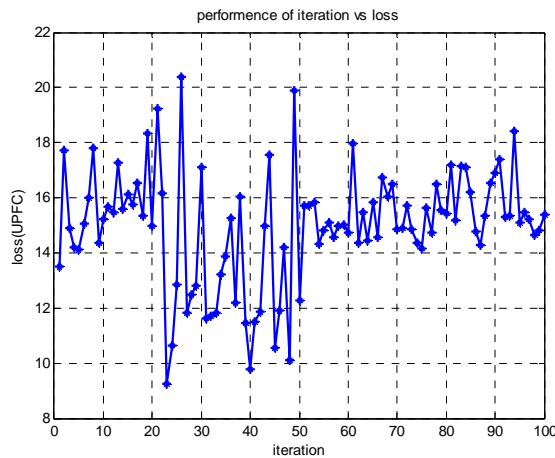


Fig. 6 Loss after connecting UPFC

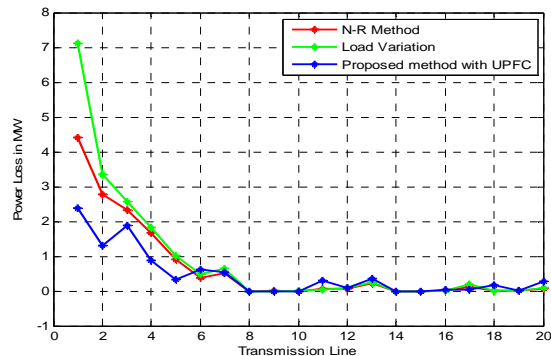


Fig. 7 Transmission line power loss comparison after connecting UPFC

Then the power loss of the system is determined after the connection of UPFC this is being illustrated in figure 4.

In figure 2(a) and (b), the GSA based voltage stability method shows that after the 8th iteration the voltage level has reached to the stable level and the power loss is less. Thus the time of convergence is reduced to achieve the solution. The computational complexity is being reduced in this case. Figure 3 depicts the improvement in voltage stability in the presence of UPFC when compared to the absence of UPFC. Nextlty figure 4 shows that the power loss of the system has

been reduced at the initial iterations after connecting the UPFC. Finally figure 5 shows that the transmission loss have been reduced when UPFC is connected in the system.

VIII.CONCLUSION

In this paper a novel approach is done to determine the location and capacity of UPFC in IEEE 14 bus system using an hybrid algorithm. The hybrid algorithm performed in a sequential manner consisting of PSO and GSA respectively. The proposed method was done for IEEE 14 and IEEE 30 bus systems. Firstly load flow analysis was conducted using N-R method for the system. Nextlty Contingency analysis was performed based on which the location for UPFC was decided by the application of PSO algorithm. Thereafter continuation power flow analysis was done for the system and using GSA the parameters of UPFC were determined in order to maintain the voltage level in the system. This proposed method for voltage stability margin enhancement quickly finds the optimal solution in determning the location and size of UPFC to be placed in the system.

REFERENCES

- [1] M. Saravanan, S. Mary Raja Slochanal, P.Venkatesh and Prince Stephen Abraham.J,“Application of PSO technique for optimal location of FACTS devices considering system loadability and cost of installation,” *IEEE Trans. On Power Engineering*, vol. 2, pp. 716-721, Nov. 29 2005- Dec.2 2005.
- [2] N.G. Hingorani, “Flexible AC transmission”, *IEEE spectrum*, April 1993, pp. 40-45.
- [3] Allen J. Wood and Bruce F. Wollenberg, *Power Generation, Operation and Control*, John Wiley, England, 2004.
- [4] Hadi Saadat, *Power System Analysis*, Tata McGRAW-HILL Edition.
- [5] N.G. Hingorani and L. Gyugyi, *Understanding FACTS: Concepts and Technology of Flexible AC Transmission Systems*, IEEE Press, New York, 1999.
- [6] D.J.Gowtham and G.T.Heydt, “Power flow control and power flow studies for system with FACTS devices,” *IEEE Trans. Power Systems*, Vol.13, No.1, Feb 1998.
- [7] G.D.Galiana etal, “ Assessment and control of the impact of FACTS devices on power

- system performance”, IEEE Trans. On power system, Vol.11, No.4, Nov.1996, pp.1931-1936.
- [8] M.A.Perez, A.R. Messina and C.R. Fuerte Esquivel, “Application of FACTS devices to improve steady state voltage stability”, *In Proceedings of IEEE Conference on Power Engineering society*, Vol.2, pp.1115-1120,2000.
- [9] L.Gyugyi, “A Unified power flow control concept for flexible AC Transmission systems”, *IEE Proc.*, Part-C, Vol.139, No.4, July 1992, pp.323-331.
- [10] Nijaz Dizdarevic, “Unified Power Flow controller in Allevation of voltage stability problem,” Ph.D. dissertation, Univ. of Zagreb, EEE Dept., Sweden, 2001.
- [11] Ashwin Kumar Shaboo, S.S.Dash and T.Thyagarajan, “An improved UPFC control to enhance Power System Stability”, *Modern Applied Science*, Vol.4, No.6, pp.37-48,2010.
- [12] M.Gitizadeh and M.Kalantar, “FACTS devices allocation to congestion Allevation Incorporating voltage dependance of Loads”, *Iranian Journal of Electrical & Electronics Engineering*, Vol.4, No.4, pp.176-190,2008.
- [13] C.R. Fuerte-Esquivel and E. Acha, “Unified Power Flow controller: a critical comparison of Newton- Raphson UPFC algorithms in power flow studies,” *IEE Proc. Gen. Trans. And distribution*, Vol.144, no.5, pp 437- 444, 1997.
- [14] Mehmet Tumay and A.Mete Vural, “Analysis and Modeling of Unified Power Flow Controller: Modification of Newton-Raphson Algorithm and User-Defined Modeling Approach for Power flow Studies”, *The Arabian Journal for Science and Engineering*, Vol.29, No.2B, pp.135-153, October 2004.
- [15] S.Gerbex, R.Cherkaoui and A.J.Germond, “Optimal location of FACTS devices in a power system using Genetic Algorithms,” in *Proceedings of the 13th Power Systems Computation Conference*, 1999, pp.1252-1259.
- [16] R. Kalavani and V. Kamaraj, “Enhancement of voltage stability by optimal location of Static Var Compensator using Genetic Algorithm and Particle Swarm Optimization”, *American Journal of Engineering and Applied Sciences*, Vol.5, No.1, pp.70-77, 2012.
- [17] Sai Ram and J. Amarnath, “Enhancement of Voltage Stability with UPFC using a Novel Hybrid Algorithm(GA-GSA)”, *IEEE Trans. On Power System*, pp. 1-6, Nov. 28 2013 – Nov. 30 2013.
- [18] Sarat Kumar Sahu, S.Suresh Reddy and S.V. Jayaram Kumar, “New Voltage Stability Index for Voltage Stability Analysis in Power System”, *International Journal of Electrical and Electronics Engineering Research*, Vol.2, No.4, pp.13-20,2012.
- [19] G.C.Ejebe and B.F.Wollenberg, “Automatic contingency selection”, *IEEE Trans. On power apparatus and systems*, Vol.98, No.1, January/February 1979, pp.92-104.
- [20] E.Eiben, J.E.Smith, *Introduction to Evolutionary Computing*, Springer, 2003.



OPTIMAL DESIGN ANALYSIS OF STANDALONE STREETLIGHT SYSTEM

¹Anu Jacob, ²Prof.Devika Menon

¹Mtech power system student, ²faculty at Christ University

Email:¹Anu.jacob@mtech.christuniversity.in,²devika.k.menon@christuniversity.in

Abstract— The uncertain nature of renewable energy sources has resulted the system design being unreliable. A hybrid system makes these energy systems more economical and reliable. Optimization of standalone hybrid renewable energy storage (HRES) is done for street light application. We mainly focuses to combine optimization process in supply side of street light..optimization is aimed to get better configuration with minimum loss and minimum cost. In this study, HRES street light uses photovoltaic (PV) as main supply, battery as storage supply and fuel cell (FC) as backup supply. Simulation of the system is done with the help of MATLAB.It is proposed to minimize loss of power supply probability LPSP and cost of energy(COE) to get better configuration

Index Terms—Hybrid standalone street light systems,HRES Optimization,PSO,Street light

I. INTRODUCTION

The energy which is harvested from the natural resources like sunlight, wind, tides, geothermal heat etc. is called Renewable Energy. As these resources can be naturally replenished, for all practical purposes, these can be considered to be limitless unlike the conventional fossil fuels. Renewable energy can replace these conventional fuels. In earlier days renewable energy is taken as single supply. but the combination of two or more renewable energy can increase their efficiency. combination of renewable energy is called Hybrid Renewable Energy Systems

One of the application of Hybrid Renewable energy system is street light system. The installation of street lamps in a city requires complex and expensive work. Moreover, to supply the lamps, an electrical network is needed. The problem is the same in remote areas where illumination is needed, as for instance on road sides. Stand-alone systems are commonly powered by solar cells with a battery to store the energy. However in regions that are far from the equator, this system cannot work all the yearlong because the solar power is weak and varies significantly according to seasons. Some studies have been conducted in term of HRES implementation.

Bernal and Rudolfo [4] present optimization HRES between PV-Wind-Battery system using simulation and optimization software. The research is aimed to find configuration with desired Net Present Cost (NPC) and Levelized Cost of Energy (LCE) as objective. Bashir and Sadeh [5] conduct the research to optimize standalone hybrid system PV-Wind-Battery using Monte Carlo algorithm. Zou and Sun design the PV -Wind system using multi-objectives optimization algorithm [6]. Optimization process is combined between Genetic Algorithm (GA) and Particle Swarm Optimization (PSO) to optimize cost of system and reliability as objectives. Load management has been proven to enhance HRES optimization. In street light application, load management is implemented to control and optimize lighting intensity and hence lighting power consumption. Poppa [1] has studied intelligent load management that can be implemented to increase

efficiency of street light system. Dynamic lighting control [1] is one kind of load management which can be implemented. In this paper, dynamic lighting control is implemented to manage lighting side with dimming method based on traffic flow condition

II. ARCHITECTURE OF THE SYSTEM

A. System Description

HRES standalone streetlight system consists of photovoltaic (PV), battery and fuel cell (FC). The FC should work during critical periods, which occur in winter. when the load is the largest (long nights) and the photovoltaic source is very weak. When the battery SOC reaches a low level (for instance 30 %), the FC starts supplying the load. When the load is switched off (i.e. during the day), the FC and the PV charge the battery simultaneously. In this way, the FC is prevented from starting and stopping each day, which would cause the FC lifetime to decrease rapidly. Finally, when the battery reaches its normal SOC, which can be even different from 100 %, the FC is turned off. The hybrid system layout is shown in fig 1.

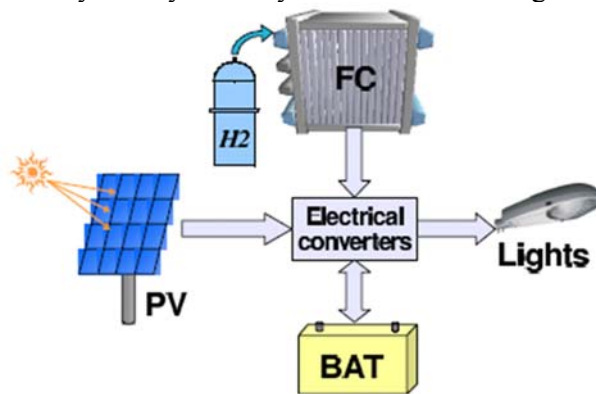


Fig 1: hybrid system layout

B. Photovoltaic model

Photovoltaic generates the power from solar radiation which is converted into electrical voltage [2]. Generated power from photovoltaic is influenced by kind of photovoltaic cell. For photovoltaic cells, three commercialized silicon technologies are currently available: amorphous, polycrystalline and monocrystalline. There are some parameters which affect the photovoltaic power, where I_{ns} is solar radiation in coverage area of pv (A_{pv}), and power efficiency from pv ..

C. Battery

A lead-acid battery is commonly associated with stationary solar systems. In this application, this type fits well with the system: a very fast response time is not necessary since the load is always constant, and the large weight of this battery has no influence in stationary applications. The battery efficiency η_b is assumed to be 80 %. Battery capacity is determined by the state of charge (SOC).

$$SOC(t) = 1 - \frac{I_{batt} * t}{C}$$

D. Fuel cell

Power is generated from hydrogen and convert it to electric power. FC power is controlled by battery condition. it will start when battery is low and will be stop when its capacity is high.

E. Lighting model

Street light uses lamp as load. For enhancement, lighting system is controlled to reduce power consumption with dimming method. Maximum power wattage from lighting system is 112W

F. Cost Analysis

The output energy is calculated as the sum of photovoltaic, fuel cell and battery. Loss of Power Supply Probability (LPSP) is used as objective function of optimization related with reliability of system. Loss system will be calculated for each time (t) to get probability loss from the system.

$$LPSP = \frac{\sum_{t=1}^T P_{load} - P_{tot}}{T}$$

Cost of energy (COE) means the total cost of the system which includes cost of PV, cost of FC and cost of battery.

G. Sizing optimization

The proposed study uses particle swarm optimization in order to obtain the optimal system. The particles in PSO algorithm continuously update the knowledge of the given searching space based on their current position, memory and cooperation of the social behaviour of the swarm. Basically their position and their velocity. Optimization process is started by selection initial configuration and its power generation

PV Capacity, FC Capacity, Battery Capacity, SOC min and SOC max are the parameters that are used for the PSO optimization. These

parameters are the state variables for the search space and thus characteristics of the potential solution.

H. Optimization results

ALGORITHM:

Begin: input the weather data

Initialize the PSO parameters

Randomly generate an initial population

While max iteration is not reached **do**

Calculate the fitness value for the Particles.

Obtain the next generation by updating the velocity and position

→ Update the pbest and gbest in each iteration

→ **Return** global best individual in the population

Fig 2: algorithm for pso

The main parameters of the optimization model are:

- Maximum Number of Iterations (Max. Iter) : 50,000
- Number of Particles: 20,000
- Inertia Weight, w: 0.729
- [c1,c2]: [1.495,1.495]

The typical performance of PSO in finding the optimal configuration of the hybrid system is shown in Fig. 3. The graph clearly shows that the swarm of particles converge to the fitness value of €506.605. Due to space limitation, the evolution trends of individual parameters have not been presented in this work, however the optimal solution set corresponding to these parameters is meticulous in Table 1.

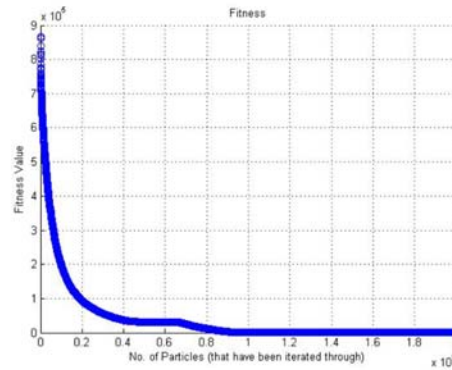


Fig 3: PSO convergence to the gbest
The optimization results without load management is given

Table 1: optimization parameters

	PV(W)	Battery(kWh)	FC(W)	COST
Value	88	2.12	237	
	SOC max(%)	SOC min(%)	LPSP	507
Value	90	40	0	

In Table 1

III. SUMMARY

This paper presented a methodology for optimal sizing of a hybrid standalone system by PSO method. The optimal energy system configuration comprise of 88W PV module, 237W fuel cell and 2.12 kWh battery that can power a LED street light application all the year at a total annualised lifetime system cost of €506. The methodology of optimisation is based on PSO using five optimization parameters to enhance the search space. Moreover, reliability constraint such as sizing penalty factor is taken into account with control parameters like the battery SOC, starting or stopping FC cycles in the optimization algorithm. The results of the proposed algorithm are validated with more economical and reliable system sizing. Moreover, PSO require lower number of convergence cycles to reach the best solution

IV. REFERENCES

- [1] M. a. C. C. Poppa, ""Energy consumption saving solutions based on intelligent street lighting control system",," in *Energy consumption*, vol. 10, , U.P.B. Sci.Bull., Series C,, 2011, pp. 296-314.
- [2] I. P. D. a. M. A. Lagorse, "Sizing optimization of a stand-alone street lighting system powered by a hybrid system using fuel cell, PV and battery",," in *Renewable Energy*, 2009,, pp. pp. 683-91..
- [3] Bashir M and Sadeh, ""Optimal sizing of hybrid wind/photovoltaic battery considering the uncertainty of wind and photovoltaic power using Monte Carlo",," in *Environment and Electrical Engineering (EEEIC) IEEE International Conference*, 2012.
- [4] M. a. D. S. Deshmukh, ""Modeling of hybrid renewable energy system",," *Renewable and Sustainable Energy Reviews*, pp. pp. 235-249, 2008,.
- [5] J. L. a. D.-L. R. Bernal-Agustin, "Simulation and optimization of stand-alone hybrid renewable energy systems",," *optimization of hybrid renewable energy systems*, pp. , pp. 2 1 1 1-2 1 18., 2009.
- [6] n. M. P. S. a. R. A. P. S. Sureshkumar, ""Economic cost analysis of hybrid renewable energy system using HOMER",," in *Advances in Engineering, Science and Management (ICAESM) IEEE 20 12 International Conference*, 2012.
- [7] B. S. V. N. P. K. C. N. Ould Bilal, ""Optimal design of a hybrid solar-wind-battery system using the minimization of the annualized cost system and the minimization of the loss of power supply probability (LPSP)",," *Renewable Energy*, pp. pp. 2388-2390, 20 10,..
- [8] D. P. a. A. M. Jeremy Lagorse, "Hybrid Stand-Alone Power Supply Using PEMFC, PV and Battery - Modelling and Optimization," in *International Conference on Clean Electrical Power*, 2009..



COMPARISON OF FUZZY LOGIC CONTROLLER AND THE PROPORTIONAL INTEGRAL CONTROLLER FOR THE APPLICATION OF SMES TO IMPROVE THE POWER QUALITY DURING VOLTAGE SAG

¹Eldose valsalan, ²Haneesh K.M

¹PG Scholar, ²Asst. Prof.,

Dept. of Electrical and Electronics Engineering,

Christ University Faculty of Engineering, Bangalore,

Email: ¹eldosenilambur@gmail.com, ²Haneesh.km@christuniversity.in

Abstract—This paper presents a comparison between superconducting magnetic energy storage (SMES) with fuzzy logic controller (FLC) and SMES with proportional integral (PI) controller to improve the power quality during voltage sag events. Service interruptions cause financial losses to both utility and consumers. A superconducting magnet is selected as the energy storage unit because of its characteristic of high energy density and quick response to improve the compensation capability in Power system. The number of member function can be minimized and the time response of the controller becomes faster by using the fuzzy logic controller. This comparison is done in the point of view of power quality and it is shown that the system with fuzzy logic controller is highly reliable. Using MATLAB Simulink, the model of SMES with PI controller and model of SMES with fuzzy logic controller are established. Simulation results in both cases are compared and analyzed.

Keywords—SMES, Voltage Sag, Power Quality

I. INTRODUCTION

Electric load is increasing day by day. Hence the power transfer in the interconnected network also increased. This leads the power system to more complex and less secure. Power quality concern has a vital role in power system. The over use of power electronics leads to power quality problems. This will affect the sensitive loads. Power system engineers are seeking solutions to overcome this problem and to operate the system in more flexible, efficient and controllable manner. Energy storage devices can overcome this problem up to some extent. Energy storage devices like flywheel and super capacitor have less power rating and energy rating. So these devices can't use for higher power application. SMES have high power rating with maximum efficiency than any other storage devices. Recent developments and advances in both superconducting and power electronics technology have made the application of SMES systems a viable choice to solve some of the problems experienced in power systems.

II. SMES

An SMES unit is a device that stores energy in the magnetic field generated by the dc current flowing through a superconducting coil.

An SMES system consists of a superconducting coil, a power-conditioning system (PCS), a cryogenic refrigerator, and a cryostat/vacuum vessel to keep the coil at a low temperature required maintaining it in superconducting state [1]. Two types of PCS are commonly used. They are current source converter (CSC) and voltage source converter (VSC).

This configuration makes highly efficient in storing electricity in the range of 95%-98% [2]-[3]. Other advantages of the SMES unit include very quick response and possibilities for high-power applications [4]. A typical SMES configuration is shown in Fig.1.

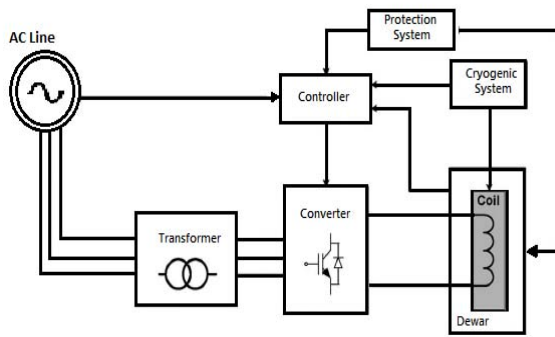


Fig. 1. Typical schematic diagram of an SMES unit.

III. CONTROL APPROACHES

There are two major configurations of SMES. They are CSC and VSC. Normally, CSC is connected through a 12-pulse converter configuration to eliminate the ac-side fifth and seventh harmonic currents and the dc-side sixth harmonic voltage, this result in savings in harmonic filters [5]. This configuration uses two 6-pulse CSCs that are connected in parallel which increase the cost. The VSC is connected with a dc-dc chopper through a dc link, which facilitates energy exchange between the SMES coil and the ac grid. Reference [6] estimates the total cost of the switching devices of the CSC to be 173% of the switching devices and power diodes required for equivalent capacity of the VSC and the chopper. VSC has a better self-commutating capability and the amount of harmonic current which can inject into the grid is lower

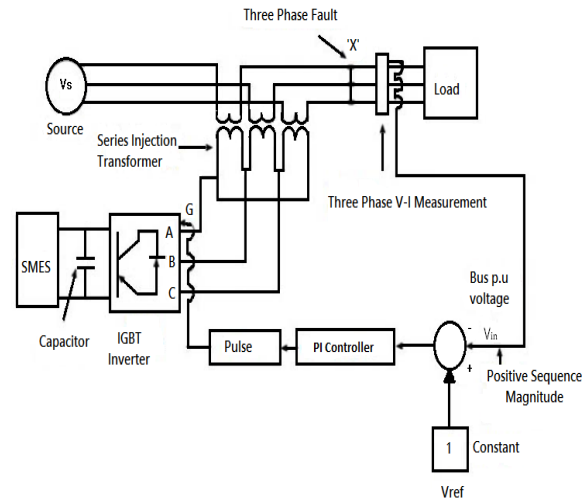


Fig. 2. SMES based DVR with PI controller

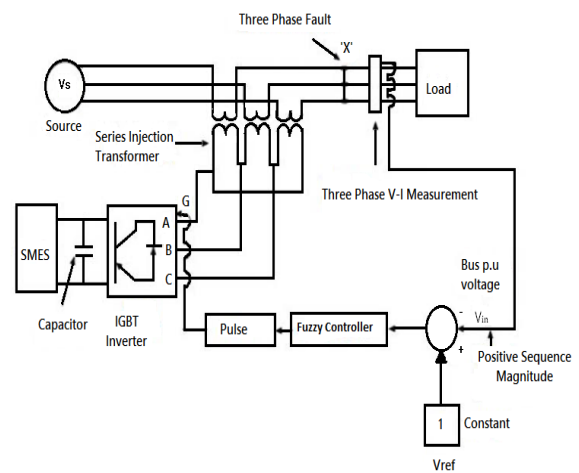


Fig. 3. SMES based DVR with fuzzy logic controller

than CSC. The switching frequency of an IGBT lies between the ranges of 2-20 KHz. But the switching frequency of GTO cannot exceed 1 KHz [7].

The SMES configuration used in this paper consists of a VSC and a dc-dc chopper. SMES with PI controller is shown in Fig.2. SMES with fuzzy logic controller is shown in Fig.3. The control strategy for pulse width modulation (PWM) converter can be divided into two, namely non-linear controller and linear controller. Fuzzy logic controller is non-linear controller. PI controller is linear controller.

Three phase fault is applied at load terminals at both cases as shown in Fig.2 and Fig.3. Load voltage is converted into per unit quantity. The magnitude is then compared with reference voltage (V_{ref}). The error signal thus produced is fed to PI controller. The PI controller processes the error signal and generates the

required angle delta to drive the error to zero. In Fig.3 fuzzy logic controller is used instead of PI controller, the remaining setup is same as that of PI controller.

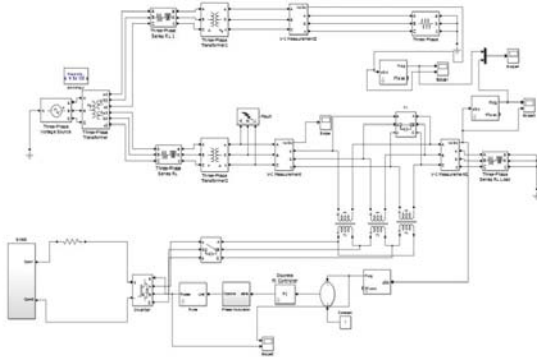


Fig.4. SIMULINK model of SMES with PI controller.

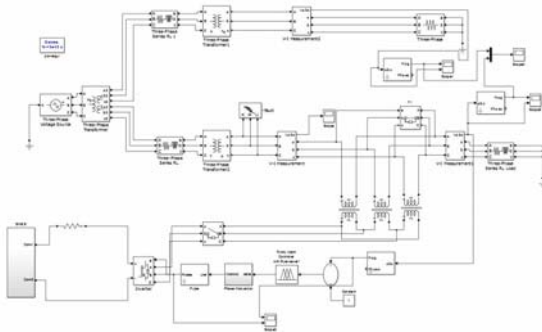


Fig.5. SIMULINK model of SMES with fuzzy logic controller

IV. SIMULATION RESULTS

To evaluate the performance of the SMES based DVR, a series of simulation is carried out with PI controller and FLC individually using MATLAB. Fig.4 shows the SIMULINK model of SMES based DVR with PI controller. Fig.5 shows the SIMULINK model of SMES based DVR with FLC.

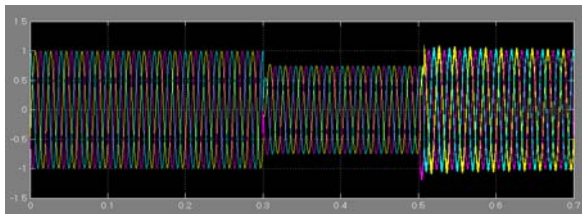


Fig.6. voltage under 3phase fault without SMES

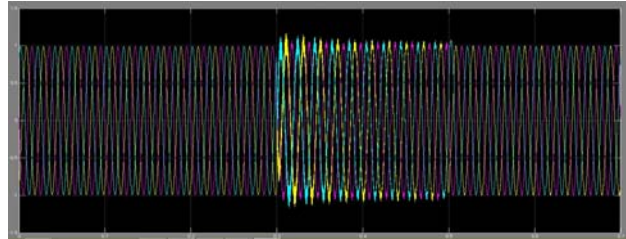


Fig.7. voltage under the action of SMES with PI controller

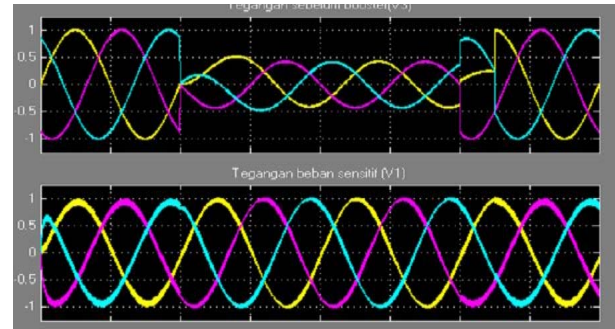


Fig 8. Three phase fault without and with the action of SMES with FLC controller..

During the simulation a three-phase voltage sag is simulated. The grid voltage drops to 50% of its nominal value and the DVR starts to operate. Fig.6 is the load voltage under fault. Fig.7 is the load voltage after compensation using PI controller. Fig.8 is the load voltage under fault and load voltage after compensation using FLC. From the obtained waveforms it is very clear that the DVR with FLC controller have better performance than the PI controller during the symmetrical fault.

V. CONCLUSION

This paper presents the SMES based DVR to compensate voltage fluctuations. It can compensate long term voltage fluctuation. Simulations results illustrate that the fuzzy logic controller has better performance than the PI controller.

VI. REFERENCES

- [1] P. F. Ribeiro, B. K. Johnson, M. L. Crow, A. Arsoy, and Y.Liu, "Energy storage systems for advanced power applications," *Proc.IEEE*, vol. 89, no. 12, pp. 1744-1756, Dec. 2001.
- [2] S. C.Smith, P. K. Sen, and B.Kroposki, "Advancement of energy storage devices and applications in electrical power system," in *proc.IEEE Power Energy Soc.*

- Gen. Meeting-Convers. Del.Elect. Energy 21st Century*, 2008, pp. 1-8.
- [3] H.Chen, T. N. Cong, W. Yang, C. Tan, Y. Li, and Y. Ding, "Progress in electrical energy storage system: A critical review," *Progr. Natural sci.*, vol. 19, no. 3, pp. 291-312, Mar. 2009.
- [4] E. Ancha, V. G. Agelidis, O. Anaya-Lara, and T. J. E. Miller, *Power Electronic Control in Electrical Systems*, Oxford, U.K, Newnes,2002.
- [5] A. Abu-siada and S.Islam, "Application of SMES unit in improving the performance of an AC/DC power system," *IEEE Trans. Sustainable Energy*, vol. 2, no. 2, pp. 109-121, Apr.2011.
- [6] I.D. Hassan, R.M. Bucci, and K. T. Swe, "400 MW SMES power conditioning system development and simulation," *IEEE Trans. Power Electron.*, vol. 8, no. 3, pp. 237-249, Jul. 1993.
- [7] T.Ackerman, *Wind Power in Power System*. West Sussex, U.K, Wiley, 2005, p. 65.



GENETICALLY OPTIMIZED LOAD SHEDDING: A CASE STUDY

¹Vijaya Margaret, ²Geethu Thomas

¹Professor, ²Student

Email: ¹vijaya.margaret@christuniversity.in, ²geethu.thomas@christuniversity.in

Abstract— The demand for electricity is increasing day by day with the expansion of industries, advancements in the field of technology and improvements in the lifestyles of people. Electric utilities all around the world strive hard to maintain a balance between demand and generation of power. Utilities resort to load shedding whenever they experience such an imbalance. The present load shedding scheme is based on round robin technique which is incapable of shedding the correct amount of load to meet the power deficit. Also there is no consideration for the importance of the load being shed. In this paper a sample system of 100 loads have been considered for load shedding. They are prioritised based on some factors to reduce the impact of load shedding for both utilities and consumers. Simultaneous optimization of load shedding error and the social impact of shedding is done by applying the artificial intelligence technique of Genetic Algorithm. The algorithm is developed on a smart grid environment under the assumption that the loads can be individually controlled from the utility side. Several case studies have been presented to test the efficiency of the algorithm in optimizing the load shedding error as well as its cost.

Index Terms— Genetic Algorithm, Grading of Loads, Load Shedding, Smart Grid,

I. INTRODUCTION

Load shedding is an important strategy adopted by the electric utilities to maintain power system stability when they are faced with generation deficiencies, lack of sufficient transmission and distribution capabilities or faults [1,2]. There has been an ever increasing demand for power owing to the technological advancements, rapid industrialisation and urbanisation. Electric utilities all around the world strive hard to tackle the situation of power crisis and to combat the imbalance between the generation and demand of power. They resort to load shedding under such circumstances.

Most of the conventional methods of load shedding causes either excessive or insufficient load reductions and have slow response time [3,4]. This necessitates the importance of an intelligent load shedding scheme that can provide optimal load shedding solutions. Artificial intelligence techniques are also widely applied to load shedding applications nowadays [5].

When a power shortage occurs, the Load Dispatch Centre (LDC) which allocates power to different substations communicates with them to shed certain amount of load as per the requirement. Currently load shedding takes place at the feeder level by round robin technique. In this method feeders will be disconnected from the supply in a cyclic manner for intervals of an hour or half hour. All the loads connected to disconnected feeder will be denied power during this interval. Usually feeders whose power consumption is greater than

the amount of load to be shed are selected for load shedding.

The present load shedding strategy suffers from many shortcomings. Since an entire feeder is disconnected it becomes impossible to shed the required amount of load. Another serious drawback is that load shedding is carried out without giving any consideration to the importance of load. Loads such as data centres, hospitals, cold storages should be exempted from load shedding to the maximum extent possible. Loads generally fall under categories such as commercial, industrial, residential etc. Each of them have a particular priority time of usage[9]. A consumer suffers from revenue loss as well as discomfort when he is neglected power during this period. At the same time distribution companies also incur revenue loss when consumers paying higher tariffs are shed. Since we cannot control the loads individually during the load shedding there is a probability that power is supplied to non critical loads rather than the important ones. Therefore the present load shedding scheme does not provide effective power distribution of available power[8].

The conventional grid system does not provide an opportunity for selective shedding of loads. However a smart grid environment provides greater flexibility for individual load control. In this paper an algorithm for load shedding in a smart grid framework is explained. Genetic Algorithm has been used for the simultaneous optimization of load shedding error as well as the impact of load shedding.

II. ANALYSIS OF PRESENT LOAD SHEDDING SCHEME

The present load shedding scheme i.e. the round robin technique is analysed based on economic and social considerations. For economic analysis we consider the real power consumption of feeders from a substation and decide the load shedding schedule based on this technique. The load profile for the feeders is noted from 10:00 am to 12:00 am and is given in Table I. Due to the peak power demand the substation receives an intimation to shed 3.1 MW for two hours. The entire load shedding duration is divided into blocks of half hour. Feeder/ feeders whose consumption is greater than the required amount

are disconnected. A possible load shedding schedule for the feeders under this case is given in Table II.

Table I. Load Profile

Time	Power consumption of different feeders corresponding to the time interval(MW)							
	F1	F2	F3	F4	F5	F6	F7	F8
10:00 AM	2.9	1.5	3	1.5	2	1.3	2.3	2.7
11:00 AM	3.1	1.6	3.4	1.6	2.2	1.4	2.6	2.7
12:00 PM	2.8	1.5	3.3	1.5	2.1	1.4	2.5	2.6

Table II. Load shedding schedule using round robin technique

Load shedding time block	Feeder/ Feeders disconnected	Load shedding error(MW)
1	F5,F6	$3.3 - 3.1 = 0.2$
2	F2,F7	$3.8 - 3.1 = 0.7$
3	F3	$3.4 - 3.1 = 0.3$
4	F1	$3.1 - 3.1 = 0$

From the load shedding schedule we can see that it is not possible to shed the correct amount of load. The extra units which are shed could have resulted in revenue generation for the utilities. While selecting the feeders for disconnection no consideration for the importance of the loads is given. Many a times non critical loads will receive supply than the critical loads. From the analysis we can see that there is a need for selectively shedding the loads which is possible only in smart grids.

III. LOAD SHEDDING IN SMART GRID SCENARIO

“A smart grid is defined as an electrical grid that uses information and communications technology to gather and act on information, such as information about the behaviours of suppliers and consumers, in an automated fashion to improve the efficiency, reliability, economics, and sustainability of the production and distribution of electricity” [6].

Smart Grid allows two way communication between the utilities and the consumers [7]. Each electrical connection from the distribution company is taken as one lumped load in a smart grid environment. Smart meters are installed

within the customer premises. They are capable of communicating the real time load data to the control centre at regular intervals. The loads can also be remotely controlled from a remote centre with the help of control signals. The major difference between load shedding in a conventional grid and that in smart grid environment is that, in a conventional load shedding system, load shedding takes place at the substation level by disconnecting an entire feeder whereas in a smart grid system load shedding takes place at the consumer end. Therefore it is possible to shed the exact amount of load required and also effectively distribute the available power to loads based on its importance and time of usage.

IV. CATEGORISATION OF LOADS

Based on the tariff structure loads are of two types- Low tension and High tension. The category of loads falling under various tariffs are given in Table III.

Table III. Category of Loads Based on Tariff

Tariff	Type of loads
LT1	Domestic (free up to 18 units)
LT2	Residential, Institutions
LT3	Commercial
LT4	Agricultural induction pumps
LT5	Industrial
LT6	Water works, Street lights
LT7	Temporary connections
HT1	Water works
HT2	Industrial, Commercial
HT3	Agriculture and Horticulture Farms

V. GRADING OF LOADS

Grading is a method which is used to assign priorities to loads of various categories as well as those within a particular category [8]. It is done to differentiate the loads based on their importance at a given time of the day. Grading or prioritising the loads helps us to realize the selective shedding of loads. Following are the factors based on which loads are prioritised :

- Number of units of power consumption.
- Social Impact of load shedding.
- Revenue loss and discomfort suffered by the

consumer.

- Revenue loss to the utilities.
- Other considerations by the distribution company.
- Time of the day.

Number of units of power consideration provides information on the size of the load as well as the number of people affected by shedding. The factor revenue loss to the distribution companies takes into account the tariff paid by the consumers. Economic loss to the consumers can be computed based on the revenue generated if he was supplied with power. Social impact of load shedding signifies the importance of the load being shed. Other factors can also be included to grade the loads based on the requirements of the distribution company. Each of these factors will be given some weightages and the loads are then graded. For each load we assign a grade point which is merely a number in the range of 0-100. A load will have high value as a grade point during its priority time compared to the less predominant ones.

VI. GENETIC ALGORITHM FOR LOAD SHEDDING

Genetic algorithms (GAs) are search methods which are based on the principles of natural selection and genetic[10]. They were originally developed by John Holland in 1975 and are inspired by the biological evolution process. Genetic algorithms use the principles of selection and evolution to produce several solutions to a given problem. GA has been used for many load shedding applications [11-13].The main reason for the use of GA in developing the algorithm is its robustness and efficiency in arriving at an optimal solution.

The algorithm for load shedding is developed based on the following assumptions:

1. A two way communication is possible between the consumer and the utility.
2. The control centre receives real time power consumption with the help of smart meters at the customer site.
3. When a power shortage occurs, the load dispatch centres intimate the substation to shed some load.
4. The load shedding requirement, real time load

profile and the grade points of the loads are given as input to the algorithm.

A. Algorithm

In Genetic Algorithms an objective function is to be defined first. The objective in this algorithm is to simultaneously optimize the error in load shedding and the cost of load shedding. Cost of load shedding is the sum of the grade points of all loads that are shed. The algorithm is briefly explained below:

1. Consider a sample system of 100 loads belonging to various tariff categories.
2. The real time input of the load to be shed, the time of the day, the load profile of the sample system and their grade tables are fed to the algorithm.
3. An initial pool of 32 chromosomes is created. The number of genes in each chromosome will be equal to the number of loads considered.
4. Binary numbers '0' and '1' represents ON and OFF state of the load.
5. The best 4 chromosomes from the initial chromosome pool are selected by using Tournament strategy.
6. The four chromosomes are subjected to objective function, crossover and mutation. We define a specific number of iterations for the convergence of the algorithm.
7. After a number of iterations the best solution for load shedding will be displayed.

VII.CASE STUDY AND RESULTS

The program for load shedding in a smart grid environment is developed using MATLAB R2012a. For testing the algorithm different case studies have been performed on a sample system of 100 loads from different categories. Load profile of the test system is shown in Table IV.

Table IV. Load Profile of the Sample System

LT1	LT2a1	LT2a2	LT2b	LT3	LT4	LT5	LT6	LT7	HT1	HT2	HT3				
0.9	1.62	0.04	1.5	0.63	3.89	3.63	13.3	9.61	6.58	74.51	21.2	35.42	56.46	68.26	85.36
0.95	1.5	1.84	0.46	1.62	3.06	4.46	12.4	7.82	13.58	33.01	24.4		79.24	102.36	160.58
	0.24	1.3	0.12	1.58	4.99	3.77	12	12.44		72.27	18.5			138.25	
	1.05	1.86	1.53	1.7	2.67	3.56	12.5	13.88		30.82	19.1				
	0.65	0.32	1.34	1.01	3.96	4.58	9.06	6.24		60.77	24.8				
	1.09	1.84	1.43	1.27	3.82	4.02	10.9			65.26					
	0.8	1.58	1.28	1.9	3.16	4.49	10.6			54.03					
	0.83	1.15	0.84	0.88	2.42	4.08	10.2			69.84					
	0.36	0.88	0.78	2.18	2.08		8.2			70.46					
	0.51	0.52	1.63	4.6	3.26		7.98			58.16					

The total power consumption of the loads is 1.716MW. The case studies done and the results obtained are presented in this section.

Case (i) Same load shedding requirement at different time of the day

We consider a load shedding requirement of 500kW at 7:00 am and 4:00 pm. The grade points for the sample system of loads and the best possible load shedding solution that is computed by the application of GA for the given load shedding requirement at 7:00 am is shown in Table V and Table VI respectively . The binary bit '1' represents all the loads that are disconnected from the supply.

Table V. Grade points of the loads at 7:00 am

LT1	LT2A1	LT2A2	LT2B	LT3	LT4	LT5	LT6	LT7	HT1	HT2	HT3				
10	53	49	51	38	50	29	25	53	51	35	11	52	51	83	78
10	40	44	55	57	48	20	28	58	49	35	20		65	73	73
	56	46	50	52	60	24	35	52		36	27			75	
	40	52	53	51	55	29	39	52		48	45				
	45	46	53	57	60	15	33	44		31	45				
	49	48	22	50	47	27	32			36					
	58	57	19	51	41	28	33			43					
	45	47	31	58	11	29	45			31					
	49	47	13	47	25		53			26					
	49	51	26	57	38		54			67					

Table VI. Load shedding solution for 500kW at 7:00 am

LT1	LT2A1	LT2A2	LT2B	LT3	LT4	LT5	LT6	LT7	HT1	HT2	HT3
1	0	0	0	0	0	0	1	1	0	0	0
1	0	1	1	0	0	1	0	0	1	0	0
	1	1	0	0	0	0	0	0	0	1	0
	1	0	0	0	0	1	0	1			
	1	0	0	0	0	0	0	1	0	0	
	0	0	0	0	1	0	0				
	0	0	0	0	0	1	0				
	0	1	0	0	0	0	1				
	1	0	0	0	0		1				
	0	0	0	0	1		1				

It is found that the load shedding error at 7:00 am is around 0.65kW which is a good result. The sum of the grade points of all the loads shed is 1200. We know that during early morning hours more power is required by the residential customers. The results obtained show that the algorithm takes care in providing maximum power to the residential customers with the help of grading scheme. Thus power is provided to the right customer at the right time.

Again the program is executed for the same load shedding requirement at 4:00 pm. The solution obtained in this case is given in Table VII.

Table VII. Load shedding solution for 500 kW at 4:00pm

LT1	LT2A1	LT2A2	LT2B	LT3	LT4	LT5	LT6	LT7	HT1	HT2	HT3
1	1	0	1	0	0	0	1	1	0	0	1
1	1	1	0	0	1	1	0	0	0	0	0
	0	0	0	1	1	0	1	1		0	
	1	0	0	0	0	0	1	0			
	1	1	0	0	1	0	0	1			
	1	1	0	0	1	0		1			
	0	1	0	0	0	1	1				
	0	1	0	1	0	0		1			
	0	0	1	1	1		0				
	0	0	0	0	1		0				

The solution obtained conveys that with the deployment of this algorithm loads which are of high priority at a given time are kept in operation whereas less important loads were shed. The algorithm provides an optimal load shedding solution and is successful in selective shedding of

loads based on their importance and social impact .
Case (ii) Different load shedding requirements at the same time of the day

The program is run by entering different load shedding requirements at 8:00 am. The results are summarised in table VIII .

Table VIII. Load shedding errors for different load shedding requirements at 8:00am

Load shedding Requirement(kW)	Load shedding Error(kW)	Percentage error in load shedding (%)
100	0.14	0.14
200	0.43	0.215
300	0.68	0.226
400	0.98	0.245
500	0.56	0.112
600	0.81	0.135
700	1.31	0.187
800	0.23	0.025
900	1.39	0.154
1000	1.01	0.001

From the results we can see that the percentage error in load shedding error is well within 0.5% of the amount of load to be shed. This is an exceptionally good result when comparing with the conventional load shedding schemes which result in excessive shedding of loads. The graph showing the minimization of load shedding error is given in Fig. 2.

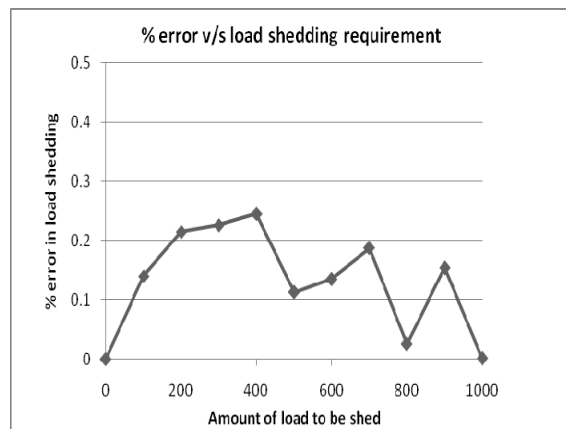


Fig. 2. Minimization of load shedding error

Case(iii) Load shedding requirement and

time of day remaining the same

The load shedding requirement and the time of day are kept fixed and the program is executed for a repeated number of times. The solution obtained for a load shedding requirement of 500kW at 7:00 am is shown in Table IX. This is then compared with the solution given in Table V.

Table IX. Solution for 500 kW at 7:00 am

LT1	LT2A1	LT2A2	LT2B	LT3	LT4	LT5	LT6	LT7	HT1	HT2	HT3
0	0	0	0	1	0	0	1	1	1	1	1
0	0	0	0	0	1	0	0	0	0	0	0
	1	0	0	0	0	1	0	0		0	
	0	0	0	0	0	1	1	0	0		
	0	0	0	0	1	1	0				
	1	0	1	0	0	1	0				
	1	1	0	1	0	1	0				
	0	0	0	0	0	0	0				
	0	0	0	1	1		0	1			
	0	0	0	0	0		1				
	0	0	0	0	0		1				

The error in load shedding is 1.43kW. We find that on comparing both the tables the solutions obtained are not unique. Loads which were shed earlier are excluded from shedding in the second case. The algorithm helps in minimising the inconvenience caused to the customers when load shedding duration is high. This is one of the advantage of using GA for load shedding application since load shedding takes place in a probabilistic manner. The solutions obtained is based on the initial chromosome pool. Since the objective function is an inequality more than one solution satisfying the problem is possible.

VIII. CONCLUSION

An algorithm for selective load shedding in a smart grid environment is developed with the help of artificial intelligent technique of Genetic algorithm. The algorithm can efficiently control the loads based on their priority. It is successful in minimising the load shedding error and also reducing the impact of load shedding. The algorithm improves customer satisfaction by providing them power during their priority time of

usage. With the help of this algorithm the critical loads such as hospitals, data centres etc can be exempted from load shedding. This method can be further extended to enable partial load shedding of a consumer which ensures a certain amount of consumer load be supplied even when load shedding becomes inevitable.

REFERENCES

- [1] Shervin Shokoo, Tanuj Khandelwal, Dr. Farrokh Shokoo, Jacques Tastet, Dr. JJ Dai, "Intelligent Load Shedding Need for a Fast and Optimal Solution", IEEE PCIC Europe 2005
- [2] Farrokh Shokoo, J J Dai, Shervin Shokoo, Jacques Tastet, Hugo Castro, Tanuj Khandelwal, Gary Donner, "An Intelligent Load Shedding (ILS) System Application in a Large Industrial Facility", Industry Applications Conference, IEEE 2005
- [3] S. Hirodantis, H. Li, P.A. Crossley., "Load Shedding in a Distribution Network", International Conference on Sustainable Power Generation and Supply, IEEE 2009
- [4] Delfino B, Massucco S, Morini A, Scalera P, Silvestro F, "Implementation and comparison of different under frequency load-shedding schemes", Power Engineering Society Summer Meeting, 2001 1,307–312.
- [5] J.A. Laghari, H. Mokhlis, A.H.A. Bakar, Hasmainsi Mohamad, "Application of computational intelligence techniques for load shedding in power systems: A review", Energy Conservation and Management 75, 2013, pp 130-140
- [6] Clark W Gellings, "The Smart Grid: Enabling Energy Efficiency and Demand Response", The Fairmount Press, 2009, pp 131-148
- [7] David Mayne, "How the smart grid will energise the world-white paper", Digi international inc.
- [8] K. Uma Rao, Satyaram Harihara Bhat, Ganeshprasad G G, Jayaprakash G, Selvamani N Pillappa, "A Novel Grading Scheme for Loads to Optimize Load Shedding Using Genetic Algorithm in a Smart Grid Environment", IEEE, ISGT Asia 2013
- [9] K. Uma Rao, Satyaram Harihara Bhat,

Ganeshprasad G G, Jayaprakash G, Selvamani
N Pillappa , " *Time Priority Based Optimal
Load Shedding Using Genetic Algorithm*",
IEEE, PEIE , 2013

- [10] David E Goldberg, "*Genetic Algorithm*",
Pearson education publication, 2011, ISBN-
978-81-7758-829-3,pp 97-105.
- [11]M. Tarafdar Hagh , S. Galvani , "*A Multi
Objective Genetic Algorithm for Weighted
Load Shedding*", IEEE, 2010
- [12] Wael M.AL-Hasawi, Khaled M.ELNaggar,
" *Optimum Steady- State Load- Shedding
Scheme Using Genetic Based Algorithm*",
IEEE MELECON 2002
- [13]Chao-Rong Chen, Wen-Ta Tsal, Hua-YI,
"*Optimal Load Shedding Planning with
Genetic Algorithm*", IEEE, 2011



Application Of TVAC-PSO For Reactive Power Cost Minimization In Deregulated Electricity Markets

¹K Rajitha Nair, ²Vara Prasad Janamala

¹PG Scholar, ²Asst. Prof. Christ University

Email: ¹rajik3@gmail.com, ²varaprasad.janamala@christuniversity.in

Abstract— for planning and proper operation of power system, optimization of reactive power is a must. The reactive power cost minimization aims at dispatching the reactive power in such a way that maximum real power is dispatched and minimum reactive power is utilized so that voltage is maintained at required level. The work presented in this paper discusses various loading conditions and the improvement after applying the optimization technique. It compares the reactive power cost both before and after optimally dispatching the reactive power and thereby ensuring the voltage stability of the power system.

Optimal power dispatch is solved using Time Varying Acceleration Coefficient and Particle Swarm Optimization. Reactive support of the generators has two functions such as voltage control and real power delivery. It explains how the application of PSO helps in reactive power control and reduction in power losses.

Index Terms— Ancillary services, Deregulated Electricity Market, Optimal Reactive Power Dispatch.

1. INTRODUCTION

The modern day power systems are required or forced to operate much closer to their stability limits due to the increased demand for electric power by the loads. In such a stressed situation, the system may have voltage instability problems and thus may lead to the problem of voltage collapse and in some cases has led to system

blackouts in many countries across the world [2]. One of the main reasons for voltage instability is the insufficient reactive power support [1]. Generation, distribution and transmission have been unbundled into separate businesses and thus the power industry has changed drastically due to development of the competitive markets for trading the wholesale power by deregulation. And reactive power became one of the ancillary services. [3]. Generation and transmission cannot do anything without reactive power, which is definitely the poorly understood but very important part of electricity. It was believed that these competitive markets may lead to a highly efficient generation of power, there will be more technological innovations and the rate of power may go down but due to the environmental aspects and economic constraints the power system became more and more complex and was forced to operate near to their limits [1] [2]. Researchers and system operators has always been keenly interested to study the optimal dispatch of reactive power, especially after the deregulation of the power industry. Reactive power and bus voltages are related to each other throughout the network, and hence reactive power services plays an important role in the system security [4], [5]. Voltage instability may lead to voltage collapse. Voltage collapses usually occur on power system which are faulted or heavily loaded or have shortage of reactive power [5]. Management of reactive power resources is vital for stable and secure operation

of power systems in the view point of voltage stability [1]. Reactive power dispatch is one of the important tasks in the operation and control of power system. Insufficient reactive power supply has resulted in one of the major blackouts of all time that is the US-Canada Power System Outage Task Force states in its report that insufficient reactive power was an issue in the August 2003 blackout [4]. In deregulated electricity markets, reactive power dispatch is related to the short-term allocation of reactive power as required from suppliers based on present operating conditions. The Independent System Operator is concerned with determining the optimal reactive power schedule for all providers based on a given objective that depends on system operating criteria. Different objective functions can be used by the Independent System Operator, besides the usual transmission losses minimization, such as reactive power cost minimization, minimizing the cost of adjusting reactive power control devices, or maximization of system loadability to minimize the risk of voltage collapse.

The reactive power cost production from a synchronous generator is divided into two main cost components they are the fixed cost and the variable operating cost. [8] The fixed cost represents a part of the generator's capital cost which goes toward providing reactive power; hence, it is very difficult to separate this fixed cost component from the total plant capital cost. The variable cost consist of two important components: the first component emerge from the increased losses in the armature and field windings of the generator because of an increase in its reactive power output, and the second component is associated with the cost of opportunity lost if the generator is required to reduce its real power generation in order to meet the reactive power requirements assigned by the ISO. [3]

II. REACTIVE POWER OPTIMIZATION

Reactive power is a quantity which is defined with alternating current systems. There are different types of electrical loads and they are classified into different categories on basis of various factors. Depending upon the nature of load we have resistive loads, capacitive loads, inductive loads and combination of above said

three. If the loads are capacitive type or inductive type or the combination of both, the current and voltage will not be in phase or in other words either the current will be leading the voltage if the load is capacitive or the current will be lagging the voltage if the load is inductive in nature and in such conditions the reactive power is produced [1] [6.] Here only the current component in phase with the voltage produces the real power. Reactive power is the reason for electric field and magnetic field in capacitors and inductors. It is the circulating power in the system that does no work. It is one of the ancillary services in the deregulated electricity market [1]. Two major requirements of reactive power are by the reactive power consumers and for system requirements and its consumption depends upon the load factor.

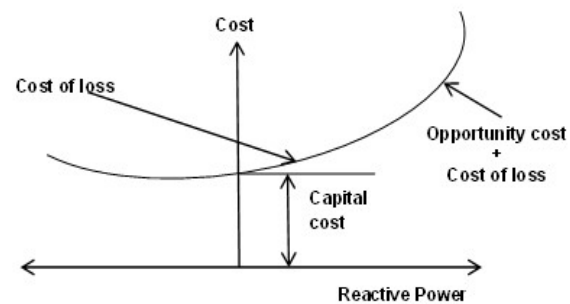


Fig.1. Cost of reactive power production from a synchronous generator

For proper operation of electrical equipment voltage regulation is necessary. Proper operation of electrical power equipment means there should not be any overheating of generators or motors, and then it should be able to minimize the losses and to make the system stable so that it does not collapse.[3] Reactive power is necessary to maintain the rated voltage at all the buses in order to deliver active power to the sending end or the loads through the transmission lines. Some of the loads like motor loads need the reactive power to do the useful works as it converts the flow of electrons for desired work. Absence of required reactive power may lead to the fall of bus voltage below its rated value and thereby the power required by the loads may not be provided [5]. If the voltage on the system is not sufficient due to insufficient reactive power required active power cannot be supplied by the system. An effective management of reactive

power should take care of three important requirements they are [10]:

- I. It should maintain the rated voltages at all the buses within the desired levels both at normal conditions and contingency conditions.
- II. To maintain the system stability and to utilize the transmission lines to its maximum [14] in order to prevent voltage collapse
- III. To minimize power losses and thereby increasing the efficiency

It is necessary to keep the terminal voltages of all the equipment in utility side and customer side within an acceptable range [4]. If the equipment on either side (utility and consumer) operates at a voltage below or above the rated voltage for a long time then the equipment performance will be affected or there is a good chance of equipment getting damaged. The difficulty of maintaining voltages within the required limits is difficult because of the fact that in power systems, the power system supplies power to a large number of loads and that is supplied from different generating stations. The generating station produces both active and reactive power [1]. If reactive power generation is decreased there is a fall in the system voltage and if the reactive power is increased the system voltage increases. When the system tries to provide more load than the voltage can support the voltage collapse happens [7]. If the system voltage falls the current must be increased in order to keep the required power demand and thereby causing the system to consume more reactive power causing the voltage to drop further [2]. If the current increases, transmission losses will increase and if the voltage drops to very small values, some generators will automatically disconnect itself for protection purpose and thereby decreasing the system voltage to further low levels which may lead to tripping of circuits and ultimately to system collapse so proper reactive power support is necessary. The problem of optimal reactive power dispatch is considered as part of optimal power flow problem.[6].If we add some controllable variable of reactive power compensators to the economic dispatch problem real power dispatch problem then it can be used to determine the optimal reactive power dispatch problem. The Optimal Power Flow consists of

two sub problem they are the economic dispatch and the optimal reactive power dispatch. They are solved until their convergence is reached. The main aim of modeling objective function is to reduce the real power losses when they are modeled for solving optimal reactive power dispatch. Reactive power cost minimization is mainly in done in terms of system losses.[1]-[7].The aim of optimal power dispatch is to reduce the overall fuel cost under certain constraints.

$$\text{Min} P_{G,i}, V_{G,i} . \text{Cost} = P_{price} * [\sum_{I=1}^n (P_{G,i})]$$

The reactive power cost is calculated from the obtained load flow studies and is compared for its rate before and after applying PSO. The cost for reactive power is calculated using the expression which is similar to the load dispatch calculation formulae and it is represented by the equation:

$$\text{Cost}_{\text{reactivepower}} = a_1 Q^2 + b_1 Q + c_1$$

Where,

$$a_1 = a \sin^2 \theta$$

$$b_1 = b \sin \theta \text{ and, } c_1 = c$$

a, b, c are the cost coefficients.

Reactive power is a must to run many electrical devices, but it can cause several harmful effects on different appliances and other motorized equipment's or loads, as well as the entire electrical infrastructure [5]. As the current passing through the electrical system is higher than the required amount to do the necessary work, excess power is dissipated in the form of heat because the reactive current flows through various resistive components like wires, switches and transformers. Keeping in mind the fact that when energy is expended, we need to pay. It does not make any difference whether the energy is utilized in the form of heat or useful work. We can determine the amount of reactive power used by the electrical devices by measuring their pf (power factor) which is the ratio between real power and true power. A pf 1 means that all the electrical power is applied towards real work that is the ideal situation.

III. TVAC-PSO

The problem of optimal power dispatch is highly non-differentiable, highly non-linear and discontinuous function and hence Time Varying Acceleration Coefficient - Particle Swarm Optimization is used to solve the real and reactive power optimal dispatch. It is search algorithm which is very helpful in solving nonlinear problems without placing any restriction on the shape of the objective function [1]. It includes Initialization, power flow analysis, evaluation of the fitness function, updating the particles and updating the best particles. The advantage of using this algorithm is that it requires minimum number of variables required for making decision. Main required thing is the power flow analysis. Only disadvantage of this search is that it requires huge calculation time.

The updating equations of TVAC-PSO are expressed as:

$$V_i^{k+1} = \omega^k * V_i^k + a_1 * rand_1(P^{k_{best,i}} - X_i^k) + a_2 * rand_2(G^{k_{best}} - X_i^k)$$

Where,

$$\omega^k = \omega_{max} - \frac{\omega_{max} - \omega_{min}}{k_{max}} * k$$

$$a_i^k = a_{i,max} - \frac{a_{i,max} - a_{i,min}}{k_{max}} * k$$

$$X_i^{k+1} = X_i^k + V_i^{k+1}$$

The optimal dispatch problem solution using PSO follows the given flowchart given in the figure below.

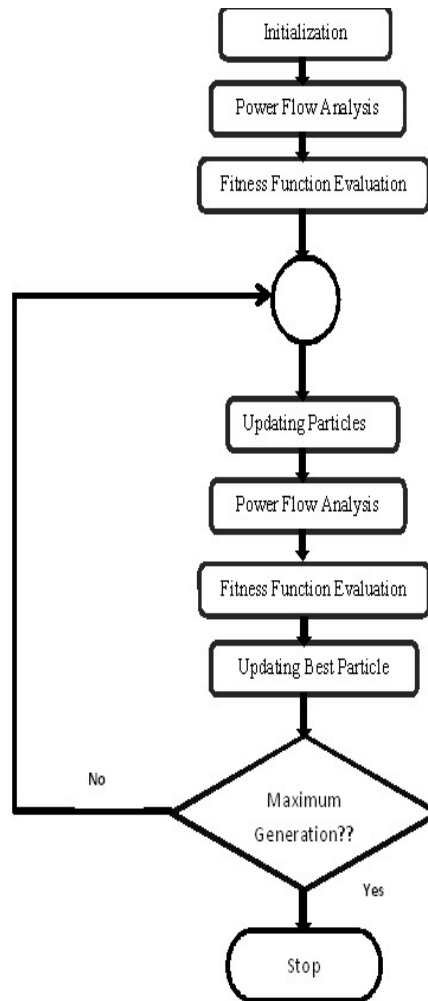


Fig.2. Optimal power dispatch in TVAC-PSO

IV. IMPLEMENTATION AND RESULTS

The TVAC-PSO was implemented on an IEEE14 bus system and hourly calculations were done for entire 24 hours:

Case (i): Base loading condition

When the incremental cost is 39\$/MWh and the optimal dispatch of generation is 274.726MW. The table I shows the comparison before and after applying PSO at the generators 1,2,3,6 and 8 when the cost coefficients are, $a= 0.04303$, $b=20$ and $c=0$ at the 8th hour and when none of the loads has exceeded its normal limit value. It is seen from the table that the voltage profile has improved when we apply TVAC-PSO as shown in the figure3.1

Generator	Before Applying PSO			After Applying PSO		
	Voltage (p.u)	Active Power	Reactive Power	Voltage (p.u)	Active Power	Reactive Power
1	1.000	236.694	-11.931	1.1000	233.676	-32.612
2	0.980	38.032	24.916	1.0900	38.032	39.016
3	0.960	0	42.155	1.0700	0	39.671
6	1.000	0	23.253	1.1000	0	13.205
8	1.000	0	15.575	1.1000	0	12.798
Cost		8266.84	3596.64		8145.39	3491.01

Table I: Comparison of active and reactive power at base load condition

Accordingly the cost of both the active power and reactive power has decreased drastically when calculated using the dispatch formula equation shown above. Minimum reactive power cost also implies that the system has minimum losses and thereby explains the optimal dispatch.

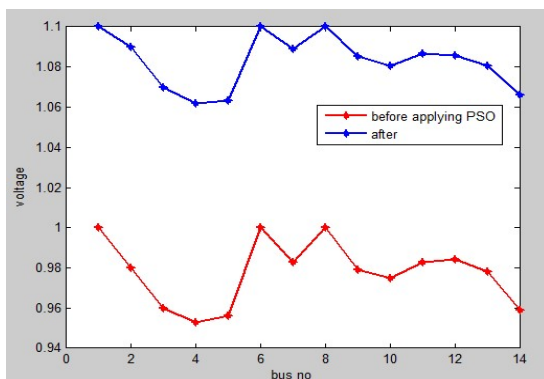


Fig.3.1. Comparison of voltage before and after applying PSO at line base loading condition

Case(ii): Maximum Load condition

When the incremental cost is 46.698 \$/MWh and the optimal dispatch of generation is 396.62 MW. The table II shows the comparison before

and after applying PSO at the generators 1,2,3,6 and 8 when the cost coefficients are, $a=0.04303$, $b=20$ and $c=0$ at the 8th hour and when there is maximum loading condition that is when generator 8 is at its maximum limit. It is seen from the table that the voltage profile has improved when we apply TVAC-PSO as shown in the figure3.2. Accordingly the cost of both the active power and reactive power has decreased drastically and is shown in the same figure.

Generators	Before Applying PSO			After Applying PSO		
	Voltage (p.u)	Active Power	Reactive Power	Voltage (p.u)	Active Power	Reactive Power
1	1.000	343.224	0.561	1.100	336.603	21.990
2	0.970	53.397	52.561	1.070	53.397	33.551
3	0.950	0	76.264	1.050	0	37.955
6	0.960	0	21.760	1.090	0	25.067
8	1.000	0	24.615	1.100	0	22.350
Cost		13714.281	7025.792		13388.177	4623.254

Table II: Comparison of active and reactive power at maximum load condition

Accordingly the cost of both the active power and reactive power has decreased drastically when calculated using the dispatch formula equation shown above. Minimum reactive power cost also implies that the system has minimum losses and thereby explains the optimal dispatch.

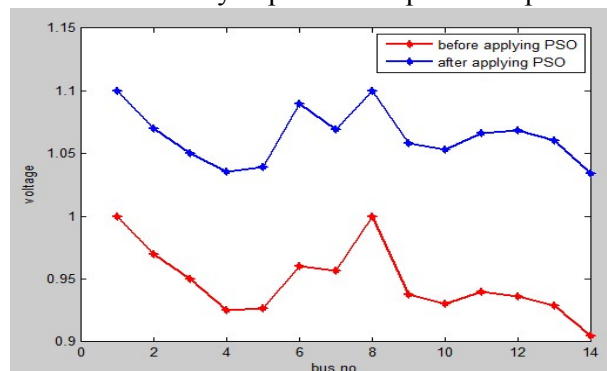


Fig.3.2. Comparison of voltage before and after applying PSO at the maximum loading condition

Case(iii): Line Contingency condition and base loading When the incremental cost is 39.061 \$/MWh and the optimal dispatch of generation is 257.05 MW and when the lines 9 to 14 are under contingency condition. The table III shows the comparison before and after applying PSO at the generators 1,2,3,6 and 8 when the cost coefficients are, a= 0.04303, b=20 and c=0 at the 8th hour. It is seen from the table that the voltage profile has improved when we apply TVAC-PSO as shown in the figure3.3. Accordingly the cost of both the active power and reactive power has decreased drastically and is shown in the same figure.

Table III: Comparison of active and reactive power at line contingency condition

Generators	Before Applying PSO			After Applying PSO		
	Voltage (p.u)	Active Power	Reactive Power	Voltage (p.u)	Active Power	Reactive Power
1	1.000	237.026	-31.244	1.1000	233.983	-33.707
2	0.990	38.032	49.108	1.0900	38.032	34.938
3	0.960	0	32.097	1.0700	0	36.959
6	1.000	0	18.344	1.1000	0	10.583
8	1.000	0	6.243	1.1000	0	4.491
Cost		8280.2507	3392.027		8157.7166	2690.606

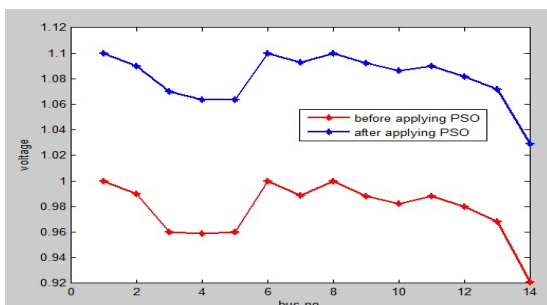


Fig.3.3. Comparison of voltage before and after applying PSO at the line contingency condition

Case(iv): Line Contingency condition and maximum loading When the incremental cost is

43.865 \$/MWh and the optimal dispatch of generation is 351.863 MW and when the lines 9 to 14 are under contingency condition with the maximum load demand. The table IV shows the comparison before and after applying PSO at the generators 1,2,3,6 and 8 when the cost coefficients are, a= 0.04303, b=20 and c=0 at the 8th hour

Table IV: Comparison of active and reactive power at maximum load condition

Generators	Before Applying PSO			After Applying PSO		
	Voltage (p.u)	Active Power	Reactive Power	Voltage (p.u)	Active Power	Reactive Power
1	1.000	304.132	2.014	1.1000	298.564	2.986
2	0.970	47.731	31.712	1.0800	47.731	29.737
3	0.950	0	61.037	1.0500	0	34.493
6	0.970	0	26.174	1.0800	0	23.532
8	1.000	0	16.764	1.1000	0	16.178
Cost		11586.937	4866.16		11331.176	3558.199

The corresponding voltage profile is shown in figure 3.4.

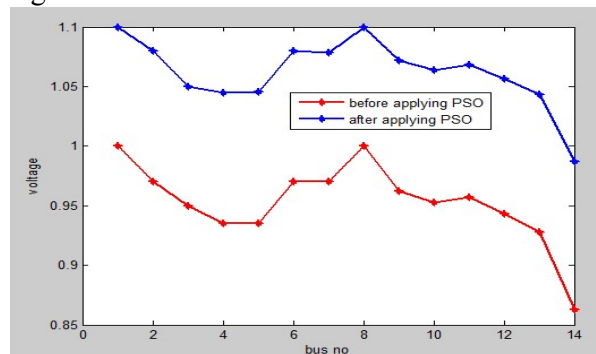


Fig.3.4. Comparison of voltage before and after applying PSO at the line contingency and maximum loading condition together

V. CONCLUSION

In this paper, a complete methodology is proposed for reactive power pricing in a deregulated electricity market. The problem of optimal power dispatch is solved using time-varying acceleration coefficients particle swarm optimization (TVAC-PSO), which is far better than conventional power flow analysis techniques because of its convergence at the

global best rather than converging at the local best. The dispatch problem is divided into two sub-problems as real power dispatch and reactive power dispatch. Total reactive power cost consists of unused capacity, costs of direct reactive power consumption and the cost of voltage control. The cost component of reactive power output is tested on the modified IEEE 14-bus. The future scope includes taking into consideration various reactive power compensating devices such as capacitors or any FACT device.

A. References

- [1] Chira Achayuthakan and Weerakorn Ongsaku, "TVAC-PSO Based Optimal Reactive Power Dispatch for Reactive Power Cost Allocation under Deregulated Environment ", IEEE Trans. On Power System, 2009.
- [2] S.Sakthivel and Dr. D. Mary, "Reactive Power Optimization for Voltage Stability Limit Improvement Incorporating TCSC Device through DE/PSO under Contingency Condition", *IU-JEEE Vol. 12(1), (2012), 1419-1430.*
- [3] Garng M. Huang and H. Zhang, "Pricing of Generators reactive Power Delivery and Voltage Control in the Unbundled Environment", IEEE Trans. On Power System, 2000
- [4] Chira Achayuthakan and Weerakorn Ongsaku, "TVAC-PSO Based Optimal Reactive Power Dispatch for Reactive Power Cost Allocation under Deregulated Environment ", IEEE Trans. On Power System, 2009.
- [5] <http://nptel.ac.in/courses/108107028/module6/lecture9/lecture9.pdf>
- [6] Weerakorn Ongsakul and Dieu Ngoc Vo, "Artificial intelligence in Power System optimization", Optimal reactive power dispatch, (pp 328-365)
- [7] Okwe Gerald Ibe and Akwukwaegbu Isdore Onyema," Concepts of Reactive Power

Control and Voltage Stability Methods in Power System Network",IOSR Journal of computerEngineering (IOSR-JCE) e-ISSN:2278-0661,p-ISSn:2278-8727 Volume 11,Issue 2(May-Jun.2013)

- [8] Shangyou Hao and Alex Papalexopoulos, "Reactive Power Pricing and Management", IEEE Trans. On Power Systems, Vol.12.No.1, February.



OPTIMIZATION IN ECONOMIC LOAD DISPATCH WITH SECURITY CONSTRAINTS

¹Debi Sankar Roy, ²Venkataswamy R,
¹M.Tech Scholar, ²Assistant Professor

Abstract—Optimization of power scheduling for dynamically varying demand in real time considering constraints like transmission line capabilities, availability of conventional and renewable power sources, change of reliability index, serving critical and forecasted loads, optimization of losses, storage capacity. The scheduling is made considering practical security aspects like line and generator outages. Deep dive analysis is made on demand side management and suggestions are proposed. Dynamic economic load dispatch problem has been modeled as inequality constrained optimization problem. The evolutionary programming is applied to optimize the solution.

Index Terms—Economic Load Dispatch, Particle Swarm Optimization, Genetic Algorithm, Distributed Generation.

I. INTRODUCTION

Now a days due to interconnection of all the various electrical networks, energy crisis in the world and continuous rising prices, it is now very much in need to reduce the operating cost of electric energy. The main aim of today's electrical utility is to provide electrical power in a reliable way and in a possible low cost. Electrical Energy cannot be stored, but it can be generated from available sources be it conventional resources or Renewable energy sources. Transmission system is used for delivery of bulk power for a considerable distance and distribution system is used for local delivery of power. Since now a days there are so many sources of energy be it

coal, oil or gas, water, solar energy, wind power, the choice of what resource should be taken, is taken in the basis of mostly economic expenditure, then other conditions are kept in mind such as Technical and Geographical.

Economic Load Dispatch in Generating units is one of the very few problems in Power system Operation. The new wave of implementing more and more renewable energy sources makes this problem even more important now a day. The main aim of Economic Load Dispatch Problem is to define the production cost of each plant so that the total cost of generation and transmission is as minimum as possible for a specific amount of load. Some factors have to be taken into account such as the generating Plant characteristics, the fuel used, heat rate of the fuel, water reserved for hydrothermal, the transmission losses etc.

II. BACKGROUND AND MOTIVATION

A. Economic Load Dispatch

As we have mentioned earlier, Economic Load Dispatch is one of the main problem now a days in our power system where dispatching the load in an economic way carries a great significance in present times power system where reducing the operating and generation cost is the most significant work to be look after.

B. Thermal Scheduling

Scheduling on plants in thermal generation carries a great significance. Thermal power plants

have to take into account the fuel cost. In present days with the increase of Load Demand, it is very much necessary to operate the generating stations in a economical way. So it is very much essential to reduce the cost of the generation. The optimum scheduling of generating plants plays a very big role in reducing the total cost. In thermal plants the main cost is of Fossil fuel. So in thermal scheduling our aim is to minimize the fuel cost to supply the load demand, considering the constraints.

c. Hydrothermal scheduling

In the present age when there are large system set up of Hydro and Thermal Power system are already existing, the idea of integrating the two power stations together cannot be ruled out looking at the economic aspect of the same. The main idea behind the integrated operation is utilization of all the available energy sources in an optimal economical way to give the customers an uninterrupted supply. In a very interesting case, the cost of operation in Thermal Power plants is high but the capital cost is low, whereas in the case of hydro, it is the opposite. The operational cost is low but the capital cost is high. So it is rather economical as well as convenient to have both the plant in the same grid. Hydro Plant can be started quickly and it has a fast response time. But thermal power plant is slow in response. Mainly the thermal plant can be preferred for base load plant and hydro electric will be as peak load plant. For Hydrothermal Scheduling, it is very much essential to use the total amount of water available to the fullest. In hydro power for consumption charge will be fixed as there is no fuel cost, regardless to the amount of power generated. So we can get the minimum overall cost can be achieved by exploiting the hydro power to the maximum. Few things that should be kept in mind is number of hydro stations, their location and their characteristics.

d. Wind based generation

In the present scenario wind power has been one of the most preferred renewable energy sources in the world. Wind energy currently generates only 1% of all the electricity, but the share of it is growing rapidly. Globally, the longterm technical potential of wind energy is

believed to be five times total current global energy production. In Denmark the share of wind power production has already gone up to 19% of the total energy generation. We can say it is the fastest growing renewable energy source. Wind power is one of the cleanest sources of energy as there are no chances of spreading pollution. With the growing energy demand in the world its very necessary to keep a balance between both normal conventional source of energy as well as Renewable energy source.

III. PROBLEM FORMULATION

here are different constraints in Economic Load Dispatch problem, mainly equality Constraints and Inequality Constraints. The objective function has to be minimized based on these constraints. Transmission loss plays a major role in this optimum dispatch of generation. The basic formula for optimization can be stated as to,

$$\begin{aligned} & \text{minimize, } F(P_{gi}) = \sum_{i=1}^{NG} F_i(P_{gi}) \\ & \text{subjected.to } \sum_{i=1}^{NG} P_{gi} = P_D \quad (1) \\ & P_{gi}^{\min} \leq P_{gi} \leq P_{gi}^{\max} \end{aligned}$$

Where P_{gi} is real power generation, P_D is the real power demand, P_{gmin} is the lower limit of the power generation.

P_{gmax} is the higher limit of the power generation $F_i(P_{gi})$ is the operating fuel cost of the i^{th} plant.

The fuel cost is given by a quadratic equation,

$$F_i(P_{gi}^2) = a_i P_{gi}^2 + b_i P_{gi} + c_i R_s/h \quad (2)$$

IV. PARTICLE SWARM OPTIMIZATION

It is one of the very few methods that are available and have been developed to solve optimization problem such as Economic Load dispatch problem. The basic concept of PSO lies in accelerating each particle toward its pbest and the gbest locations, with a random weighted acceleration at each time step. The two things considered for particle swarm optimization is Pbest, and Gbest. In PSO, a swarm of n individuals communicate either directly or indirectly with one another search directions

(gradients). Each particle keeps track of its coordinates in the solution space which are associated with the best solution (fitness) that has achieved so far by that particle.

Application of PSO in Power System are Economic Load Dispatch, Power System Reliability, State Estimation, Load Flow and Power Flow and Power System Identification and Control.

V. GENETIC ALGORITHM

It is a method that mimics the natural selection process of nature. It is one of those methods used as a solution to optimizing problems. It is one of those methods belonging to Evolutionary algorithms, which generate its solution using the natural evolution such as mutation, crossover etc. In a genetic algorithm, a Population of candidate solutions is evaluated as towards a better solution. Each candidate solution will have a set of properties (chromosomes) which can be mutated. Normally, solutions are represented in binary as strings of 0s and 1s, but other encodings are also possible. At first many numbers of random solutions are generated from a given initial population. The population size depends on the nature of the problem, but generally it contains several hundreds or thousands of possible solutions. Traditionally, the population is generated randomly which allows a full range of possible solutions.

Genetic Algorithm problems have five main components,

- A genetic representation for potential solution to the problem; solution coding.
- To create an initial population of potential solutions; Initialization.
- Fitness function
- Genetic operators that alter the composition of children, Genetic operators.
- Values of different parameters that are used for using the problem with GA.

The main usage of Genetic Algorithm is for getting an optimized solution for a given problem. Same as in for Power system also, aim is to get the optimum solution. In power system one of the main criteria is to dispatch the load in an economical way, so for that we need to get the optimum solution on which price we can dispatch

the load to the customer. That's why Genetic Algorithm is used.

VI. DISTRIBUTED GENERATION

In present world it is very much needed for the power system to be very user friendly and for that distributed generation, which is also known as decentralized generation, is very much needed. Because in this present times, most of the power plants as thermal, nuclear or coal fired power plants are all of centralized generation type and sometimes it needs to be transmitted to a long distance which creates a problem when there is a problem in the line that affects the whole system. But as of distributed generation, it is located near the consumer place where the serve the load as it is decentralized, making it more flexible and not prone to face the failures if any problem happens in the neighborhood. The distributed generation uses mainly renewable energy resources.

VII. RESULTS

The sample problem was considered for different type of generation. The economic load dispatch is done using GA and PSO algorithm.[2]

VIII. CONCLUSION

The economic load dispatch problem has been simulated for different types of generation like wind, hydrothermal, thermal as well as IEEE-30 bus system using genetic and particle swarm optimization. The comparative study has been made with respect to consistency of optimal solution and simulation time. It has been observed that PSO gives better consistency

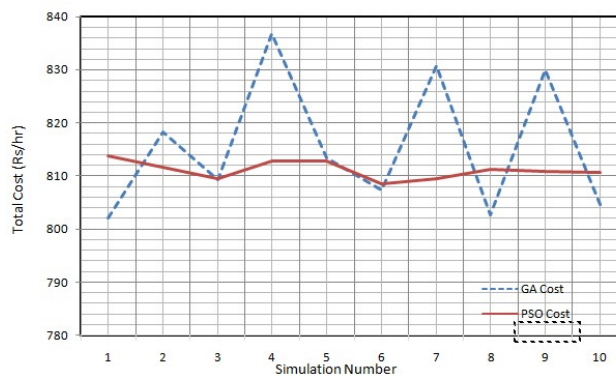


Fig. 1. Consistency of optimal cost using PSO algorithm and GA algorithm in IEEE-30 bus system

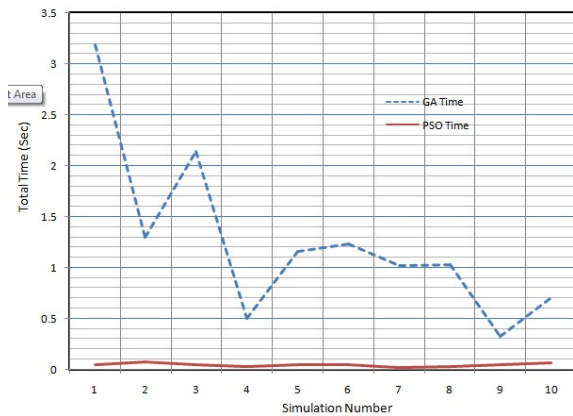


Fig. 2. Simulation time taken by PSO algorithm and GA algorithm for IEEE30 bus system

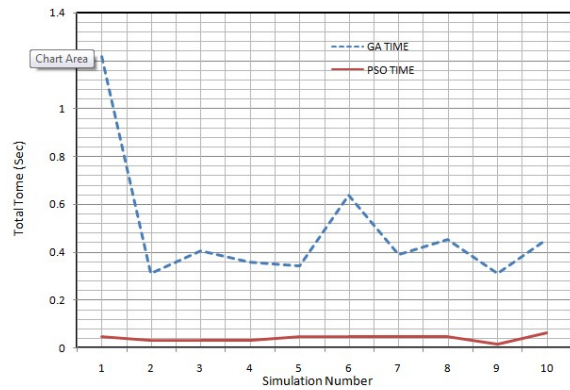


Fig. 5. Simulation time taken by PSO algorithm and GA algorithm for thermal generation

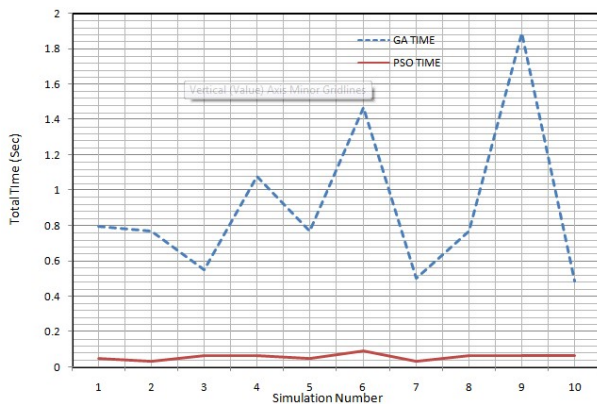


Fig. 3. Consistency of optimal cost using PSO algorithm and GA algorithm in hydrothermal generation

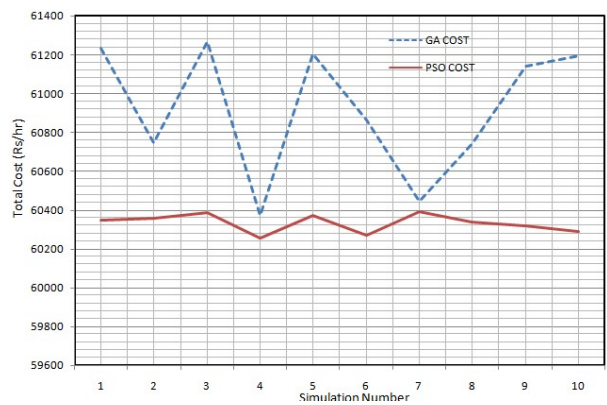


Fig. 6. Consistency of optimal cost using PSO algorithm and GA algorithm in wind generation

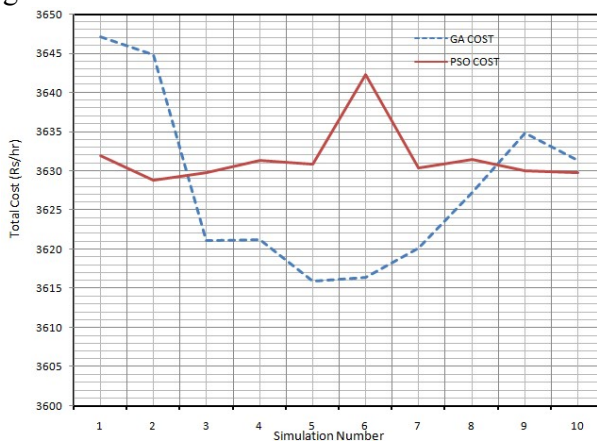


Fig. 4. Consistency of optimal cost using PSO algorithm and GA algorithm in thermal generation

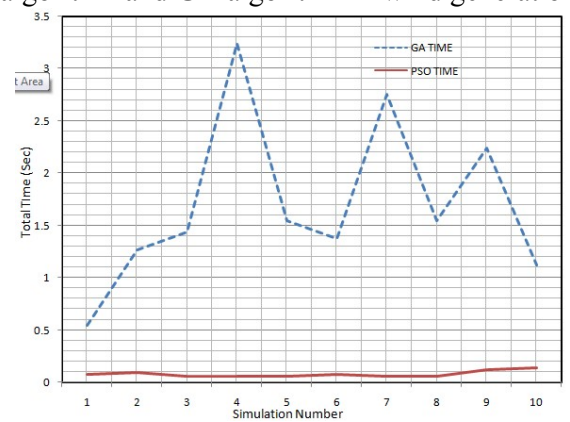


Fig. 7. Simulation time taken by PSO algorithm and GA algorithm for wind generation

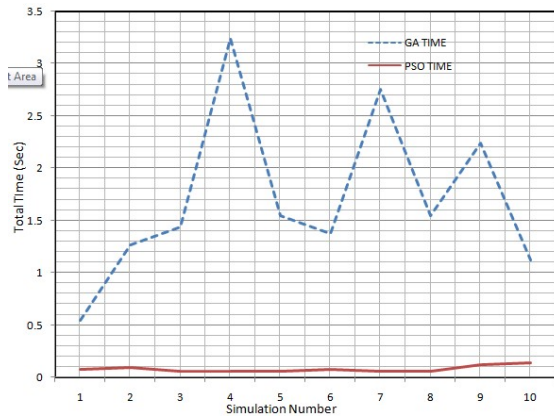


Fig. 8. Simulation time taken by PSO algorithm and GA algorithm for wind generation

	P1	P2	P3	P4
GA	187.5416	154.6825	215	14.40933
PSO	222.8415	121.2677	206.3063	12.25443
GA	171.951	170	215	12.05497
PSO	234.85	129.6718	182.1369	11.4813
GA	170.1678	170	215	13.26017
PSO	239.691	118.6862	189.7223	10.13045

Fig. 9. Simulation time taken by PSO algorithm and GA algorithm for wind generation

	P1	P2	P3
GA	169.2242	45.68567	100
PSO	191.009	47.72342	74.00755
GA	207.9703	24.51265	82.18814
PSO	188.0822	50.15988	74.21794
GA	184.0009	71.15463	57.41803
PSO	190.5246	46.46327	75.54208

Fig. 10. Simulation time taken by PSO algorithm and GA algorithm for wind generation

	P1	P2	P3
GA	175.1879	48.4664	21.94559
PSO	202.0029	34.31468	19.54208
GA	167.5313	29.53974	19.86533
PSO	185.531	43.1274	20.32467
GA	164.8007	44.79349	19.55504
PSO	187.7028	48.20544	15.76577

Fig. 11. Simulation time taken by PSO algorithm and GA algorithm for wind generation

	P4	P5	P6
	21.41068	11.4499	14.17757
	10.91632	11.02748	14.62658
	30.82075	13.89978	29.84902
	11.63676	15.74007	16.1601
	16.63857	24.46285	21.53492
	17.01052	10.93732	12.61814

Fig. 12. Simulation time taken by PSO algorithm and GA algorithm for wind generation and takes lesser time than genetic algorithm. The local and global optima is converging very fast in PSO compared to the fluctuating response of GA. The detailed study made considering the different parameters which affects the cost characteristics. Line and generator outage constraints were considered for IEEE-30 bus system and the stress on the transmission line, increase in the transmission loss and the non-reliability has been studied.

Line Outage	Overloading factor
No outage	1.339
1-2	1.971
6-7	1.412
2-4	1.222
6-8	1.431
14-15	1.339

Fig. 13. Line Outage and its impact on transmission line

Generator Outage	Overloading factor
No outage	1.339
2	1.608
3	1
4	1.166
5	1.332
6	1.364

Fig. 14. Generator Outage and its impact on transmission line

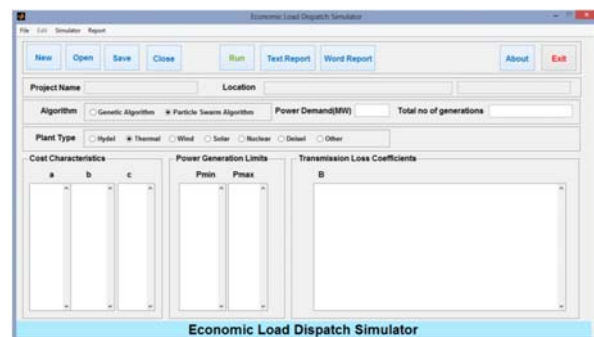


Fig. 15. ELD Simulator

APPENDIX A SIMULATOR

The tool is developed to simulate PSO and GA for economic load dispatch problem to different types of generations.

REFERENCES

- [1] H. Kopka and P. W. Daly, *A Guide to L^AT_EX*, 3rd ed. Harlow, England: Addison-Wesley, 1999.
- [2] D. P. Kothari and J. S. Dhillon, *Power System Optimization*, Second Edition, PHI Learning, 2003.
- [3] Shaik Affijulla and Sushil Chauhan, *Swarm Intelligence Solution to Large Scale Thermal Power Plant Load Dispatch*, IEEE, 2003.
- [4] F. Benhamida, Y. Salhi, S. Souag, A. Graa, Y. Ramdani, A. Bendaoud *A PSO Algorithm for Economic Scheduling of Power System Incorporating Wind Based Generation*, IEEE, 2003.
- [5] Dimple Singla, Sanjay K. Jain, *A Review on Combined Economic and Emission Dispatch using Evolutionary Methods*, International Journal of Advanced Research in Electrical, Electronics and Instrumentation Engineering, Vol. 2, Issue 6, June 2013.
- [6] K. Balamurugan and Sandeep R Krishnan, *Differential Evolution Based Economic Load Dispatch Problem*, National conference on Advances in Electrical Energy Applications, Vol. 2, Issue 6, June 2013.
- [7] Ravinder Singh Maan, Om Prakash Mahela, Mukesh Gupta, *Economic Load Dispatch Optimization of Six Interconnected Generating Units Using Particle Swarm Optimization*, IOSR Journal of Electrical and Electronics Engineering, Vol. 6, Issue 2, pp. 21-27, June 2013.
- [8] Tripti Gupta and Dr. Manjaree Pandit, *PSO-ANN for Economic Load Dispatch With Valve Point Loading Effects*, International Journal of Emerging Technology and Advanced Engineering, Vol. 2, Issue 5, June 2012.
- [9] R. Mudumbai and S. Dasgupta, *Distributed control for the smart grid: the case of economic dispatch*, IEEE.
- [10] T. Kumano, *A Functional Optimization Based Dynamic Economic Load Dispatch Considering Ramping Rate of Thermal Units Output*, IEEE.
- [11] F. Benhamida, Y. Salhi, S. Souag, A. Graa, Y. Ramdani, and A. Bendaoud, *A PSO Algorithm for Economic Scheduling of Power System Incorporating Wind Based Generation*, IEEE.
- [12] A. Naresh Kumar, D. Suchitra, *AI Based Economic Load Dispatch Incorporating Wind Power Penetration*, IEEE.
- [13] Warsono, D. J. King, and C. S. zveren, *Economic Load Dispatch for a Power System with Renewable Energy using Direct Search method*, IEEE.
- [14] Shahab Bahrami, Farid Khazaeli, Mostafa Parniani, *Industrial Load Scheduling in Smart Power Grids*, International Conference on Electricity Distribution, Stockholm, pp.10-13, June 2013 .



LOW POWER STAND-ALONE MICRO-GRID WITH WIND TURBINE

¹Pooja Prasad, ²Prof. Manikandan.P

^{1,2}Department of Electrical and Electronics, Christ University Faculty of Engineering
Bangalore, India

Email: ¹pujaprasad07@gmail.com, ²manikandan.p@christuniversity.in

Abstract—The energy demand around the world is increasing, the need for renewable energy source that will not harm the environment has been increased in which wind power is one among them. There are many loads that are away from the main grid. For isolated localities, one practical approach to self-sufficient power generation involves using a wind turbine with battery storage to create stand-alone systems. The power conversion system consists of Wind turbine driven Permanent Magnet Synchronous Generator (PMSG), a Diode Rectifier, a DC-DC boost converter to which the high voltage DC loads are connected. Battery is connected to store the excess power generated from wind turbine. The low voltage loads are connected to a system through a DC-DC buck converter, this entire system forms the DC micro grid. The proposed system is demonstrated using MATLAB/SIMULINK based simulations.

Keywords—Wind Energy, PMSG, Uncontrolled Diode Rectifier, DC-DC converters, DC link voltage.

I. INTRODUCTION

In recent years, the electrical power generation from renewable energy sources, such as solar and wind, is increasingly attracting interest because of environmental problems and shortage of the traditional energy like fossil fuels etc, in the near future. The two configurations used for wind energy conversion system are the stand-alone or autonomous systems and the grid or

utility connected systems. Standalone systems directly supply electrical load especially in isolated areas which will eliminate the need for extensive transmission lines from the utility. However the wind is an ever changing energy source, continuous power generation is not possible without energy storage. Wind power mainly depends on geographic and weather conditions and varies with time. So it is necessary to construct a system that can generate maximum power for all operating conditions. Permanent Magnet Synchronous generator is used for stand-alone wind power generation because of its advantages such as reliability, low maintenance and high efficiency.

In order to achieve variable speed operation, power electronic converter interface is used to supply load. The converter consists of uncontrolled three-phase diode rectifier, and DC-DC converters.

In this paper, the modeling of generator and the power electronic interface is carried out in steady state condition [2].

Power electronic devices with variable speed system are very important, where AC-DC converter is used to convert AC voltage with variable amplitude and frequency at the generator side to DC voltage and that voltage is boosted to DC link voltage (380V) by boost converter. This in turn is connected to the loads which operate at higher voltages. The loads which operate at lower voltages are connected to the link through a DC-DC buck converter which bucks the DC link voltage to 24V. The reliability

of the variable speed wind energy system can be improved significantly by using a direct drive permanent magnet synchronous generator (PMSG). PMSG has several advantages when compared to other types of generators which are used in wind energy conversion systems such as simple structure, can operate at slow speed, self excitation capability, leading to high power factor and high efficiency operation. When PMSG is used, there is no need of a gearbox which suffers many times from faults and requires regular maintenance, which makes the system inefficient.

Battery energy storage system is essential for a standalone system to meet the required load. As a variable speed wind system which has a fluctuating generated power due to the variability of wind speed. It can store the excess energy when the generated power from the wind is more than the required load power for a time. When the generated power from the wind is less than the required load, battery supplies the required power to maintain the power balance between generated and required load power. The varying power from wind energy system can be removed and the reliability of power to the load can be maximized with battery storage system.

Most residential households are currently supplied with 240V AC, requiring rectifiers for DC operated appliances to convert the AC voltage to usable DC, leading to power losses in the conversion. Standby power loss also factors into AC distribution for DC electronics and appliances, since the rectifiers will continue draw power even if the device is in standby. DC distribution in a building would require rectification only from the grid to the internal grid in the household, or micro-grid, and would use DC-DC converters for the rest.

With the interest in reducing dependency on foreign petroleum and CO₂ emissions, renewable energy has been a rapidly expanding area. Renewable energy generation helps strengthen the case for DC distribution since renewable energy sources generate DC power. With DC distribution, DC-DC conversion is all that is required to interface with the grid and battery storage to a micro-grid compared to AC, which would require AC-DC conversions in addition. By maximizing energy efficiency with renewable energy sources, the demand on the power grid is also reduced, which leads to less

reliance on foreign petroleum and reduced CO₂ emissions.

In this paper, author derived and presented the following models: wind turbine, Permanent Magnet synchronous generator, rectifier, Boost converter and the buck converter. The simulink model was constructed and implemented using the power system simulation tools in MATLAB/SIMULINK. This model is used to predict the performance of the wind turbine generator system.

II. STAND-ALONE WIND ENERGY CONVERSION SYSTEM

The circuit topology for the variable speed stand-alone wind energy supply system is shown in fig. 1. The system consists of the following components: Wind turbine which is connected to Permanent Magnet Synchronous Generator of kW. The Permanent Magnet Synchronous Generator is driven directly without using gearbox. Uncontrolled diode rectifier is used to convert AC output from generator to DC voltage and this voltage is fed to DC-DC boost converter which will boost the voltage to DC link voltage (380V). Battery bank is connected to the DC link of which the nominal voltage is maintained at 380V. The proposed model has been modeled and simulated using MATLAB/SIMULINK.

III. MODELLING OF THE SYSTEM

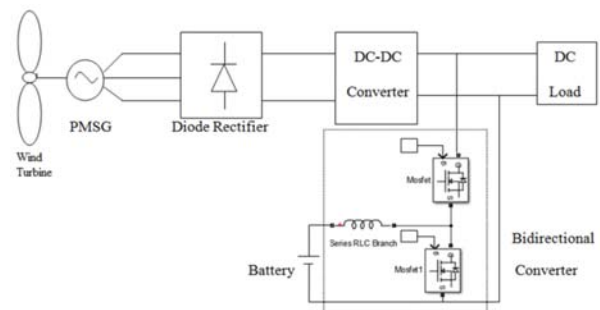


Fig 1: Power circuit topology of a stand-alone wind energy supply system

A. Modelling of Wind Turbine

The Wind Power is given by,

$$P_w = \frac{dW_w}{dt} \tag{1}$$

Energy drawn by wind turbine is,

$$W_w = V_a \frac{1}{2} \rho (V_1^2 - V_3^2) \quad (2)$$

Where,

W , is Energy drawn by wind turbine, ρ is the Air density(kg/m³) V_a is the air stream volume element, V_1 is undisturbed far upstream wind speed, V_2 is wind speed at turbine.

The power in the wind in an area is given by ,

$$P_w = 0.5 \rho A V_w^3 \quad (3)$$

Where, V_w is the wind velocity (m/s)

But the turbine captures only a fraction of this power. The power captured by the turbine (P_m) can be expressed as

$$P_m = P_w \times C_p \quad (4)$$

Where, C_p is a fraction called the Power coefficient. The power coefficient represents a fraction of the power in the wind captured by the turbine and has a theoretical maximum of 0.55.

The power coefficient can be expressed by a typical empirical formula as,

$$C_p(\lambda, \beta) = C_1 \left(\frac{C_2}{\lambda_i} - C_3 \beta - C_4 \right) e^{\frac{C_5}{\lambda_i}} + C_6 \lambda \quad (5)$$

Where, β is the pitch angle of the blades in degrees

λ is the Tip speed ratio of the rotor blade tip speed to wind speed

$$\lambda = W_r \cdot R / V_w \quad (6)$$

Where, W_r is the Turbine rotor speed

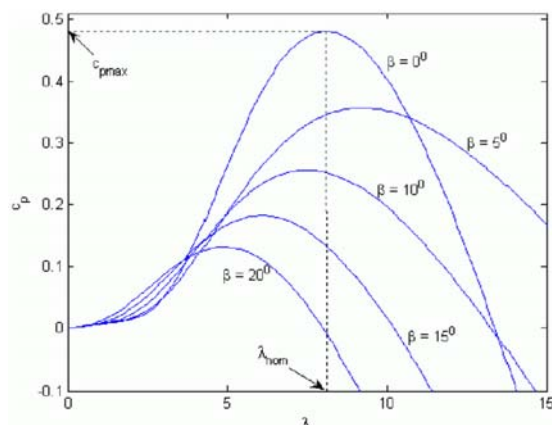


Fig 2: Cp versus lambda[4]

$$\frac{1}{\lambda_i} = \frac{1}{\lambda + 0.08\beta} - \frac{0.035}{\beta^3 + 1} \quad (7)$$

Where, $C1 = 0.5176$, $C2 = 116$, $C3 = 0.4$, $C4 = 5$, $C5 = 21$, $C6 = 0.0068$

Substituting these values in equation 5, it becomes

$$C_p(\lambda) = 0.5176 \left(\frac{116}{\lambda} - 9.06 \right) e^{\frac{21}{\lambda_i} + 0.735} + 0.0068 \lambda \quad (8)$$

The power and torque characteristics of a wind turbine are governed by equations (4) and (5). With the power coefficient function given by (3), the mechanical power (P_m) of the turbine can now be represented as[3],

$$P_m = 0.5 \rho A C_p V_w^3 \quad (9)$$

$$P_m = 0.5 \rho A (0.5176 \left(\frac{116}{\lambda} - 9.06 \right) e^{\frac{21}{\lambda_i} + 0.735} + 0.0068 \lambda) W_r^3 \quad (10)$$

The volume of aerodynamic torque T_w in N-m is given by the ratio between the power from the wind and the turbine rotor speed W_r in rad/s, as follows

$$T_w = P_m / W_r \quad (11)$$

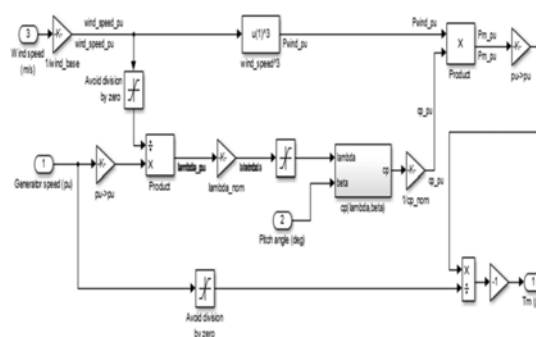


Fig 3: Matlab/SIMULINK model of Wind Turbine

B. Modeling of Permanent Magnet Synchronous Generator

A Permanent Magnet Synchronous generator is a generator in which the excitation coil, normally in the rotor, has been replaced by a system made up of permanent magnets which provide a constant excitation field, which eliminate the need of additional excitation system.[3]

It is used in those cases where small voltage drops by a certain degree or when power converters are connected to the output of the generator. The power converters can convert a

voltage range into continuous voltage of a constant value. The operation of the PMSG is different from that of normal synchronous generator. In a normal generator, voltage is controlled by means of excitation, but in PMSG, excitation is constant that is why, when the generator is charged, voltage drops without the option to regulate.

The main advantage is its simplicity. The manufacturing and assembly of the rotor will be cheaper if the magnets are used. They do not have brushes, thus the maintenance is not required. The mechanical consistency of a PMSG is superior and it does not require additional systems for its excitation. By eliminating the excitation, energy savings of about 20% can be attained by simply using magnets.

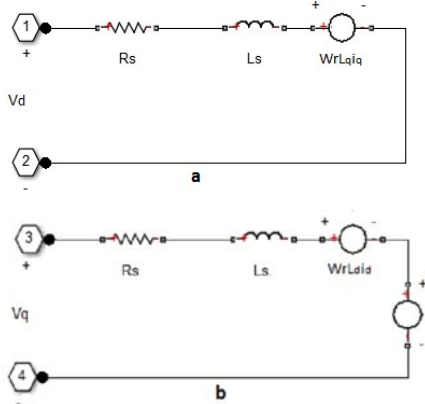


Fig 4: d-q-axis equivalent circuit model of the PMSG (a) d-axis (b) q-axis

The analysis of the PMSG can be made using quadrature equivalent circuit in which the damper windings are replaced with two equivalent windings in direct and quadrature axis respectively and permanent magnet is replaced with an equivalent superconductor winding placed in the direct-axis. The current through the equivalent winding of the permanent magnet (I_f) will be constant in all modes of operation.

The voltage equations of the PMSG can be derived from the voltage equations of the synchronous machine in dqo reference frame.

The voltage equations for the synchronous machine can be written as:

$$\begin{aligned} V_d &= R_s i_d + \frac{d\lambda_d}{dt} - \omega_s \lambda_q \\ V_q &= R_s i_q + \frac{d\lambda_q}{dt} - \omega_s \lambda_d \\ V_o &= R_s i_o + \frac{d\lambda_o}{dt} \end{aligned} \quad (12)$$

The flux linkage in d direction can be written as:

$$\lambda_d = L_d i_d + \lambda_m$$

$$\lambda_q = L_q i_q \quad (13)$$

When equations 13 are substituted in equations 12, we get,

$$\begin{aligned} V_d &= R_s i_d + L_d \frac{di_d}{dt} - \omega_s L_q i_q \\ V_q &= R_s i_q + L_q \frac{di_q}{dt} - \omega_s L_d i_d + \omega_r \lambda_m \end{aligned} \quad (14)$$

This is the standard current dynamics model of a PMSG where, R_s is the stator resistance, L_d and L_q are the d -axis and q -axis inductance, λ_m is the flux linkage due to permanent magnets, V_d and V_q are the dq -axis voltages, ω_r is the rotor speed, i_d and i_q are dq -axis current components.

The total input power into the machine when the rotor dq reference plane rotates at a speed of $\omega_r = d\theta_r / dt$ (θ_r is the rotor angular position), equation becomes,

$$P_{in} = \frac{3}{2} (V_q i_q + V_d i_d) \quad (15)$$

Where, the zero sequence components are neglected.

The mechanical output power is given by[3],

$$P_{out} = \frac{3}{2} (\omega_r L_d i_d i_q + \omega_r \lambda_m i_q - \omega_r L_q i_q i_d) \quad (16)$$

For a P pole machine, with $\omega_r = (P/2)\omega_m$, where ω_m is the rotor speed in mechanical radians per second.

$$P_{out} = \frac{3}{4} P \omega_{rm} (L_d i_d i_q + \lambda_m i_q - L_q i_q i_d) \quad (17)$$

The equation for electromagnetic torque is obtained by,

$$T_e = \frac{P_{out}}{\omega_{rm}} = \frac{3}{4} P (L_d i_d i_q + \lambda_m i_q - L_q i_q i_d) \quad (18)$$

If P is the number of pole pairs then electromagnetic torque becomes:

$$T_e = 1.5 (\lambda_m i_q + (L_d - L_q) i_q i_d) \quad (19)$$

Mechanical system:

$$\begin{aligned} \frac{d}{dt} \omega_r &= \frac{1}{J} (T_e - F \omega_r - T_m) \\ \frac{d\theta}{dt} &= \omega_r \end{aligned} \quad (20)$$

Where, T_m is the shaft mechanical torque, θ is the rotor angular position, J is the combined inertia of rotor and the load.

C. Modeling of uncontrolled diode Rectifier

The diode rectifier is the most commonly used topology in converting AC to DC voltage output. The circuit of a uncontrolled diode rectifier is shown in figure 4. The AC power generated from the PMS generator is converted into DC power through diode bridge rectifier. The same system is modeled in Matlab/Simulink

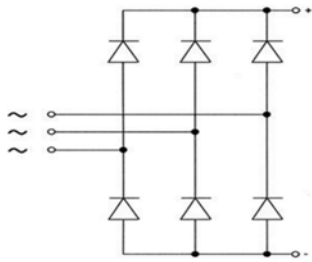


Fig 5: 3-Phase Uncontrolled diode Rectifier[10]

The DC output voltage (V_{dc}) from a rectifier is given by the expression:

$$V_{dc} = \frac{3}{\pi} \int_{\frac{\pi}{3}}^{\frac{2\pi}{3}} \sqrt{3} V_m \sin \omega t d\omega t = \frac{3\sqrt{3}V_m}{\pi} = \frac{3\sqrt{2}V_{LL}}{\pi}$$

$$= 1.654V_m = 1.3505V_{LL}$$

(21)

Where, V_{dc} is the output voltage, V_m is maximum peak voltage, V_{LL} is line to line voltage, R is the load resistance.

The output DC current (I_{dc}) is given by the expression,

$$I_{dc} = \frac{3\sqrt{3}V_m}{\pi R} = \frac{3\sqrt{2}V_{LL}}{\pi R} = \frac{1.654V_m}{R} = \frac{1.3505V_{LL}}{R}$$

(22)

The RMS voltage (V_{rms}) is given by the expression,

$$V_{rms} = \sqrt{\frac{3}{\pi} \int_{\frac{\pi}{3}}^{\frac{2\pi}{3}} (\sqrt{3} V_m \sin \omega t)^2 d\omega t} = \sqrt{\frac{3}{2} + \frac{9\sqrt{3}}{4\pi}} V_m$$

$$= 1.6554V_m = 1.3516V_{LL}$$

(23)

D. Modeling of DC-DC converters

Boost converter:

The voltage and current equations of dc-dc converter under steady state conditions can be found by using the two basic principles such as, the principle of volt-second balance and the principle of capacitor amp-second or charge balance. The principle of inductor volt-second balance says that the average value, or the dc component of the voltage applied across an ideal inductor winding must be zero and the principle of capacitor amp-second or the charge balance says that the average current that flows through an ideal capacitor must be zero. Thus, to determine the voltages and currents of dc-dc converters operating in periodic steady state, one averages the inductor current and capacitor voltage waveforms over one switching period, and equates the results to zero [1].

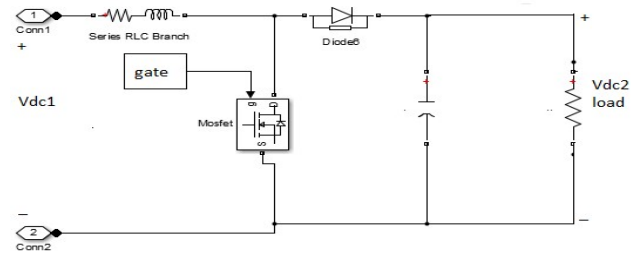


Fig 6: Simulink model of Boost converter

The expression for output Voltage and current is given

by,

$$V_{dc2} = \frac{V_{dc1}}{(1-D) \left[1 + \frac{R_L}{(1-D)^2 R_{load}} \right]} \quad (24)$$

Assuming a lossless circuit,

$$V_{dc1} I_{dc1} = V_{dc2} I_{dc2}$$

(25)

$$I_{dc2} = (1-D) \left[1 + \frac{R_L}{(1-D)^2 R_{load}} \right] \quad (26)$$

E. Battery Energy storage:

In this proposed topology Battery bank is connected to the DC link through DC-DC bidirectional converter as shown in fig 1.

Bidirectional Buck-boost converter:

In this paper, the battery bank is connected to the DC link voltage through a bidirectional DC-DC buck-boost converter. In addition to,

charge/discharge current to/from the batteries bank according to the generated power from the wind and the demanded load power, the DC-link voltage can be maintained constant as a reference value. This can be attained by controlling the bidirectional DC-DC buck-boost converter. The batteries bank voltage will be kept same as the DC-link voltage i.e. 380V.

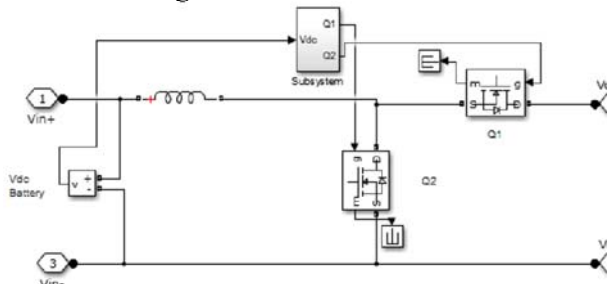


Fig 7: Birectional DC-DC converter

The control strategy is shown in the figure. To regulate the DC output voltage at a reference value, the control strategy of DC-DC bidirectional buck-boost converter uses a PI controller. In this control technique the DC voltage V_{dc} is sensed and compared with the reference DC voltage V_{ref} . The error signal is sent to the PI controller. The output signal is the duty cycle for the switches Q1 or Q2 according to the case of charging or discharging [2].

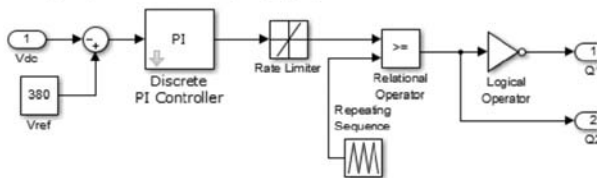


Fig 8: Control strategy for bidirectional DC-DC converter

During charging, the current flows from DC-link voltage to the battery bank. In this mode, Q1 is the active switch while Q2 is kept off. On the contrary, during discharging, the current transfers from battery bank to the DC-link voltage. In this mode, Q2 acts as a controlled switch and Q1 is kept off. Also, presence of the inductor at the batteries bank side results low ripple current which achieves higher efficiency and longer lifetime for the battery storage system.

IV SIMULATION RESULTS

The proposed topology for PMSG based variable speed stand alone wind turbine is simulated in

MATLAB/SIMULINK. Fig. 9 shows the simulation circuit of the proposed topology. The value of the power coefficient C_p was kept at optimum value which is equal to 0.48 with varying wind speed.

The performance of bidirectional DC-DC buck-boost converter controller to achieve the main purpose of storing power is demonstrated. It has been able to charge current to the battery bank when the generated power is more than the demanded power and discharge the power when the generation is less than the demanded power. It also helps in maintaining the DC link voltage to 380V. Table 1 shows the wind turbine and PMSG parameters considered.

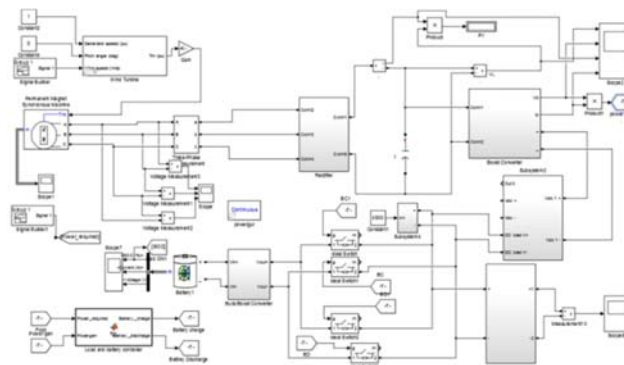


Fig 9: Simulation diagram of the proposed system

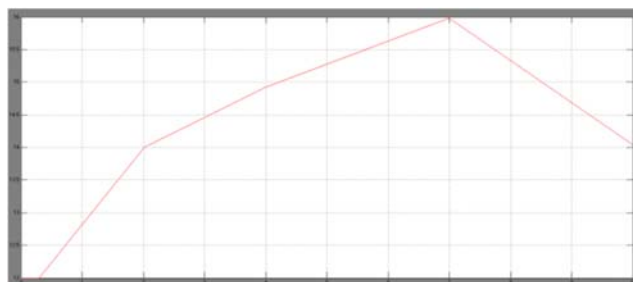


Fig 10: Wind speed



Fig 11: Constant DC link voltage (380V)

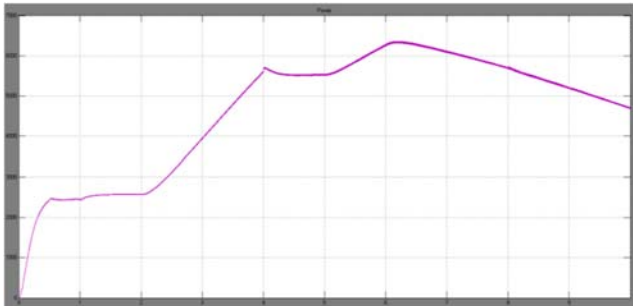


Fig 12: Power generated from the Boost Converter

Table 1: Wind Turbine and PMSG parameters

Wind Turbine	
Rating	10KW
Air Density	1.225Kg/m ³
Blade Radius	3.7m
Rated Wind Speed	16m/s
Inertia constant	0.6s
Permanent Magnet Synchronous Generator(PMSG)	
Rating	12KVA
Rated phase voltage	200V
Pole number	42
Inertia constant	0.4s

V CONCLUSION

The comprehensive and performance analysis of a variable speed stand-alone wind turbine with a PMSG using MATLAB/SIMULINK is presented in this paper. From the simulation results it can be seen that the control strategy used in the boost converter system helped in attaining 380V which is taken as a DC link voltage. The control used in the bidirectional converter which is connected between battery bank and DC-link voltage, is capable of maintaining the DC link voltage at a constant value, further it helps the battery to store surplus of wind energy and supply power to the load when the power generated from the wind turbine is less. With that the optimum value of the power

efficient is obtained which means that the maximum power is obtained from the available wind energy.

REFERENCES

- [1] Mohammed Aslam Husain, Abu Tariq , —Modelling and Study of a Standalone PMSG Wind Generation System Using MATLAB/SIMULINK in Universal Journal of Electrical and Electronic Engineering, issue:2(7), pp : 270-277
- [2] Mahmoud M. Hussein, Tomonobu Senjyu, Mohamed Orabi, Mohamed A. A. Wahab, and Mohamed M. Hamada, Control of a Variable Speed Stand Alone Wind Energy Supply System, IEEE International Conference on Power and Energy (PECon), 2-5 December 2012, Kota Kinabalu Sabah, Malaysia
- [3] Janardan Gupt1, Ashwani Kumar, —Fixed Pitch Wind Turbine-Based Permanent Magnet Synchronous Machine Model for Wind Energy Conversion Systems, Journal of Engineering and Technology, Jan-Jun 2012, issue: Vol 2, Issue 1
- [4] A. B. Cultura II, Z. M. Salameh, —Modeling and Simulation of a Wind Turbine-Generator System, IEEE, 2011, volume 6 no. 4, pp:5-11
- [5] Moulay Tahar Lamchich and Nora Lachguer, Matlab Simulink as Simulation Tool for Wind Generation Systems Based on Doubly Fed Induction Machines, MATLAB – A Fundamental Tool for Scientific Computing and Engineering Applications – Volume 2, pp:1-22
- [6] J. Mendez, A. Falcon and D. Hernandez, —Simulation of Storage Systems for increasing the Power Quality of Renewable Energy Sources in International Conference on Renewable Energies and Power Quality (ICREPQ'10) Granada (Spain), 23th to 25th March, 2010
- [7] S. Drouilhert, —Power flow management in a high penetration wind-diesel hybrid power system with shortterm energy storage, NREL Tech. Rep. CP-500-26827, July, 1999.
- [8] A.D. Hansen, P. Sorensen, F. Blaabjerg and J. Becho, —Dynamic modelling of wind farm grid interaction, Wind Engineering, Vol. 26, No. 4, pp 191-208, 2002.

- [9] Rajveer Mittal, K.S.Sandu and D.K.Jain —*Battery Energy Storage System for Variable Speed Driven PMSG for Wind Energy Conversion System*”, International Journal of Innovation, Management and Technology, Vol. 1, No. 3, 2010 pp.300-304
- [10] Semistack classics
- [11] L. Barote, C. Marinescu, M. Georgescu, “*VRB Modeling for Storage in Stand-Alone Wind Energy Systems*” IEEE Bucharest Power Tech Conference, June 28th - July 2nd, Bucharest, Romania, pp.1-6
- [12] Kazuki Ogimi, Akihiro Yoza, Atsushi Yona, Tomonobu Senjyu, and Toshihisa Funabashi, —*A Study on Optimum Capacity of Battery Energy Storage System for Wind Farm Operation with Wind Power Forecast Data*” IEEE Conference, pp 118-123
- [13] Mahmoud M. Hussein , Tomonobu Senjyu , Mohamed Orabi , Mohamed A. A. Wahab and Mohamed M. Hamada “*Control of a Stand-Alone Variable Speed Wind Energy Supply System*” Appl. Sci. 2013, 3, 437-4
- [14] Bing Hu, Liuchen Chang, Yaosuo Xue, “*Control and Design of a Novel Buck-Boost Converter for Wind Turbine Applications*” IEEE 2008, pp. 234-238
- [15] T. Tafticht, K. Agbossou and A. Chériti —*DC Bus Control of Variable Speed Wind Turbine Using a Buck-Boost Converter*”. IEEE Conference 2006, pp.1-5
- [16] D. L. Yao, S. S.Choi, K. J. Tseng, and T. T. Lie —*Determination of Short-Term Power Dispatch Schedule for a Wind Farm Incorporated With Dual-Battery Energy Storage Scheme*” IEEE transactions on sustainable energy, Vol. 3, No. 1, 2012, pp.74-84



RELIABLE OPERATION OF A HYBRID DC MICRO GRID FOR CRITICAL APPLICATIONS

¹Sankeerth Sudhan , ²Prof . Manikandan.P

^{1,2}Department of Electrical and Electronics,Christ University, Faculty of Engineering
Bangalore, India

Email:¹sankeerth24@gmail.com, ²manikandan.p@christuniversity.in

Abstract—Renewable Energy Sources are becoming more significant in the present era to meet growing energy demands and also to decrease environmental pollution. Reliability is an important factor for any power system. Micro grids with Distributed Generation is developed to provide power in remote areas as well as for military, college institutional applications to improve reliability even when isolated from the main grid. This paper mainly deals with the reliable operation of a stand-alone DC Micro grid with two Renewable Energy Sources, Solar Photovoltaic array and Fuel cell array to meet the generation capacity of the micro grid so as to supply the load without any interruptions along with an energy storage device to store excessive energy when demand is less.

Keywords—Renewable Energy Sources,Solar PV array,Proton Exchange Membrane Fuel cell array,DC Micro grids,Battery

I. INTRODUCTION

Due to rapid increase in population and industrial growth, there has been tremendous increase in power requirements as well as various power quality problems associated with the same. So the use of Renewable Energy Sources (RES) for power generation has become a hot topic nowadays. Distributed

Generation (DG) is the use of small power generation technologies located close to the load that has to be served. DG of RES helps to reduce environmental pollutions. Due to the advancements in RES and Energy Storage, integration of RES into Micro grids have become possible. Micro grids are basically any isolated electrical system that has its own generation. They can work in isolated mode from the main grid or stay connected with the main grid.[1],[4],[6].

In this paper we consider a stand-alone DC Micro grid with two RES technologies mainly Solar Photovoltaic array and PEM Fuel cell array supplying DC power for telecommunication applications for military purposes. Micro grids are developed mainly to improve the reliability and quality of power supplied. Any excessive power generated is stored in a battery storage device which provides power when any of the RES are not active. Emerging Smart grid technologies helps the utilities to easily control the DG systems. The RES technologies used in this paper are connected to a DC grid via DC-DC converters. An energy storage device is also connected to the DC grid via a controller to store excessive power when demand is less and provide power when demand is more.

II. SOLAR PV ARRAY MODELING

Solar cells convert light into electricity. Some materials exhibit a property known as the photoelectric effect that causes them to

absorb photons of light and release electrons. The electrons flow through the external circuit to produce electricity. Power generation from solar energy using Photovoltaic (PV) has emerged in last decades since it has many advantages and less maintenance, no wear and tear. The main applications of PV systems are in either stand-alone systems such as water pumping, domestic and street lighting, electric vehicles, military and space applications or grid-connected configurations like hybrid systems and power plants.

The equivalent circuit for a PV cell is shown in the figure. It consists of a current source, a diode, shunt resistance R_{sh} and series resistance R_s . [8], [2] and [1].

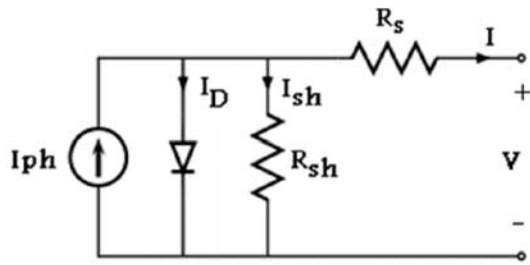


Fig1: Equivalent model of a solar cell

Each solar cell behaves as a p-n diode. When sunlight strikes a solar cell, the incident light energy is converted directly into electrical energy without any mechanical effort. For simplicity, a single diode model is used in this paper. I_{ph} represents the cell photocurrent.[1] and [8].

Nomenclature

V_{PV} – Output voltage of a PV module (V)

I_{PV} – Output current of a PV module (A)

T_R – Reference temperature=298 K

T – Module operating temperature

I_{ph} - light generated current in a PV module (A)

I_o - PV module saturation current (A)

$A = B$ is an ideality factor = 1.6

k - Boltzmann constant = 1.3805×10^{-23} J/K

q - Electron charge = 1.6×10^{-19} C

R_s is the series resistance of a PV module

I_{SCr} is the PV module short-circuit current at 25°C , 1000W/m^2

K_i - short-circuit current temperature co-efficient at $I_{SCr} = 0.0017\text{A}/^\circ\text{C}$

λ -PV module illumination (W/m²) = 1000W/m^2

E_{go} - Band gap for silicon = 1.1 eV

Number of cells per module=60 s

N_s - Number of cells connected in series

N_p - Number of cells connected in parallel

Photocurrent: The module photocurrent I_{ph} of the photovoltaic module depends linearly on the solar irradiation and is also influenced by the temperature according to the following equation-

$$I_{ph} = [I_{sr} + k_i(T - 298)] * \frac{\lambda}{1000} \quad (1)$$

Module reverse saturation current – I_{rs} :

$$I_{rs} = I_{rs} / [\exp(qv_{oc}/N_s K A T) - 1] \quad (2)$$

The module saturation current I_o varies with the cell temperature, is given by

$$I_o = I_{rs} [T/T_r]^3 \exp [q * E_{go} / B_k \{1/T_r - 1/T_r\}]$$

The output current of a PV module is given by –

$$I_{pv} = N_p * I_{ph} - N_p * I_o \left[\frac{\exp \{q * (v_{pv} + I_{pv} R_s) / N_s A K T\}}{N_s A K T} \right] \quad (4)$$

Module reverse saturation current – I_{rs} :

$$I_{rs} = I_{scr} / \exp(qv_{oc}/N_s K A T) - 1 \quad (5)$$

The module saturation current I_o varies with the cell temperature, is given by

$$I_o = I_{rs} [T/T_r]^3 \exp [q * E_{go} / B_k \{1/T_r - 1/T_r\}] \quad (6)$$

The output current of a PV module is given by –

$$I_{pv} = N_p * I_{ph} - N_p * I_o \left[\frac{\exp \{q * (v_{pv} + I_{pv} R_s) / N_s A K T\}}{N_s A K T} \right] \quad (8)$$

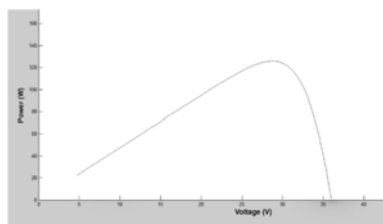


Fig2: P-V curve

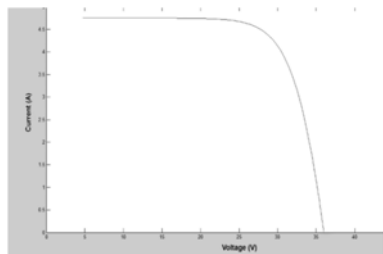


Fig3: V-I curve

III. BOOST CONVERTER

The PV modules are always used with DC-DC converters to obtain the maximum power point operation. [1] and [8]. For battery charging applications buck-boost configuration is preferred. Boost converters are used for grid-connected applications to step up the low module voltage to higher load voltages. Hence, DC-DC boost converter is used for the design of MPPT controller. Typical Boost converter configuration is shown in figure. It consists of a DC input voltage source V_s , boost inductor L , controlled switch S , diode D , filter capacitor C , and load resistance R . If the switch operates with a duty ratio D , the DC voltage gain of the boost converter is given by

$$M_v = V_o / V_s \quad (9)$$

Where V_s is input voltage, V_o is output voltage, and D is the Duty cycle of the pulse width modulation (PWM) signal used to control the MOSFET ON and OFF states.[8]

Inductance value is given by the equation

$$L = (1-D)^2 DR / 2f \quad (10)$$

The minimum value of the filter capacitance that results in the ripple voltage V_C is given by

$$C_{min} = DV_o / V_r Rf \quad (11)$$

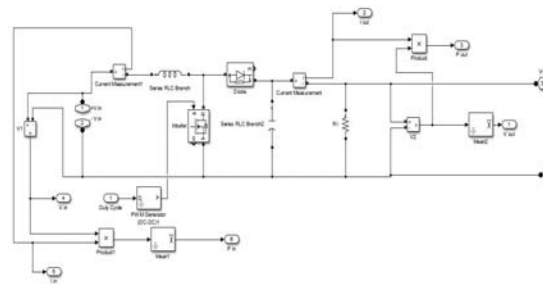


Fig4: Boost Converter SIMULINK model

IV. FUEL CELL MODELING

Proton Exchange Membrane Fuel cell (PEMFC) is used in this simulation. PEMFC is widely used as DG for solving the problem of clean power requirement.[7], [9] and [10]

A. Steady State model

The cell voltage of a PEMFC can be represented by the equation

$$V = E - V_{act} - V_{ohm} - V_{con} \quad (12)$$

Where V_{act} , V_{ohm} and V_{con} are in the form of voltage drop

(better for representing losses). The cell voltage equations can also be written as

$$V = E + \eta_{act} + \eta_{ohm} + \eta_{con} \quad (13)$$

Where η , η and η are in the form of voltage gain

So we have

$$\eta_{act} = -V_{act}, \eta_{ohm} = -V_{ohm}, \eta_{con} = -V_{con} \quad (14)$$

The open circuit voltage in equation (12) can be expressed by Nernst potential:

$$E = 1.229 - 8.5 * 10^{-4} (T - 298.15) + 4.308 * 10^{-5} T + 0.5 \ln p_{O_2} \quad (15)$$

The losses in equation (10) can be expressed as referred in [7],[9] and [10].

Activation loss:

$$-V_{act} = -0.9514 + 3.12 * 10^{-3} T - 1.87 * 10^{-4} T \ln i + 7.4 * 10^{-5} c_{O_2} \quad (16)$$

Ohmic loss:

$$-V_{ohm} = -i - R_{int} \quad (17)$$

Where R_{int} is the internal resistance which can be expressed by

$$R_{int} = 1.605 * 10^{-2} - 3.5 * 10^{-5} T + 8 * 10^{-5} i \quad (18)$$

Concentration loss:

$$-V_{con} = B \ln(1 - i / i_{lim}) \quad (19)$$

Here T is cell temperature in Kelvin, i_{lim} is current and the limit current.

The output voltage of a single PEM fuel cell will be in the order of 0.7 to 0.9V. TO obtain high voltages, cells are connected in series to form arrays.

Parameters used in simulation are shown in the TABLE 1

TABLE 1
Model parameters of PEMFC

Parameters	Values
Number of cells	50
Fuel cell resistance	0.76218 ohms
Nernst voltage of one cell (E_n)	1.2037V
Operating temperature	55
Nominal power	2496W
Nominal stack efficiency	46%

V. BATTERY MODEL AND CHARGE CONTROLLER

“Batteries are one of the most cost-effective energy storage technologies available, with energy stored electrochemically. A battery system is made up of a set of low-voltage/power battery modules connected in parallel and series to achieve a desired electrical characteristic. Batteries are “charged” when they undergo an internal chemical reaction under a potential applied to the terminals. They deliver the absorbed energy, or “discharge,” when they reverse the chemical reaction. Advantages of using batteries for storage applications include: high energy density, high energy capability, cycling capability, life span, and initial cost.”[8]

Battery model is directly available from MATLAB SIMULINK library. Battery type used is Lead acid battery. Lead acid batteries are cheaper than lithium ion batteries and have better tolerance to voltage fluctuations. A battery bank is used in a DC Micro grid to store excessive power during low demand times and to supply power during peak load times. The battery banks are to be designed to supply the load for a day or two even when there is no power generation from the RES in

the case of any natural calamities. Battery banks play an important role in improving the reliability of the entire power system.

TABLE 2

Model parameters of Battery

Parameters	Values
Nominal Voltage (V)	230
Rated Capacity (Ah)	500
Initial State Of Charge	100
Fully Charged Voltage (V)	250.4275
Nominal Discharge Current (A)	100
Internal Resistance (ohms)	0.0046

A charge controller is modeled using MATLAB and is used to protect the battery from over charging. It also helps to improve the life span of the battery. Based on the State Of Charge (SOC) of the battery, charging and discharging of the battery is controlled by switching process.

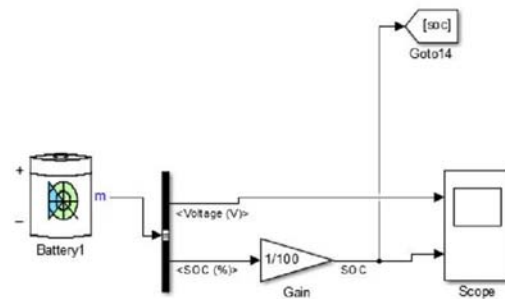


Fig5: Battery model in SIMULINK

VI. MAIN CONTROLLER

A Main Controller is designed in MATLAB SIMULINK to control the operation of the two RES (Solar PV array and PEMFC array) to meet the load requirements in the most reliable manner [3] and [4]. Total power generated is given by:

$$P_{Total} = P_{Solar} + P_{Fc} + P_{Bat}$$

The controller always keeps track of the solar power generated and the load demand. If the load is less than that of the power generated by the Solar PV array, the load is supplied by Solar

alone. Any excessive power is stored in Battery Banks.

$$P_{Load} = P_{Solar}$$

If Load exceeds the generation of solar power, Fuel cell is turned on to meet the excessive load demand.

$$P_{Load} = P_{Solar} + P_{Fc}$$

Any excessive energy is stored in the Battery banks depending on the SOC of the Battery banks.

When the load increases even more, the battery banks can supply the load within its capacity limit.

$$P_{Load} = P_{Solar} + P_{Fc} + P_{Bat}$$

During night time, when solar power is not available, the load is driven by fuel cell power and battery bank power. During any natural calamities, battery bank supplies the entire power to the load.

VII. INTERCONNECTION

The output from Solar PV array and PEMFC array are connected to DC-DC Boost converters and then to a DC grid. From the DC grid, the Main controller supplies it to the load based on demand and switches the input power sources based on the demand. Energy storage system is integrated with the DC Micro Grid to supply power during low generation periods as well as to store excess energy.

VIII. SIMULATION RESULTS

The Solar PV Array is designed to have 2.7KW capacity and Fuel cell array is designed to have 2.2KW capacity. The battery storage is of 230V with 500Ah capacity. When load is less than solar power, solar PV array supplies the load. When load is more than that of PV array, Fuel cell also takes up the load. Any excessive energy is stored in battery. When solar is not available, Fuel cell and battery supplies the load. When both the RES are not available, the battery supplies the load as it is designed to have a backup capacity for two days.

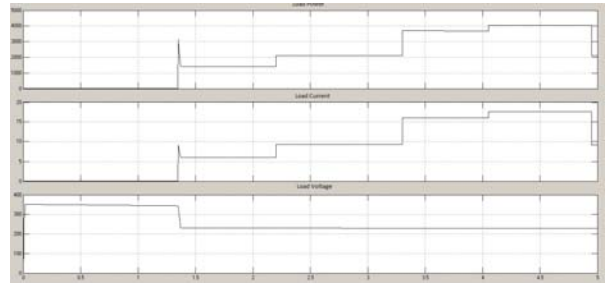


Fig6: Load voltage, load power.

IX. OVERALL SYSTEM MODEL AND SIMULINK BLOCKS

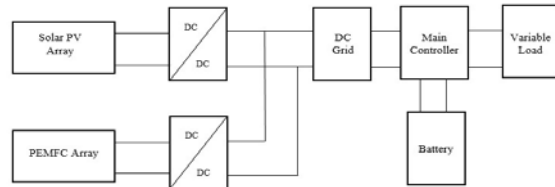


Fig-7 Overall system model of DC Micro grid with RES

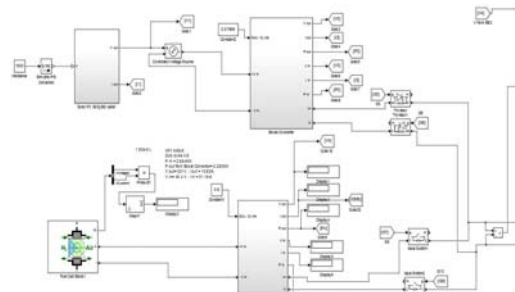


Fig8: Solar PV Array and PEMFC SIMULINK model with Boost converters connected to a DC bus

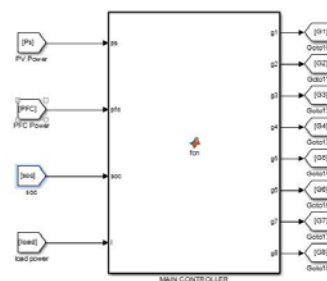


Fig9: Main Controller for Power Flow Control

X. CONCLUSION

Since the Renewable Energy Sources are highly varying in nature, the reliability of the system using only one RES as power source is very low. This paper deals with the simulation of a DC Micro grid for critical applications like military communications, in hospitals to provide continuous power supply at all costs. Battery

energy storage system is also used to store any excess energy and supply power during peak loads.

REFERENCES:

[1] Caisheng Wang, "Modelling and Control of Hybrid Wind/Photovoltaic/Fuel cell Distributed Generation Systems." July 2006. Montana State University, Bozeman, Montana.

[2] Manuela Sechilariu, Baochao Wang and Fabrice Locment, "Building Integrated Photovoltaic System with Energy Storage and Smart Grid Communication" IEEE Transactions on Industrial Electronics, vol.60, no.4, April 2013.

[3] Y. Jaganmohan Reddy, Y. V. Pavan Kumar, K. Padma Raju, and Anilkumar Ramsesh, "Retrofitted Hybrid Power System Design With Renewable Energy Sources for Buildings" IEEE Transactions on Smart Grid, vol. 3, no. 4, December 2012.

[4] Caisheng Wang, M. Hashem Nehrir, "Power Management of a Stand Alone Wind/ Photovoltaic/ Fuel cell Energy system, IEEE Transactions on Energy Conversion, vol. 23, no. 3, September 2008.

[5] Paulo F Rebeiro ,Brian K Johnson, Mariesa L Crow, Aysen Arsoy and Yilu Lui "Energy Storage Systems For Advanced Power Applications" Proceedings of the IEEE, vol. 89, no. 12, December 2001.

[6] Mesut E Baran, Hossein Hooshyar, Zhan Shen and Alex Huang, "Accommodating High PV Penetration on Distribution Feeders" IEEE Transactions on Smart Grid, vol. 3, no. 4, June 2012.

[7] Caisheng Wang, M. Hashem Nehrir, and Steven R. Shaw, "Dynamic Models and Model Validation for PEM Fuel Cells Using Electrical Circuits" IEEE Transactions on Energy Conversion, vol.20, no.2 June 2005.

[8] Natarajan Pandiarajan, Ramabadrana Ramaprabha and Ranganath Muthu

"Application of Circuit Model for Photovoltaic Energy Conversion System "International Journal of Photo Energy, vol.2012, article ID

[9] J. M. Correa, F. A. Farret, L. N. Canha, M. G. Simoes "An electrochemical- based fuel-cell model suitable for electrical engineering automation approach". IEEE Transactions on Industrial Electronics 2004, 51 (5), 1103-1112.

[10] Yancheng Xiao, Kodjo Agbossou, "Interface Design and Software Development for PEM Fuel Cell Modelling based on Matlab/Simulink Environment" World Congress on Software Engineering.



CONTROL OF A FOUR LEG INVERTER FOR UNBALANCED POWER NETWORKS

¹Jofey Simon,

¹MTPS,CUFE,Bangalore,India

Email: ¹jofey000@gmail.com

Abstract—The operations of three-phase, four-leg inverter under unbalanced load conditions, have to be controlled. The inverter is proposed for hybrid power system applications, in order to provide simultaneous supply of three-phase and single-phase ac loads with balanced voltage and constant frequency. An outer voltage regulation loop is used to provide current reference to the inner current control loop to regulate the inverter current using PI regulators. A control strategy for the four-leg inverter based on the decomposition of the supply voltages and currents into instantaneous positive, negative and homo-polar sequence components using phasor representation is described, to ensure balanced voltage. The three sequences are controlled independently in their own reference frames as dc signals, so that the disturbance of the output voltage due to the load unbalances is eliminated. Aim is to develop a Psim model for the inverter control during unbalanced voltage conditions.

Keywords— Four leg inverter; Hybrid power system; Current Control.

I. INTRODUCTION

In recent years there is growing interest in four leg converters for three-phase four-wire applications [1][2], such as controlled rectifiers, active power filters and many others applications that require neutral current control. One of the most promising

applications of this topology is the Hybrid Power Systems (HPS). An HPS (Figure 1) can be generally defined as an electricity production and distribution system which consists of a combination of two or more types of electricity generating sources (e.g. wind turbine generators, solar photovoltaic panels, picohydro plant, diesel generators...). An HPS usually also includes an energy storage system. In such a system the different power generators interconnected with the AC load in an isolated grid can be subject of unbalanced voltages. Unbalanced utility grid voltages which is one of the most common utility voltage quality problem in this kind of system, may arise due to the simultaneous supply of three-phase and single-phase loads, a short-circuit or a starting up of a large induction machine. Such an unbalance in voltage at the point of common coupling can cause increased losses in motor loads and abnormal operation of sensitive electronic and electrical equipment. For low voltage distribution, when the HPS has a four wire configuration to supply both single-phase and three-phase loads, a 0-sequence current flows through the neutral conductor.

A major drawback in such HPS is voltage unbalance. Unbalanced loading conditions can occur in HPS for a variety of reasons. In general, small loads (relative to the power range of the system) are configured to draw power from only one phase. When several single-phase loads are placed on a distribution system, the fluctuating power required from each of these loads can cause unbalance in the power system. Even for

dedicated three-phase motor drives, a significant (up to several percents) unbalance in the phase impedances can exist.

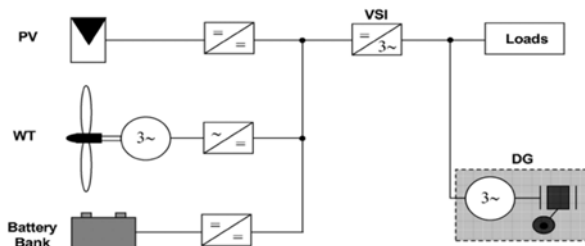


Fig. 1: HPS application with VSI

Today, most inverters are designed for balanced three-phase loads and consequently the associated control strategies are quite effective for three-phase, three-wire systems but are not able to manage loads that require a fourth (neutral) connection.

In three-phase applications with three-leg inverters, if the load requires a neutral point connection, a simple approach is to use two capacitors to split the dc link and tie the neutral point to the midpoint of the two capacitors. In this case, unbalanced loads will cause neutral currents that flow through the fourth wire between the load neutral point and the midpoint, distorting the symmetrical output voltage. Another drawback of this inverter topology is the need for excessively large dc-link capacitors [3].

Another possibility to provide a neutral connection for three-phase, four-wire systems is to use a four-leg inverter. This topology involves an additional leg, expanding the control capabilities of the inverter using the same dc-link capacitor and voltage. The fourth leg provides a path for the neutral current when the load is unbalanced.

This paper proposes fully digital voltage and current controllers for a four-leg inverter allowing simultaneous balanced voltage supply of three-phase and single-phase ac loads in an HPS application. The controllers are implemented in two different reference frames rotating at fundamental frequency after the link.

decomposition of the inverter ac voltage and current into positive, negative, and homopolar sequence components.

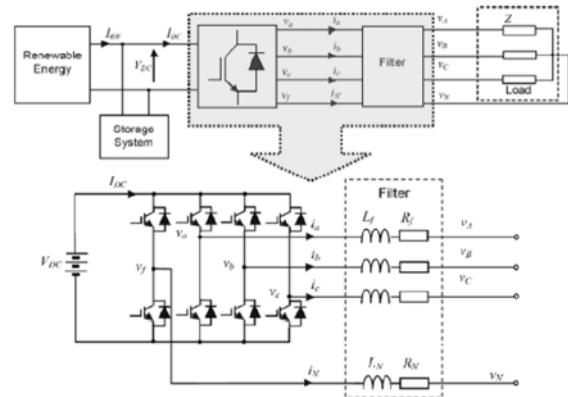


Fig. 2. Three-phase, four-leg inverter.

II. MODEL OF THE FOUR-LEG INVERTER UNDER UNBALANCED OPERATING CONDITIONS

The four-leg inverter in an HPS environment is described in Fig.2. As mentioned in Section I, its topology is characterized by the connection of the neutral point of the load to the midpoint of the fourth leg of the inverter. Due to load unbalances, an intruding current flows through the fourth wire between the load neutral point and the midpoint of the fourth leg of the inverter, and a voltage drop occurs, distorting the symmetrical output voltage. The three phases of the converter are independent of each other and the current flowing through each leg depends only on the position of the associated switches and its phase voltage.

Because studying the switches is not part of this study, the averaging technique [4] has been used to model the four-leg inverter. Assuming the switching frequency is much higher than the fundamental frequency of the ac signals, so that all voltage and current ripples due to the switches are negligible, the average inverter model can be obtained from the switching model. The dc-link voltage V_{dc} is kept at a constant value by controlling the energy flow from the storage system to the dc

Consequently, the line-to-neutral three-phase output voltages V_{af} , V_{bf} , and V_{cf} for the three-phase, four-leg inverter can be expressed as the product of the dc-link voltage and the duty ratios d_{af} , d_{bf} , and d_{cf} .

The equations describing the behavior of the inverter voltages and currents under balanced and unbalanced conditions are expressed as follows:

$$\begin{bmatrix} v_{AN} \\ v_{BN} \\ v_{CN} \end{bmatrix} = -V_{dc} \begin{bmatrix} d_{af} \\ d_{bf} \\ d_{cf} \end{bmatrix} + R_f \begin{bmatrix} i_a \\ i_b \\ i_c \end{bmatrix} + L_f \frac{d}{dt} \begin{bmatrix} i_a \\ i_b \\ i_c \end{bmatrix} \\ - R_N \begin{bmatrix} i_N \\ i_N \\ i_N \end{bmatrix} - L_N \frac{d}{dt} \begin{bmatrix} i_N \\ i_N \\ i_N \end{bmatrix} \\ i_a + i_b + i_c + i_N = 0$$

where R_f and R_N , and L_f and L_N are the resistances and the inductances of the inverter filter, V_{AN} , V_{BN} , and V_{CN} are the line-to-neutral filter output voltages, i_a , i_b , and i_c are the three-phase inverter output currents, and i_N is the neutral current.

III. DECOMPOSITION INTO SYMMETRICAL COMPONENTS

In terms of control loop design, the conventional control strategy of the four-leg inverter uses voltage and current dq0-components. If the load is balanced, the d- and q-components are DC quantities and the 0-component is zero. If the load is unbalanced both d- and q-components contain an additional AC quantity, which oscillates with the double frequency of the output voltage. The 0-component is not zero and oscillates with the same frequency as the output voltage. To solve this problem the proposed control strategy uses the symmetrical components of the output voltage and current decomposed into dq DC quantities. According to the Fortescue theorem, three-phase variables can be symmetrically decomposed into positive, negative and homopolar sequence components. Therefore, the inverter output voltages can be expressed as:

$$\begin{bmatrix} \bar{v}_{AN} \\ \bar{v}_{BN} \\ \bar{v}_{CN} \end{bmatrix} = \begin{bmatrix} \bar{v}_{AN,p} + \bar{v}_{AN,n} + \bar{v}_{AN,h} \\ \bar{v}_{BN,p} + \bar{v}_{BN,n} + \bar{v}_{BN,h} \\ \bar{v}_{CN,p} + \bar{v}_{CN,n} + \bar{v}_{CN,h} \end{bmatrix}$$

where ($V_{AN,p}$, $V_{BN,p}$, $V_{CN,p}$) is the positive-sequence voltage, ($V_{AN,n}$, $V_{BN,n}$, $V_{CN,n}$) is the negative-sequence voltage and ($V_{AN,h}$, $V_{BN,h}$, $V_{CN,h}$) is the homopolar sequence voltage.

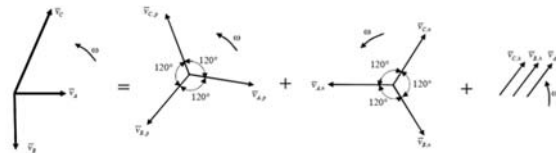


Fig. 3: Decomposition of a three-phase unbalanced system in three balanced systems

The transformation of the ABC signals into symmetrical components can be expressed by the following compact form:

$$[\bar{x}_{i,p}] = [F_p] \cdot [\bar{x}_i]$$

$$[\bar{x}_{i,n}] = [F_n] \cdot [\bar{x}_i]$$

$$[\bar{x}_{i,h}] = [F_h] \cdot [\bar{x}_i]$$

where x can be voltage or current, \bar{x} denotes the phasor of x , and $i = A, B, C$. The transformation matrices F_p , F_n , and F_h have the following expressions:

$$[F_p] = \frac{1}{3} \begin{bmatrix} 1 & a & a^2 \\ a^2 & 1 & a \\ a & a^2 & 1 \end{bmatrix}$$

$$[F_n] = \frac{1}{3} \begin{bmatrix} 1 & a^2 & a \\ a & 1 & a^2 \\ a^2 & a & 1 \end{bmatrix}$$

$$[F_h] = \frac{1}{3} \begin{bmatrix} 1 & 1 & 1 \\ 1 & 1 & 1 \\ 1 & 1 & 1 \end{bmatrix}$$

where $a = ej2\pi/3$.

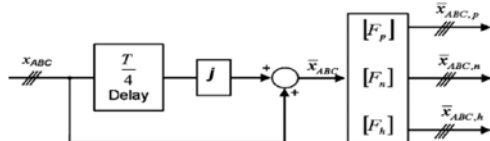
Let us consider X_{ABC} the three-phase (balanced or unbalanced) sensed voltage or

current in the output filter of the investigated four-leg inverter.

The mathematical expression of this signal is:

$$x_{ABC} = x_{ABC \max} \cos(\omega t + \varphi_{ABC})$$

For the proposed control strategy, a simple way to obtain the symmetrical components of the supply voltage and current is presented in Fig. 5.



This method implies delaying the measured voltage and current X_{ABC} by one-fourth of the period at the fundamental frequency ($T = 1/f$, $f = 50$ Hz). The addition of the measured voltage and the same signal delayed by one-fourth of the period and multiplied by the complex operator j ($j = \sqrt{-1}$) gives the phasor representation \bar{X}_{ABC} . Using this representation and the transformation matrix (F_p , F_n , and F_h), the positive, negative, and homopolar sequence components are obtained. Fig. 6 shows the real part of the three-phase system (X_{ABC}) decomposition into symmetrical components and the effect of the delay when applying the method proposed earlier. Until 0.04 s, the three-phase system is balanced and becomes unbalanced after this moment. For the inverse transformation, it is sufficient to add phase-by-phase the real part of the positive, the negative, and the homopolar sequences in order to regain the original sensed signal.

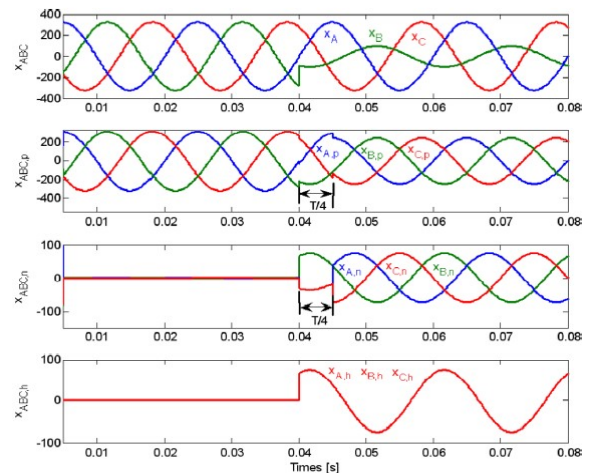


Fig. 4. Three-phase system decomposition into symmetrical components.

From Fig. 4, the following conclusions can be drawn.

- 1) Starting with three real variables, X_A , X_B , and X_C , after transformation, we obtain three new sets of three real variables: $X_{ABC,p}$, $X_{ABC,n}$, and $X_{ABC,h}$ (positive, negative, and homopolar sequence components).
- 2) The three sequence components are completely independent of each other, from the amplitude point of view.
- 3) The three sequence components turn at the same speed and in the same direction. Only the negative system has reversed phase sequence.
- 4) The negative and the homopolar sequences appear only when the original three-phase system is unbalanced.
- 5) The homopolar sequence components are superposed.

Because the symmetrical components are always balanced, the voltage and current regulation is performed in a dq synchronous reference frame rotating at the fundamental frequency.

Thus, using a positive reference frame, which rotates counterclockwise, the positive sequence dq voltages and currents appear as dc signals. In contrast, the dc quantities of the negative sequence dq voltages and currents are obtained using a negative reference frame, which rotates clockwise. The homopolar sequence voltage or current appears as a disturbance in the θ -variable at the fundamental angular frequency ω in any rotating system reference frame (positive or negative), while d and q components are inexistent. Thus, it is not possible to rotate the θ -variable voltage in order to transform it into a dc signal and to facilitate its regulation. As shown in Fig. 4, the vectors of the homopolar sequence system are in phase and equal in amplitude. They are also independent, from the point of view of the amplitude, with regard to the positive- and negative-sequence systems. Thus, it is possible to apply a spatial rotation of 120° and 240° to the homopolar phasors B and C and the transformation matrix F_h becomes

$$[F_h^*] = \frac{1}{3} \begin{bmatrix} 1 & 1 & 1 \\ a & a & a \\ a^2 & a^2 & a^2 \end{bmatrix}.$$

The obtained three-phase balanced voltage system is transformed in dc dq signals using the rotating negative reference frame. Once transformed in dc signals, the homopolar sequence can be easily regulated by PI controllers. This technique, which allows obtaining dc signals, and thus, a good regulation of the homopolar sequence voltage and current, is possible because the applied transformations do not affect the amplitude of the processed signals. The complete transformation of the measured signals (voltage and currents). As it can be seen, only the real part of the phasor representation is used to obtain dc signals.

IV. VOLTAGE AND CURRENT REGULATION

The voltage and current signals obtained after decomposition into symmetrical components are

regulated using an inner current loop controller and an outer voltage loop controller. Both loops are disposed in three-channel arrangement (Figure 5). The first channel allows controlling the positive sequence of the current and voltage, the second is for the negative sequence and the third is for the homopolar sequence.

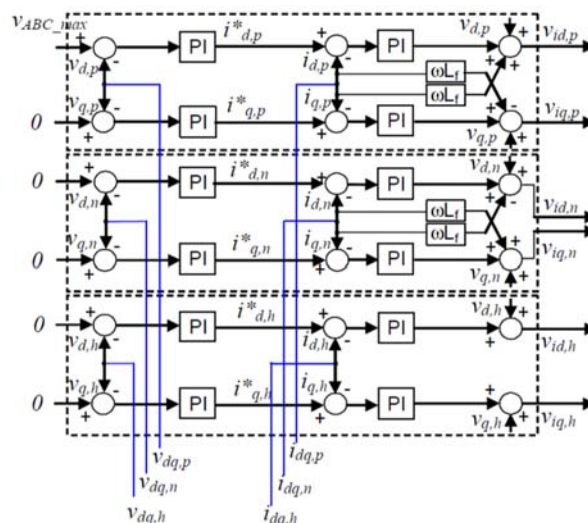


Fig. 5: Voltage and current regulation loops

In the inner current loop, the positive-sequence current ($i_{d,p}$, $i_{q,p}$ in the first channel of the control structure presented in Fig. 8) is regulated in the positive reference frame. The terms $\omega L_f i_{q,p}$, $-\omega L_f i_{d,p}$ are inserted to decouple dq axes dynamics. The negative-sequence current ($i_{d,n}$, $i_{q,n}$) in the second channel of the control structure is controlled in the negative rotating reference frame. The homopolar-sequence current ($i_{d,h}$, $i_{q,h}$) in the third channel of the control structure is controlled in the negative rotating reference frame. The outer voltage loops give the reference currents $\{i^*_{d,p}, i^*_{q,p}, i^*_{d,n}, i^*_{q,n}, i^*_{d,h}, i^*_{q,h}\}$ in order to keep the measured voltages at constant values. The positive-sequence voltage $v_{d,p}$ is compared with the desired output voltage amplitude and the error is processed in a PI controller. All the remaining sequence voltages are kept at zero value using the same procedure. These voltage set-points correspond to a balanced three-phase AC voltage. The control

signals to be applied to the inverter are obtained using the inverse Park and

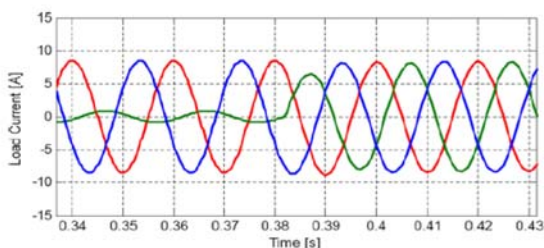


Fig. 6. Simulation result of the load current.

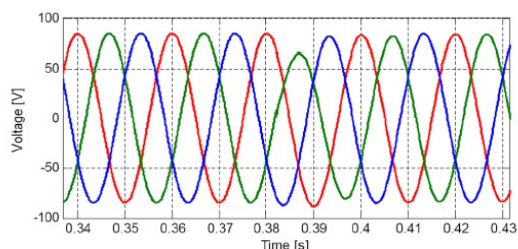


Fig. 7. Simulation result of the load voltage

V. OUTLOOK AND CONCLUSIONS

The issues in the modeling and control of four leg inverter were investigated. The ability of a four leg inverter in dealing with unbalanced and non-linear loads was presented. It was established that in order to deal with unbalanced load, the loop gain must have sufficient gain at 2ω where ω is the fundamental output frequency.

Operation of a four-leg inverter under unbalanced load conditions for HPS applications has been investigated. The four-leg inverter is controlled using an innovative

Clarke transformations with the addition of the symmetrical components. The addition is carried out phase by phase, using only one phase from the homopolar sequence

control strategy based on the decomposition of the supply three-phase voltage and current into instantaneous positive, negative, and homopolar sequence components using phasor representation. The proposed control strategy has the ability to decompose into dq dc quantities not only the positive and negative current and voltage sequences, but also the homopolar sequence. Consequently, regulation has been easily done with classical PI controllers.

REFERENCES

- [1] Ryan M.J., De Doncker R.W., Lorenz R.D. "Decoupled control of a 4-leg inverter via a new 4×4 transformation matrix" (IEEE, Transaction on Power Electronics, 2001, Volume 16, No. 5.)
- [2] Benhabib M.C., Saadate S. "New Control Approach for Four-Wire Active Power Filter Based on the Use of Synchronous Reference Frame", Electric Power Systems Research March, 2005, Volume 73, Issue 3, pp. 353-362
- [3] S. El-Barbari and W. Hofmann: "Digital control of four-leg inverter for standalone photovoltaic systems with unbalanced load," in Proc. 26th Annu. Conf. IEEE Ind. Electron. Soc. 2000 (IEcon), Oct., vol. 1, pp. 729-734.
- [4] J. Sun and H. Grotstollen, "Averaged modelling of switching power converters," in Proc. IEEE PESC, 1992, pp. 1166-1172.



SCREENING AND ANALYSIS OF RESPIRATORY SYSTEM USING CONTROLLER

¹Ms. Dipti P. Kulkarni , ²Prof. S. S. Patil

^{1,2}Department of Electronics and Telecommunication, Rajarambapu Institute of Technology, Islampur, Sangli Shivaji University, Kolhapur. Maharashtra, India
Email: ¹kulkarnidipti9@gmail.com, ²shaila.nalawade@ritindia.edu

Abstract— Asthma is a chronic disease related with respiratory system. So screening of asthma will help patient to monitor their level of asthma and from the analysis guideline is provided to control their asthma level. In this system, Peak flow meter is used for acquisition of breathing signal. Microcontroller is used for a decision making according to reading from peak flow meter. A graphical user interface is provided. In this way a self management system is designed for asthmatic patient. So the system is very efficient for patient as they can monitor their asthma level at their residential place. People in villages having their financial problem then for them the system can be installed to their central clinic which can help them to diagnose their asthma at local place.

Keywords— Screening, Peak flow meter, Peak expiratory flow

I. INTRODUCTION

Asthma is a chronic inflammatory disease of airway characterized by airflow obstruction and bronchospasm. Common symptoms are wheezing, coughing, chest tightness, shortness of breath. According to world health organization (WHO) in the world around 300 million people suffer from asthma in that children are affected by the chronic diseases.

Asthma patients do not having much of facility to recover their problem. Many of them have some mechanical or digital devices but patient cannot operate that device or discover the problem. In all age group people want some help of other person to manage their asthma. Also for checking or some kind of fear in mind about the asthma they have to visit doctor many times in a week for their mental satisfaction.

In many cases at villages or in town only specialist doctors are having well equipped laboratory as well as instrument for detection of asthma. So it is difficult for the patient to travel for a long distance to have a proper action on their asthma. So there is a need to have such system which provides guidelines for patient to live fit.

So there is need of self management system for asthmatic patients which can help them to manage their asthma before it create some danger situation. Also the system can be beneficial for patient in both categories as in financial as well as in mental and physical health. Also the system is beneficial to the clinics which are in the villages as well as in town.

Nowadays in allover world wireless systems are famous for data mining as well as healthcare management. So the main aim of the project is to develop a system which can monitor the level of asthma of the patient and also guide them at their residential place. Also if some people in villages having their financial problem then for them the system can be

installed to their central clinic which help them to diagnose their asthma at local place.

II. LITERATURE ON RELATED WORKS

A. Kassem, M. Hamad, C. El-Moucary, E. Neghawi, G. Bou Jaoude, and C. Merhej [1] have explained android application for asthmatic patients so they can easily diagnose their asthma level. This application will allow doctors to follow their patients. It helps patient to live healthy and with less stress. Also due to graphical interface system is becoming user friendly. The system is low cost and easy to use for asthmatic patient. So it is useful for patient to control their asthma.

Jabłoński, G. Głomb, T. Guszowski, B. Kasprzak, J. Pękała, A. G. Polak, A. F. Stępień, Z. Świerczyński, and J. Mrocza [2] have presented pulmotel 2010 which include different data transfer module such as router, wire-telephone system, and cellular network. At home unit different medical sensors are used and data from those sensors are transferred through Bluetooth, modem, Ethernet. From that communication network via Internet data will be transferred to doctor.

Zhe Cao, Rong Zhu, *Member, IEEE*, and Rui-Yi Que [3] have explained system of microsensors nodes which are having Bluetooth connectivity. The sensors are used for measuring respiratory airflow, blood oxygen saturation and body posture. Mobile or PC is connected to internet for monitoring and diagnosis of COPD and asthma.

Ana Filipa Teixeira, Octavian Postolache [4] have developed web information system and wireless sensor network which are used for indoor and outdoor monitoring with application in asthma. Wireless sensor network consist of sensing nodes like temperature, humidity, carbon monoxide. The information can be accessed anywhere which allows the users to know elements about risk condition for their respiratory health.

O. Postolache, P. Girão, M. Dias Pereira G. Ferraria, N. Barroso, G. Postolache[5] have explained continuous monitoring of indoor temperature, humidity, gases which are responsible for pollution Bluetooth scattering sensor networking architecture is formed. By using this and smart phone the risk factor for the asthma is reduced. In this persons can send

sms in order to provide alert to health care provider.

Kelly L. Andrews, Sandra C. Jones, Judy Mullan [6] have developed self management system for asthma diseases is important because it reduce cost of the diagnosis as well as it gives mental stability. By the survey it is clear that self management system can reduce health problem regarding the asthma. This can help in developing health literacy. Self management programs for chronic conditions, such as asthma, have an important place in healthcare delivery.

Antoinette Bumatay, Remy Chan, Keith Lauher, Alice M. Kwan, Tod Stoltz, Jean-Pierre Delplanque, Nicholas J. Kenyon, Cristina E. Davis [7] have explained PFM (Peak flow meter) interfacing custom software interface to forward this stored data electronically. E-mail forwarding and “telemedicine” capabilities will give physicians a better way to monitor the patient’s PEF over time, leading to a more convenient method for physicians to make appropriate changes in patient medication regimens.

Vilas D. Ghonge, Vijay S.Gulhane, Nitin D.Shelokar [8] have described an ingenious system approach to the doctor to inform a complete health information control of a distant patient using real time system. The discussed system is a medical electronic informational platform for diagnostic use, which permits the doctor to carry out complete health information of remote patients in real time. The system consists of two parts: a patient station and a doctor station, both compact and light easily transportable both the positions are composed of committed laptop, hardware and software.

B O Adeniyi and G E Erhabor [9] have explained use of peak flow meter. A peak flow meter is a small hand-held device that measures how fast a person can blow air out of the lungs when there is forceful exhalation, after maximum inhalation. The peak flow meter helps to assess the airflow through the airways and thus help to determine the degree of obstruction along them. Peak flow meters are available in medical equipment and drug stores worldwide and can be acquired without prescription.

Surajit Bagchi, Dr. Madhurima Chattopadhyay [10] have presented cost effective on-line ventilation monitoring system for impaired

elderly persons using optical wireless sensory system. The analysis process is done by the distantly located physician. If physician is in sleep then the artificial decision making system is developed.

III. PROPOSED SYSTEM ARCHITECTURE

In this proposed system Peak flow meter is used to acquire breathing signal. Patient has to take 3 reading for the proper diagnosis of disease. Processing (Signal conditioning) on signal will be carried out. Standard data of normal person will be collected for comparison with patient data. Normal expected value depends on a person's sex, age, height etc. Program will be developed for microcontroller/processor for comparing. Microcontroller will be selected as per sampling rate and memory requirement. After comparison data will be transferred form the Wi-Fi device to computer/mobile. Computer/mobile will be used as a graphical user interface

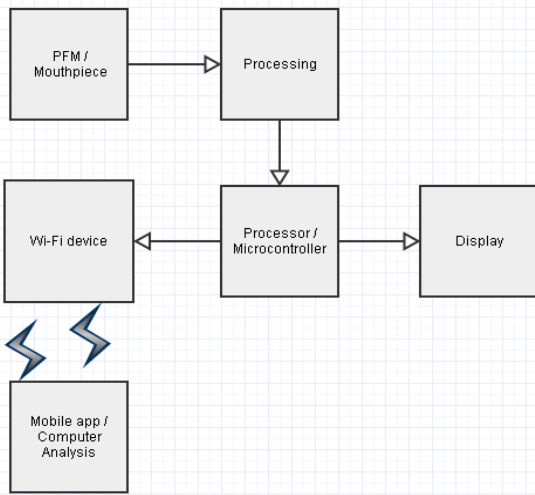


Fig. 1 Proposed system

IV. PROPOSED SYSTEM FLOWCHART

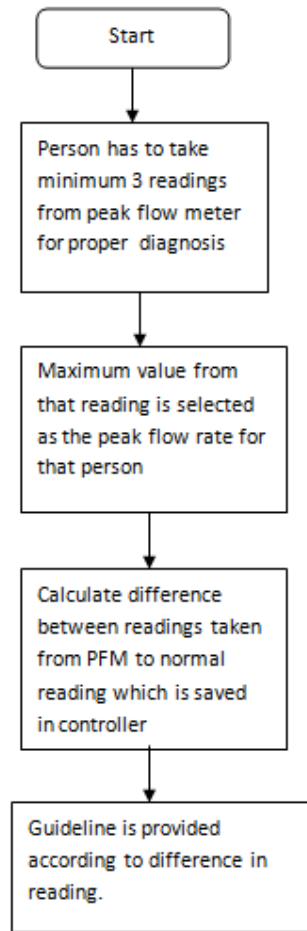


Fig.2 Flow chart

V. HARDWARE IMPLEMENTATION FOR PROPOSED SYSTEM

A. Peak flow meter

Peak flow meter is used to measure peak expiratory flow rate in the breathing signal. So peak flow rate is a maximum value occurred during one expiration. So Peak flow rate is proportional to maximum flow rate. So in this proposed system flow sensor is used to measure maximum flow rate.

Flow sensor used which gives constant 5v at output.



Fig.3 Flow sensor

B. *Microcontroller*

Microcontroller is used in this system to compare patient data which is taken from the peak flow meter to the standard data of normal person. Normal data is collected from patient's age, height, gender. Then comparison of that two data will take place with the help of microcontroller. Maximum value from 3 readings of patient is displayed on LCD 16X2. After comparison data will be wirelessly transferred to mobile/computer. Computer/mobile is used as a graphical user interface.



Fig. 4 Proposed system hardware

VI. RESULTS AND OBSERVATIONS

In the proposed system with the help of peak flow meter the minimum 3 readings of patient is carried out. From these readings comparison is made by controller. Maximum value from that 3 reading is displayed on the LCD.

A. Age = 8 years , Gender : male , Height = 4



Fig.5 Result1- Maximum flow rate = 175L/Min

B. Age = 34 Years, Gender = Male ,
Height= 5'3



Fig. 6 Result2- Maximum flow rate = 595L/Min

VII. CONCLUSION AND FUTURE WORK

From these readings it is clear that controller is display maximum reading from the 3 successive reading taken from patient and these peak expiratory flow rates are equal to the standard readings which are taken from patient's data that is height, weight, gender.

Currently we are working on wirelessly data transfer and graphical user interface.

VIII. REFERENCES

- [1] A. Kassem, M. Hamad, C. El-Mougary, E. Neghawi, G. Bou Jaoude, and C. Merhej, "Asthma care apps", 2ND international conference on advances in biomedical engineering, IEEE 2013, PP. 42 - 45
- [2] I. Jabłoński, G. Głomb, T. Guszowski, B. Kasprzak, J. Pękala, A. G. Polak, A. F. Stępień, Z. Świerczyński, and J. Mroczka,, "Internal Validation of a Telemedical System for Monitoring Patients with Chronic Respiratory Diseases", 32nd Annual International Conference of the IEEE EMBS Buenos Aires, Argentina, August 31 - September 4, 2010, PP.2172 - 2175
- [3] Zhe Cao, Rong Zhu,, Member, IEEE, and Rui-Yi Que "A Wireless Portable System With Microsensors for Monitoring Respiratory Diseases", IEEE Transactions On Biomedical Engineering, Vol. 59, No. 11, November 2012, PP.3110 - 3116
- [4] Ana Filipa Teixeira, Octavian Postolache, "Wireless Sensor Network and Web based Information System for Asthma Trigger Factors Monitoring", IEEE 2014, PP.1388 - 1393

- [5] O. Postolache, P. Girão, M. Dias Pereira, G. Ferraria, N. Barroso, G. Postolache, “*Indoor Monitoring of Respiratory Distress Triggering Factors Using a Wireless Sensing Network and a Smart Phone*”, International Instrumentation and Measurement Technology Conference Singapore, IEEE 5-7 May 2009, PP.451 - 456
- [6] Kelly L. Andrews, Sandra C. Jones, Judy Mullan [6], “*Asthma self management in adults: A review of current literature*”, ELSEVIER journal, Volume 21, Issue 1, March 2014, PP.33-41
- [7] Antoinette Bumatay , Remy Chan , Keith Lauher , Alice M. Kwan, Tod Stoltz, Jean-Pierre Delplanque, Nicholas J. Kenyon, and Cristina E. Davis, Member, IEEE, “*Coupled Mobile Phone Platform With Peak Flow Meter Enables Real-Time Lung Function Assessment*”, IEEE Sensors Journal, Vol. 12, No. 3, March 2012, PP.685 - 691
- [8] Vilas D. Ghonge, Vijay S.Gulhane, Nitin D.Shelokar, “*A Real-time Ingenious System for Remote Health Assistance*”, International Journal of Application or Innovation in Engineering & Management (IJAIEM), Volume 2, Issue 3, March 2013, PP.350-355
- [9] B O Adeniyi and G E Erhabor, “*The peak flow meter and its use in clinical practice*”, Journal of Respiratory Medicine, March 2011, PP.5-8
- [10] Surajit Bagchi, Dr. Madhurima Chattopadhyay, “*Real-time monitoring of respiratory diseases of distantly located elderly impaired patients*”, IEEE 2012 Sixth International Conference on Sensing Technology (ICST), PP.146 – 150



FEATURE EXTRACTION OF MES (MYOELECTRIC SIGNAL TO DESIGN CALF STIMULATOR

¹Ms. Rutuja U.Bachche, ²Prof. R.T.Patil

^{1,2}Department of Electronics and Telecommunication, Rajarambapu Institute of Technology, Islampur, Sangli Shivaji University, Kolhapur. Maharashtra, India
Email: ¹rutuja.bachche27@gmail.com, ²ramesh.patil@ritindia.edu

Abstract— Bio-medical domain is the widely emerging technology from past recent years. In today's world many people have born with disability or have an accident and are unable to perform daily routine work. Mostly spinal cord and brain gets injured. Due to spinal cord injury person may suffer from paralysis of different parts of body. Stimulating the lower limb with electrodes can awaken the circuitry and gets functioning without instruction from brain. Taking into consideration these problems electric stimulator concept has been introduced to maintain and restore the movements. Fast method for feature extraction and design of stimulator is the main aim of the project. This paper will describe method of analyzing MES signal in Matlab tool and also design stimulator with the help of microcontroller using Proteus tool. Activation of the stimulator will be based on the extracted signal and setting the threshold value. The proposed stimulator is EMG-triggered stimulator and it helps to pass the current of 0-50Ma to do the ankle movement.

Keywords— Myoelectric signal, Feature extraction, Electrodes, Electric Stimulator.

I. INTRODUCTION

Bio-medical domain is the widely emerging technology from past recent years. During past years, a number of digital stimulator have been developed and successfully implemented. This

research work describes the methodology of collecting EMG signal and hardware and software approach to drive the stimulator. For designing the stimulator, firstly we have to collect the myoelectric signals. Biological signals are called EMG signals which are electrical signals produced by the activation of the muscles motor unit. EMG signals which are collected from the surface of body (calf muscle) are non-stationary, non-linear, complexity and have large variation. This nature creates difficulty in analyzing EMG signal. There are two techniques for data collection of EMG signal which includes surface method and intramuscular method. In these experiment we have used surface method for data collection. Common EMG signals strength can range from μV to few mV .

Noise is the major concern in analysis of EMG signal which affects on the accuracy of feature extraction. To achieve the movements we have to perform steps like EMG signal collection, feature extraction and movement variation. There are several methods for EMG feature extraction. In this work we have used time based temporal approach. Feature extraction is an important step in process of pattern recognition, especially if the pattern is represented by a temporal or spatial signal like acoustic, geodetic, electromyographic signal. Feature extraction method like FFT and Wavelet Transform are helpful to compare with temporal approach. From temporal approach, we have evaluated MES feature extraction using mean absolute value, average value, root mean square value, minimum voltage,

maximum voltage, integrated EMG, simple square integral.

Nowadays, the electric portable stimulators plays the important role in clinical studies. There are different types of stimulators that are used to restore the muscle activity in rehabilitation treatment of paralysed person like Transcutaneous Electric Nerve Stimulation(TENS),Functional Electrical Stimulation(FES),Galvanic Stimulation(GS), Electric Nerve Stimulation(ENS),etc.

The proposed system developed a electric calf stimulator.Electric stimulation means to influence the natural bio-electric process within the body,i.e.,creating action potentials that are conducted along the excitable cells.It uses el electric current to cause a single muscle or nerve or group of muscle/nerve to contract..Using this stimulator person can do ankle movement like dorsalflexion and plantarflexion so that they can walk and live independently.

II.LITERATURE ON RELATED WORKS

Nowadays, the electric portable stimulators plays the important role in clinical studies.There are different types of stimulators that are used to restore the muscle in rehabilitation treatment of paralysed person like Transcutaneous Electric Nerve Stimulation(TENS),Functional Electrical Stimulation (FES), Galvanic Stimulation(GS), Electric Nerve Stimulation(ENS),etc. .Recently clinical studies demonstrates the recovery of functionality of paralyzed portion that contributed by electrical stimulation of different nerves that generates missing function of upper limb due to spinal cord injury.A portable,programmable,battery operated stimulator is designed which can be used for stimulation of minor muscles defect as well as critical muscle defect[1]. Walking after partial paralysis assisted with EMG-triggered or switch-triggered functional electric stimulation.FES shows walking afters paralysis by activating the muscles of lower extremities[2].There are normally two non-parametric approaches in feature extraction.Feature extraction is important step in pattern recognition.Temporal and Spectral Approach are the two non-parametric

parameters for feature extraction of EMG signal [3]. The comparative study of multi-purpose Functional Electric Stimulation (FES) that is used to restore the mobility to spinal cord injury patients by applying low level current to the paralyzed muscle of the patients to function,activate and live independently[7].The

proposed stimulator has closed loop stimulation paradigm which is more suitable for various FES application that are used for both experimental and clinical studies which has high degree of flexibility but less power consumption[9]. There are different types of electrodes used in FES system but they prefer skin surface electrodes. Here, they defined an FES system as an application of suitable electric current to muscle fibres to restore the control function of body and proposed low cost FES System that has targeted person which suffered from hemiplegic stroke condition.The skin surface electrodes has been chosen due to its simplicity which can be easily available for clinical settings[10].

III. PROPOSED SYSTEM ARCHITECTURE

Myoelectric(EMG) signals are useful in intelligently recognizing intended limb motion of person.This proposed work is an attempt to develop multi-channel EMG signal acquisition system which can be used to control the stimulator. Electrical stimulator uses electric current of 0-50 mA to cause single nerve/muscle or group of muscles/nerves to contract and by contracting these muscles/nerves helps to strengthen the affected muscle. Following fig.1 shows the block diagram of my proposed work.

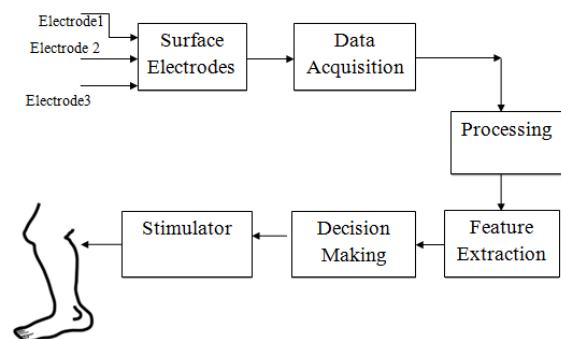


Fig.1 Block diagram of proposed work

In this proposed system, database of standard EMG signal has been collected from normal person according to the condition for comparison purpose. EMG signal has been acquired using NI DAQ 6009 Card with the help of surface and disk electrodes. Further processing of EMG signal is done to remove unwanted part using signal conditioning. Preprocessing on the acquired EMG signal will be carried out to extract the time domain features.

A. Hardware Approach-

It includes instrumentation amplifier, filter design, precision rectifier.

1. Instrumentation amplifier (INA118)- An instrumentation amplifier is a type of differential amplifier which includes very low DC offset, low drift, low noise very high open loop gain very high common mode rejection ratio and very high input impedance.

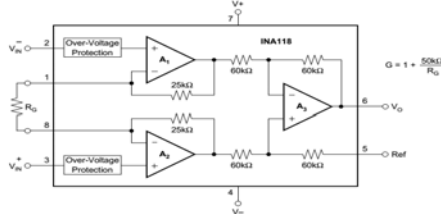


Fig.2 Design of Instrumentation amplifier

2. Design of filter-

a) High Pass Filter: The second order high pass filter circuit is shown in fig 3.

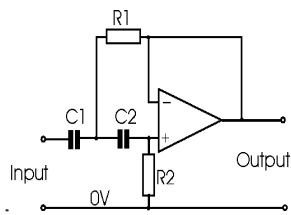


Fig.3 Operational amplifier two pole high pass filter

The calculations for the circuit values are very straightforward for the Butterworth response and unity gain scenario. The formula for cut-off frequency is $F_c = 0.707 / 2 \pi RC_2 = 50\text{Hz}$.

Where $R_1 = R_2 = 6.8\text{Kohm}$, $C_1 = 0.22\mu\text{F}$, $C_2 = 2C_1 = 0.44\mu\text{F}$

b) Low Pass Filter:

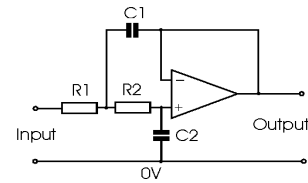


Fig.4 Operational amplifier two pole low pass filter

The formula for cut-off frequency is $F_c = 0.707 / 2 \pi RC_2 = 150\text{Hz}$ where, $R_1 = R_2 = 6.8\text{Kohm}$, $C_2 = 0.11\mu\text{F}$, $C_1 = 2C_2 = 0.22\mu\text{F}$.

Using the two-pole low-pass active filter and two-pole high pass active filter the second order Butterworth band pass filter is designed. The cut-off frequency for band pass filter is $f_{c1} 50\text{ Hz}$ and $f_{c2} 150\text{Hz}$.

c) Signal conditioning circuit:

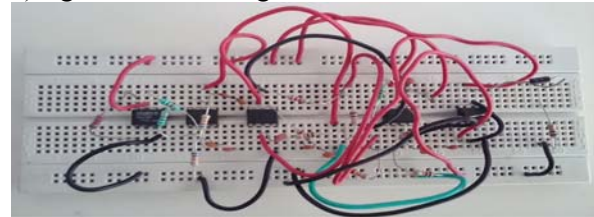


Fig.7 Total signal conditioning circuit

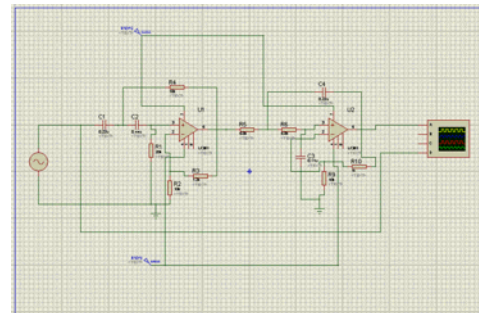


Fig.5 Design of Butterworth Band pass filter

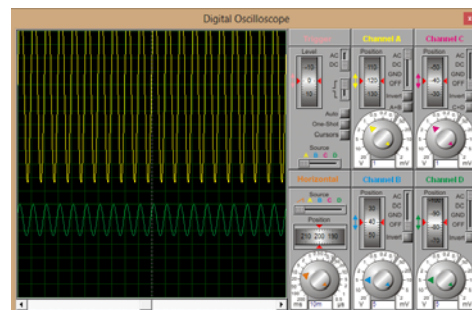


Fig.6 Filter simulation

B. Software Approach-

In proposed work,the signal acquired from the surface of body are to be processed for finding the time domain features like-

A] Mean Absolute Value (MAV): MAV is similar to IEMG that normally used as an onset index to detect the muscle activity. MAV is the average of the absolute value of EMG signal amplitude. MAV is a popular feature used in EMG leg movement recognition application.

$$MAV = \frac{1}{N} \sum_{n=1}^N |X_n|$$

B] Integrated EMG (IEMG): IEMG is normally used as an onset detection index that is related to EMG signal sequence firing point. IEMG is the summation of the absolute values of EMG signal amplitude, which can be expressed as

$$IEMG = \sum_{n=1}^N |X_n|$$

C] Root Mean Square (RMS): RMS is related to constant force and non fatiguing contraction. Generally, it similar to SD, which can be expressed as

$$RMS = \sqrt{\frac{1}{N} \sum_{n=1}^N |X_n|^2}$$

D] Simple Square Integral (SSI): SSI captures the energy of the EMG signal as a feature. It can be expressed as

$$SSI = \sum_{n=1}^N |X_n|^2$$

E] Average voltage:

F]Maximum(Peak) voltage:

For collection of EMG to design calf stimulator we have used calf muscles , Tibialis anterior and Gastrocnemius muscle to do the ankle movement.

For Tibialis anterior muscle:

	Peak voltage reading before RF contracting in Voltage	Average of voltage reading before contraction	Peak voltage reading after RF contracting in Voltage	Threshold set in Voltage
Normal Person 1	0.0061	3.2264e-06	0.0063	0.0062
Normal Person 2	0.0066	2.9373e-06	0.0068	0.0067
Patient 1	0.0018	0.0026	0.0023	0.0020
Patient 2	0.0016	0.03741	0.0021	0.0018

Table1. EMG signal observed and threshold in terms of voltage

For Gastrocnemius muscle:

	Peak voltage reading before RF contracting in Voltage	Average of voltage reading before contraction	Peak voltage reading after RF contracting in Voltage	Threshold set in Voltage
Normal Person 1	0.0490	3.4071e-06	0.0876	0.0683
Normal Person 2	0.0163	3.0526e-06	0.0236	0.0199
Patient 1	0.0015	0.0026	0.0026	0.0019
Patient 2	0.0021	0.0102	0.0039	0.0030

Table 2. EMG signal observed and threshold in terms of voltage

C. Design of Stimulator-

1.Analog to Digital design-

The microcontroller consists of built in Analog-to- Digital (ADC) converters. These enable the conversion of our analog inputs into quantized values. The voltage from the rectifier is fed to one ADC pin (AN0). The ADC of the microcontroller divides these analog inputs into 1024 quantized levels. These values are 0 (for 0V input) and 1023 (for 5V input). In this way, rectified EMG voltage sensing is achieved.

2.EMG signal voltage measurement-

The EMG signal is acquired using instrumentation amplifier and filtered using band pass filter. Then the signal is rectified, rectified output is given to the microcontroller

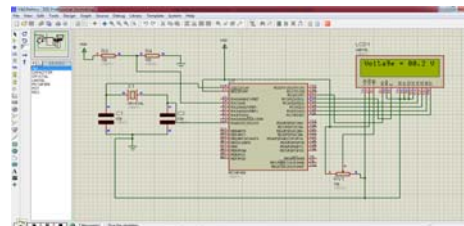


Fig.8 EMG signal voltage sensing

3.Pulse Width Modulation-

To adjust the period of stimulating pulse the pulse width modulator is used. By changing the duty cycle of PWM waveform the pulse duration adjustment is achieved. The duty cycle like the ADC, must be quantized into digital outputs. For this purpose the PORTB and PORTC are declared as outputs and the PWM

port is initialized with input frequency .The duty cycle of the PWM pin is set with a quantized value which is 0 for minimum (0%) duty cycle and 255 for maximum (100%) duty cycle. The simulation for this is shown in Fig 9, and output of PWM is shown in Fig.10.

4.Current Source-

At the output of the PWM, the amplifier is connected to increase the voltage of the PWM. Then that voltage is converted into the current using voltage to current converter with grounding load. To adjust the amplitude of the PWM the 10K log plot is used at the output of controller.The simulation for this is shown in Fig 9, and output of PWM is shown in Fig.10.

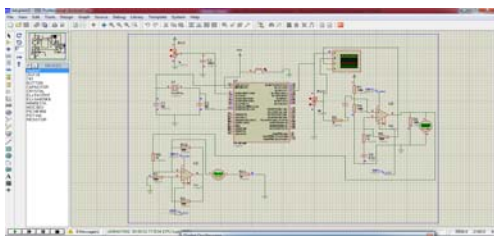


Fig.9 Simulation of PWM and current source

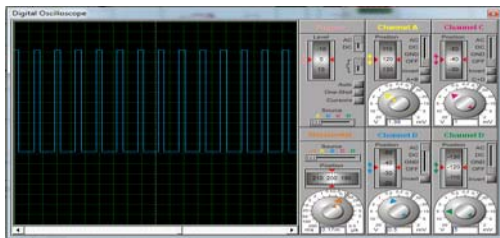


Fig.10 Output of simulation of PWM

IV RESULTS & OBSERVATIONS

With this system we have extracted the time domain features to design the calf stimulator. The filtered EMG signals of different persons are collected using Daq-Card, and different features of EMG signals are extracted using MATLAB tool. The different features extracted are (MAV) Mean absolute value, (RMS) Root mean square, Maximum amplitude, Minimum amplitude, Average level . The Mean absolute value of the EMG signal is related to the muscle contraction level of that muscle of the person. RMS value of EMG signal is directly proportional to the contraction force applied on that muscle to contract.

We had done the feature extraction with the help of five-six parameters.MAV is the most important parameter for contraction of EMG

signal. As MAV represents the contraction level of the muscle, the MAV before contraction is less than MAV after contraction. The contraction level of Normal person is greater than the contraction level of Patients. The threshold voltage level to drive the stimulator is calculated from the average and peak voltages before and after RF contraction. The current value for the stimulator is set between 1 mA to 50 mA. The different current levels will be given to the patient according to the patient's response for certain period of time.

V.CONCLUSION AND FUTURE IMPROVEMENT

The proposed work is to develop Electrical Calf Stimulator.Electrical stimulator uses electric current of 0-50 mA to cause single nerve/muscle or group of muscles/nerves to contract and by contracting these muscles/nerves helps to strengthen the affected muscle. It is used to maintain or restore the muscle activity of lower extremity.The work reflects the study of Myoelectric signal (MES) acquired from the surface of the body by specially design surface electrode are to be processed for finding the time domain features which can be further used to design the stimulator.

REFERENCE

- [1] Debabrata Sarddar, Madhurendra Kumar, Suman Kumar Sikdar presented "Functional Electric Stimulation using PIC Microcontroller," International Journal of Computer Application, vol.44, issue no.12, April 2012, pp 31-35.
- [2] Anirban Dutta and Rudi Kobetic., "Walking after partial paralysis assisted with EMG triggered or switch-triggered Functional Electrical Stimulation –two case studies" IEEE International Conference on Rehabilitation Robotics. 2011, pp 1 – 6, July 2011.
- [3] Sijiang Du and Marko Vuskovic presented "Temporal Vs.Spectral Approach to Feature Extraction from Prehensile EMG signals" IEEE International Conference, ,November 2004, pp 344-350.
- [4] Thomas C. Bulea, , Rudi Kobetic, , Musa L. Audu, John R. Schnellenberger, and Ronald J. Triolo, "Finite State Control of a Variable

Impedance Hybrid Neuroprosthesis for Locomotion After Paralysis” IEEE transaction on Neural System and Rehabilitation Engineering,vol.21, issue no.1,January 2013,pp 141-151.

[5] Cheryl L.Lynch, Milos R.Popovic,“A Comparison of Closed-Loop Control Algorithms for Regulating Electrically Stimulated Knee Movements in Individuals With Spinal Cord Injury”IEEE transaction on neural system and rehabilitation engineering,vol.20, issue no.4,July 2012, pp 539-548.

[6] Ryan J. Farris, Hugo A. Quintero, and Michael Goldfarb,“Preliminary Evaluation of a Powered Lower Limb Orthosis to Aid Walking in Paraplegic Individuals”IEEE transaction on Neural System and Rehabilitation Engineering,vol.19, issue no.6,December 2011, pp 652-659.

[7] Aizan Masdar,B.S.K.K.Ibrahim,M.Mahadi Abdul Jamil, DirmanHanafi ,M.K.I.Ahmad, and K.A.A.Rahman,“Current Source with Low Voltage Controlled for Surface Electrical Stimulation”,IEEE 9th International Colloquium on Signal Processing and its Applications, 2013, Kuala Lumpur, Malaysia.

[8] Matthew A. Schiefer, , Ronald J. Triolo, , and Dustin J. Tyler,“A Model of Selective Activation of the Femoral Nerve With a Flat Interface Nerve Electrode for a Lower Extremity Neuroprosthesis”IEEE transaction on neural system and rehabilitation engineering,vol.16,issue no.2, 2008, pp 195-205.

[9]QiXu,TaoHuang,JipingHe,YizhaoWang,Hau lunZhou,“A programmable multi-channel stimulator for array electrodes in

transcutaneous electrical stimulation”, Proceedings of the IEEE/ICME International Conference on Complex Medical Engineering,Harbin, China,2011,pp 652-656.

[10] Amelia W Azman, JannatulNaeem, YasirMohd,Mustafah,“The Design of Non-Invasive Functional Electrical Stimulation (FES) for Restoration of Muscle Function”International Conference on computer and communication engineering,2012, pp.612-616

[11]Ming,DingYaun,YananLi,MinpengXu,Wei jieWang,RamiAbboud,“Neuroprosthesis System for Lower Limbs Action Based on Functional Electrical Stimulation”, Electrical and control Engineering International conference,2011, pp.4583-4586

[12] Emily Waltz Photography by Greg“Electrical stimulation of the spinal cord could let paralyzed people move again”.



IMPLEMENTATION OF PERTURB AND OBSERVE MPPT OF PV SYSTEM USING BUCK-BOOST CONVERTER

¹Snehali Shankar Patil, ²Prof. M. S. Kumbhar

^{1,2}Electronics and Telecommunication Engineering, Rajarambapu Institute of Technology, Islampur, Sangli, Maharashtra, India

E-mail: ¹snehalipatil1992@gmail, ²Mahesh.kumbhar@ritindia.edu

Abstract— This paper presents a study of Perturb and Observe MPPT Algorithms in MATLAB/Simulink. Maximum power point tracking algorithm of PV array gives highest possible power to load by changing the conditions of solar irradiance & Temperature. This MPPT algorithm is used to maximize the output power of PV array. MPPT algorithm is implemented using Buck-Boost converter. DC-DC converter transfers maximum power to the load. This system is simulated at different solar irradiance and temperature. Simulation results are obtained by varying the solar irradiance & temperature of PV panel.

Keywords— PV system, MPPT algorithm, Buck-Boost converter.

I. INTRODUCTION

With increasing demand of fossil fuel reserves and global warming, for future generation, we are looking at sustainable energy to save the earth. Solar energy has lots of attention in recent year because of electricity problem. Solar energy has been applied to variety of field like water heating, building lightning, cooling & building heating. Sun radiation in solar energy, which is present in throughout the day but intensity of sun radiation which is different at different time. The different radiation intensity of sun that make it unreliable by using different MPPT algorithm

for the improvement of system power efficiency and reliability.

Perturb and Observe algorithm is used for residential photovoltaic system. it is implemented using microprocessor for improving the power [1]. MPPT algorithm is used for PV generator, that can be used for tracking maximum power point by comparing with incremental conductance and result obtain at different atmospherics condition [2]. MPPT combined with a step down DC-DC converter to a PV converter to produce maximum continuous power [3]. Perturb and Observe MPPT algorithm is used to increase efficiency of PV module compare with other method [4]. MPPT algorithms compare Perturb & Observe, Incremental Conductance and Constant Voltage for different atmospherics condition [5].

II. PROPOSED WORK

Solar cell is an electrical device that converts the energy of light directly into electricity. Solar cell is a form of Photovoltaic cell defined as a device whose electrical characteristics current, voltage or resistance vary when exposed to light. MPPT algorithm, this is a maximum power point tracking algorithm. MPPT is a technique that solar battery chargers and similar devices use to get the maximum power from one or more photovoltaic device. Therefore, the MPPT

B. Buck-Boost Converter

PV array generated voltage & current is fed to the buck-boost converter & buck-boost converted output is current, voltage & power, by varying the duty cycle then the voltage gain of buck-boost converter can be set higher or lesser than unity [7]. fig4. shows Buck-Boost simulation model.

Table.2 Buck-Boost converter component Parameter

1	Inductance	L= 80uH
2	Capacitance	C= 10uF
3	Switching frequency	F _{sw} = 25 kHz

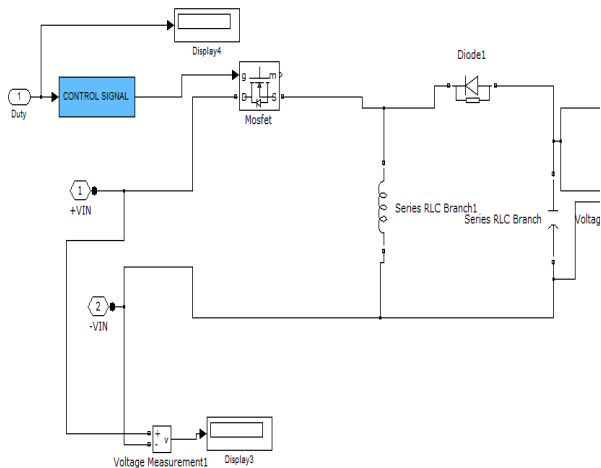


Fig4. Buck-Boost simulation model

C. MPPT

MPPT is used for improve the efficiency of solar panel. Output power of any circuit can be maximize by adjusting the source impedance equal to load impedance according to mppt. Buck-boost converter is used for impedance matching device between input and output by varying the duty cycle of converter circuit. Duty cycle of converter is depend on the output voltage, so MPPT is used to the calculate duty cycle for obtain the maximum output voltage [8]. In this Perturb and Observe, constant duty cycle technique is used because less hardware complexity [9].

1) Perturb & Observe MPPT

Perturb & Observe is simple method which is used to obtain the maximum power point. Here we use voltage and current sensor to sense voltage and current of PV array. In this, operating point reaches very close to MPPT but it does not reach at the MPP and keeps increasing or decreasing on both the direction. If $\frac{dP}{dV} > 0$ then the operating point of PV array moves towards MPP. If $\frac{dP}{dV} < 0$ then the operating point of PV array moves away from MPP. If $\frac{dP}{dV} = 0$ then the operating point at MPP. State flow chart implementation of Perturb & observe method is shows in fig. 5 [10].

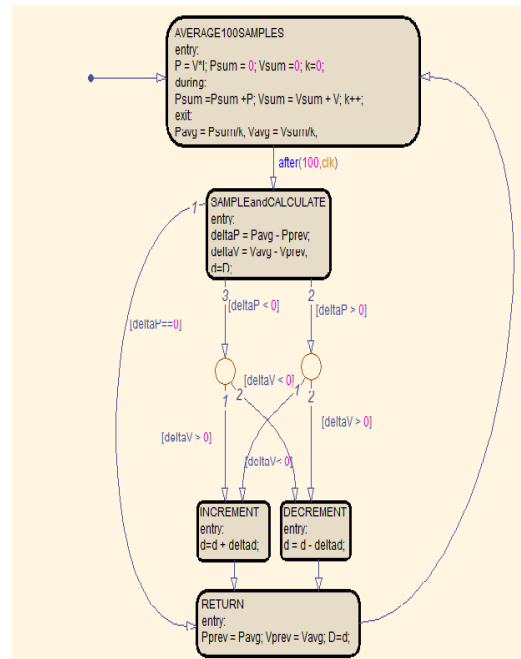


Fig.5 State flow chart of P&O method

IV. SIMULATION RESULT

The Matlab/Simulink model of PV model with Buck-Boost converter using Perturb & Observe algorithm is shown in fig.6

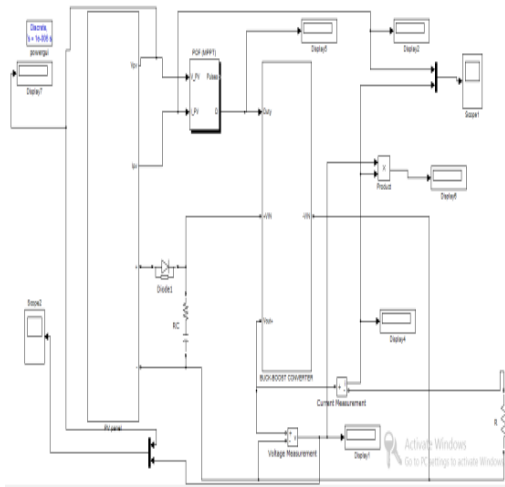


Fig.6 PV system with P&O algorithm

Perturb & observe algorithm is implemented in Matlab for tracking maximum power. The simulation result of output power of PV module and DC-DC converter for different solar irradiance and constant temperature are obtained. From the simulation results for different solar irradiance and temperature that output power increases with increasing solar irradiance.

PV panel and DC-DC converter output power curve for temperature 30 degree and solar irradiance 1000W/m² as shown in fig.7 and temperature 30 degree and solar irradiance 1100W/m² as shown in fig.8 for P&O.

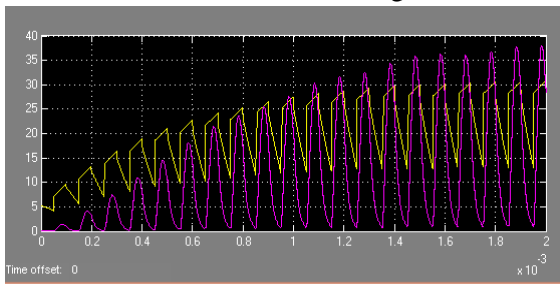


Fig.7 Output power curve for Perturb & observe 30 degree & Solar irradiance 1000W/m²

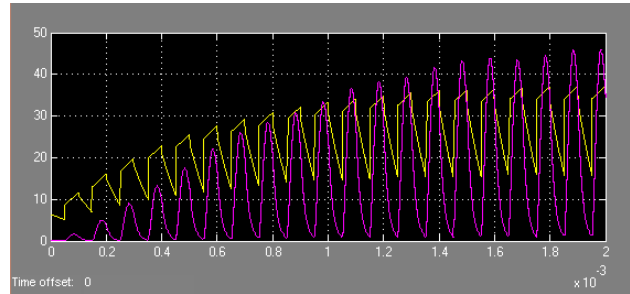


Fig.8 Output power curve for Perturb & observe 30 degree & Solar irradiance 1100W/m²

The output power of PV system and DC-DC converter for Perturb and Observe under constant temperature and different solar irradiance as well as constant solar irradiance and different temperature are shown in table.3 & table.4 [12].

Table.3 Output of PV system for constant T=30 centigrade

Algorithm	Solar irradiance (W/m ²)	PV Module Power(Watt)	Buck-Boost Converter Power(Watt)
P&O	1000	30.38	27.97
P&O	1100	37.79	33.88

Table.4 Output of PV system for constant Solar irradiance =1000W/m²

Algorithm	Temperature(Centigrade)	PV Module Power(Watt)	Buck-Boost Converter Power(Watt)
P&O	30	30.38	27.97
P&O	40	29.01	27.1

V. CONCLUSION

This paper presents Perturb and Observe MPPT algorithms are implemented using Buck-Boost converter in Matlab/Simulink. In this

result of simulation of PV system and DC-DC converter is depend on solar irradiance & temperature. Implementation of Perturb & observe is easier to implement. This algorithm gives maximum power point by increasing solar irradiance. Temperature increases Maximum power point voltage decreases.

REFERENCES

- [1] Mohamad A. S. Masoum, Seyed Mahdi Mousavi Badejani, and Ewald F. Fuchs, "Microprocessor-Controlled New Class of Optimal Battery Chargers for Photovoltaic Applications", IEEE Transaction on Advanced Packaging, 2003, Volume: 26, Issue: 4, pp 453.
- [2] Eftichios Koutroulis, Kostas Kalaitzakis, "Development of a Microcontroller-Based, Photovoltaic Maximum Power Point Tracking Control System", IEEE transactions on Power Electronics, Vol. 16, No .1, January 2001, pp. 46-54.
- [3] Sachin Jain, Vivek Agarwal, "A New Algorithm for Rapid Tracking of Approximate Maximum Power Point in Photovoltaic Systems", IEEE Conference Paper, 2004, Volume 2, Issue1, pp. 16-19.
- [4] UmaShankar Patel ,Ms. Dhaneshwari Sahu, Deepkiran Tirkey, "Maximum Power Point Tracking Using Perturb & Observe Algorithm & Compare with Another Algorithm", International Journal of Digital Application & Contemporary research Conference, September 2013, Volume 2, Issue 2.
- [5] Roshan Kini, Geetha.Narayanan, Aditya Dalvi, "Comparative Study and Implementation of Incremental Conductance method and Perturb and Observe method with buck converter by using arduino", International Journal of Research in Engineering and Technology, Jan-2014, Volume 03, Issue 01.
- [6] Y.P. Siwakoti, B.B. Chhetri, B. Adhikary and D. Bista, "Microcontroller based intelligent DC/DC converter to track Maximum Power Point for solar photovoltaic module", IEEE Conference on Innovative Technologies for an Efficient and Reliable Electricity Supply (CITRES), 2010, pp. 94-101.
- [7] Ahmed M. Atallah, Almaoataz Y. Ahdelaziz, an Raihan S. Jumaah, "Implmentation of Perturb & Observe MPPT of PV System with direct control method using buck & boost converters", International Journal on Electrical, Electronics & Instrumentation engineering, February 2014, Volume 1, no.1.
- [8] Priety and Vijay Kumar Garg, "To Perform MATLAB/Simulink of battery charging using solar power with Maximum Power Point Tracking(MPPT)", International Journal of Electronics & Electrical Engineering, 2014, volume 7, no.5, pp. 511-516.
- [9] Hassan Abouobaida, Mohamed Cherkaoui, "Comparative Study of Maximum Power Point Trackers for fast changing Environment condition", IEEE conference, May 2012, pp.1131-1136.
- [10] Ioan Viorel BANU, Razvan BENIUGA, Marcel ISTRATE, "Comparative Analysis of Perturb and Observe and Incremental Conductance methods", International Syposium on Advanced Topics in Electrical Engineering, May 2013.
- [11] Tekeshwar Prasad Sahu, T.V. Dixit, "Modelling and Analysis of Perturb & observe and Incremental Conductance MPPT algorithms for PV array using Cuk converter", IEEE conference on Electrical, Electronics & Computer Science, March 2014, pp.1-6.



SECURE QUESTION PAPER TRANSFERRING USING LSB STEGANOGRAPHY TECHNIQUE

¹Tejashri Shivajirao Jadhav, ²Dr. S. A. Pardeshi

^{1,2}Electronics and Telecommunication Engineering, Rajarambapu Institute of Technology, Islampur,
Sangli, Maharashtra, India

E-mail: ¹jadhavtejashri@gmail, ²sanjay.pardeshi@ritindia.edu

Abstract- Steganography is an important area of research in recent years involving a number of applications. It is the science of embedding information into the cover image. Visual Attacks can potentially be implemented in many ways, picking on different properties of the image in each implementation such that a wide range of embedding strategies are examined. For example, a visual attack could be set up to display the spatial LSB plane of the image on its own, the two lowest bit planes, the second lowest bit plane only, and so on[3]. When all possible bit plane combinations have been exhausted, the steganalyst will be better placed to determine whether or not the image was subjected to spatial steganographic embedding such as that defined by the Hide & Seek method (or a slight modification of that algorithm that embeds in a different bit plane or combination of bit planes). Similarly, the steganalyst could also exhaust all possible bit plane combinations in a particular transform. Steganalysis is the process of identifying steganography by inspecting various parameter of a stego media at the receiver. At the receiver the video will be displayed and various parameters of video will be read like peak signal to noise ratio (PSNR), mean squared error.

Keywords- peak signal to noise ratio (PSNR), mean squared error (MSE).

I. INTRODUCTION

Steganography literally means covered writing. Its goal is to hide the fact that communication is taking place. In the field of Steganography, some terminology has been developed. The term cover is used to describe the original, innocent message, data, audio, still, video and so on. The growing possibilities of modern communications need the special means of security especially on computer network.

One of the reasons that intruders can be successful is the most of the information they acquire from a system is in a form that they can read and comprehend. Intruders may reveal the information to others, modify it to misrepresent an individual or organization, or use it to launch an attack. One solution to this problem is, through the use of steganography. Steganography is a technique of hiding information in digital media. In contrast to cryptography, it is not to keep others from knowing the hidden information but it is to keep others from thinking that the information even exists.

Steganography[1] become more important as more people join the cyberspace revolution. Steganography is the art of concealing information in ways that prevents the detection of hidden messages. Steganography include an array of secret communication methods that hide the message from being seen or discovered.

Due to advances in IT, most of information is kept electronically.

Consequently, the security of information has become a fundamental issue. Besides cryptography, steganography can be employed to secure information. In cryptography, the message or encrypted message is embedded in a digital host before passing it through the network, thus the existence of the message is unknown. Besides hiding data for confidentiality, this approach of information hiding can be extended to copyright protection for digital media: audio, video and images.

The growing possibilities of modern communications need the special means of security especially on computer network. The network security is becoming more important as the number of data being exchanged on the internet increases. Therefore, the confidentiality and data integrity are required to protect against unauthorized access and use. This has resulted in an explosive growth of the field of information hiding.

Information hiding is an emerging research area, which encompasses applications such as copyright protection for digital media, watermarking, fingerprinting, and steganography.

Steganography hides the secret message within the host data set and is imperceptible and is to be reliably communicated to a receiver. The host data set is purposely corrupted, but in a covert way, designed to be invisible to an information analysis.

II. LITERATURE ON RELATED WORKS

Steganography[1] is the science that involves communicating secret data in an appropriate multimedia carrier, e.g., image, audio, and video files. It comes under the assumption that if the feature is visible, the point of attack is evident, thus the goal here is always to conceal the very existence of the embedded data. Steganography has various useful applications. However, like any other science it can be used for ill intentions. It has been propelled to the forefront of current security techniques by the remarkable growth in computational power, the increase in security awareness by, e.g., individuals, groups, agencies, government and through intellectual pursuit. Steganography's ultimate objectives, which are undetectability, robustness (resistance to various image processing

methods and compression) and capacity of the hidden data, are the main factors that separate it from related techniques such as watermarking and cryptography[1]. Today's computing systems which consist of a broad range of processors communication network, are vital to operation of many sectors of our society from manufacturing to education and healthcare. The explosive growth and the open nature of internet and E-commerce[2]. Have caused organization to become more vulnerable to electronic attack on IT assets companies have been suffering from breach of the data loss of customers confidence and job productivity degradation all which eventually lead to loss of revenue.

That is rise of internet one of the most important factors of information technology communication has been the security of the information. It is also often said that the goal of steganography is to hide a message in one-to-one communications and the goal of watermarking is to hide message in one-to-many communications[3].

Shortly, one can say that cryptography is about protecting the content of messages, steganography is about concealing its very existence.

Steganography methods usually do not need to provide strong security against removing or modification of the hidden message. Watermarking methods need to be very robust to attempts to remove or modify a hidden message.

There are three security systems watermarking, steganography and encryption. Steganography and watermarking bring a variety of very important techniques how to hide important information in an undetectable and/or irremovable way in audio and video data. Steganography and watermarking are main parts of the fast developing area of information hiding.

The main goal of steganography is to hide a message m in some audio or video (cover) data d , to obtain new data d' , practically indistinguishable from d , by people, in such a way that an eavesdropper cannot detect the presence of m in d' . The main goal of watermarking is to hide a message m in some audio or video (cover) data d , to obtain new data d' , practically indistinguishable from d , by

people, in such a way that an eavesdropper cannot remove or replace in d'.

It is also often said that the goal of steganography is to hide a message in one-to-one communications and the goal of watermarking is to hide message in one-to-many communications.

Shortly, one can say that cryptography is about protecting the content of messages, steganography is about concealing its very existence.

Cryptography hides the contents of the message from an attacker, but not the existence of the message. Steganography/watermarking even hide the very existence of the message in the communicating data.

III. PROPOSED SYSTEM ARCHITECTURE

Security of exam paper is an important issue in these competitive era . So to transfer exam paper from university to respective collage securely ,We will develop software using steganography using MATLAB. To hide a message inside an image without changing its visible properties, the cover source can be altered in "noisy" areas with many color variations, so less attention will be drawn to the modifications. The most common methods to make these alterations involve the usage of the least-significant bit or LSB method on the cover image[2]. These techniques can be used with varying degrees of success on different types of image files.

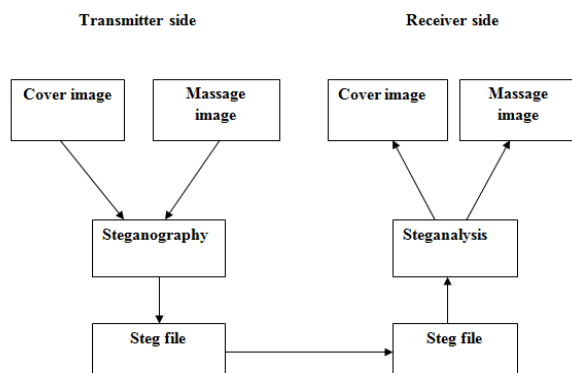


Fig. 1 Proposed system

Least significant bit (LSB) insertion is a common, simple approach to embedding information in a cover image. The least significant bit (in other words, the 8th bit) of some or all of the bytes inside an image is

changed to a bit of the secret message. When using a 24-bit image, a bit of each of the red, green and blue colour components can be used, since they are each represented by a byte. In other words, one can store 3 bits in each pixel. For example a grid for 3 pixels of a 24-bit image can be as follows:

```

(00101101 00011100 11011100)
(10100110 11000100 00001100)
(11010010 10101101 01100011)
    
```

When the number 200, which binary representation is 11001000, is embedded into the least significant bits of this part of the image, the resulting grid is as follows:

```

(00101101 00011101 11011100)
(10100110 11000101 00001100)
(11010010 10101100 01100011)
    
```

A. Mean Squared Error-

- The MSE is cumulative squared error between the compressed and the original image.
- If x_i and y_i are the i-th pixels in the original and distorted video signals respectively and N is the number of pixels in the video signal, MSE is defined as:

$$MSE = \frac{1}{N} \sum_{i=1}^N (x_i - y_i)^2$$

B. peak signal to noise ratio-

- The PSNR is most commonly used and traditional objective quality metric to measure of the quality of video. A higher PSNR would normally indicate higher quality.
- The Peak Signal-to-Noise Ratio (PSNR) is defined as:

$$PSNR = 10 \log_{10} \frac{L^2}{MSE}$$

- Where L is the dynamic range of the pixel values or the maximum possible reference intensity value.

IV. RESULTS & OBSERVATIONS

If the value of PSNR is higher then it indicates higher quality of image. For low quality image value of PSNR is small.



Fig.2 Cover ,Message, Stego images and output message image

Table.1 PSNR value for above stego images

Number of Replaced bit plane	PSNR value	Number of Replaced bit plane	PSNR value
0	5.2836	4	4.5007
1	5.2370	5	3.6224
2	5.0551	6	1.6880
3	4.7714	7	2.2458

V. CONCLUSION AND FUTURE IMPROVEMENT

Steganography can be used as beneficial tool for privacy than other security systems. Steganalysis is the technique to detect steganography. The stego multimedia produced by mentioned methods for multimedia steganography are more or less vulnerable to attack are like media formatting and compression etc., a visual attack could be set up to display the spatial LSB plane of the image on its own, the two lowest bit planes, the second lowest bit plane only, and so on. From output , using LSB plane replacing method to hide the message image ,we get the larger PSNR value. Using MSB plane replacing ,we get the smaller PSNR value. Larger the PSNR value the smaller the possibility of visual attack by human eye.

VI. REFERENCE

[1] Abbas Cheddad, Joan Condell, Kevin Curran and Paul Mc Kevitt, "Digital image steganography: Survey and analysis of current methods". Signal Processing 90 (2010),pp. 727-752.

[2]Bin Li, Junhui He, Jiwu Huang ,"A Survey on Image Steganography and Steganalysis." Ubiquitous International Volume 2, Number 2,pp.142-172, April 2011.

[3] Joan Condell, Kevin Curran, Paul Mc Kevitt, "Enhancing steganography in digital images", Canadian Conference on Computer and Robot Vision,2008 pp.326-332.

[4]V.Lokeswara Reddy, Dr. A. subramanyam and Dr.P.Chenna Reddy "on Implementation of LSB Steganography and its Evaluation for Various File Format."

[5] Fatiha Djebbar, Beghdad Ayady,Habib Hamamzand karim ,Abed Meraim, "A view on latest audio steganography technique", 2011 international conference on innovations in information technology,pp.409-414.

[6] S. Changder, S. Das, D. Ghosh, "Text Steganography through Indian Languages Using Feature Coding Method", 2010 2nd international onference on Computer Technology and Development (ICCTD 2010), pp.501-505.



DESIGN OF A NOVEL PRESSURE SIGNAL BASED BIOMETRIC SYSTEM FOR AUTOMATED IDENTIFICATION OF COCKPIT PERSONNEL

¹Eswaran.R ²Rajatha, ³Viswanath Talasila

^{1,2,3}Dept. of Telecommunication Engg, M.S.Ramaiah Institute of Technology
Bangalore, Karnataka, India.

Email: ¹eswaranrathinam@gmail.com, ²rajatha2893@gmail.com

³viswanath.talasila@gmail.com

Abstract—Airplane cockpit security is a crucial function of flight management. One important aspect is the identification of the persons occupying the pilot and co-pilot seats. Existing biometric techniques have certain drawbacks, and this paper presents an automated method to identify the person sitting in a seat, based on the pressure patterns. In this paper, Principle Component Analysis is used to compute specific patterns in the pressure signature; these patterns are compared with existing patterns in a database to identify the correct person.

Keywords- *biometric system, pressure signature, PCA, Threshold.*

I. INTRODUCTION

Cockpit security and pilot health are critical aspects of an airplane's functioning.

Voice biometrics is one standard approach for pilot authentication, [1]. Here the pilot is prompted, at certain intervals, for a voice sample either by the air traffic controller or the flight management system and an authentication is performed. Note that this procedure requires pilots to focus, temporarily, on the biometric tasks and may interfere with the routine flight tasks. Further, voice identification is not a fully accurate procedure, and thus cannot be used as a single biometric source of authentication. The

standard biometric systems available are the on ground systems, where pilots are required to be verified before boarding a flight, [2]. In [3] aircrafts are installed with biometric systems (including retinal scanning, fingerprint identification etc) to monitor the cockpit personnel in flight. The problem with this system is that in case real time (or online) authentication is required, the pilot is forced to delay the regular flight tasks and perform a biometric authentication. This can interfere with flight procedures and could lead to potentially dangerous situations. *Ideally, the biometric system should be non-invasive and should not require the pilot to ignore any in flight task.*

In the medical rehabilitation community, when considering motion signatures of the entire human body, there is a theory that each individual has unique signatures. This is employed in various biometric applications, for e.g. in [4] the authors analyze the spatial and temporal characteristics of human motion in the frequency domain, and discriminate between two individuals based on their Fourier descriptors. In further applications of biometrics, [5] has employed gait analysis, where the gait is computed through radar signatures, in order to detect if a person is carrying a bomb. The relation with this specific paper is that it is possible to identify unique patterns in the human body through appropriate sensor measurements. Indeed, camera measurements, radar

measurements, inertial sensor measurements etc can all be used to identify specific patterns in the human body. For e.g., inertial sensing is a standard tool to identify specific movement disorders in the human body [6] [7]; here machine learning techniques are used to identify specific patterns based on the motion signatures.

Finally, in the medical rehabilitation community, the pressure map of the human body is used to identify specific muscle (and joint) weakness and disorders. For e.g. in [8], the pressure signature from the forearm was used as a predictor of grip force, which is then used to model the muscle strength and related issues in rehabilitation.

The use of the whole body pressure signature in biometrics is a novel concept that we introduce in this paper. *While pressure signature itself has been traditionally used in fingerprint based biometrics, the focus of this paper is a whole body signature when the person is sitting in a chair.*

Fingerprinting is essentially a pressure signature, and based on the specific patterns the identification is made. Though this is a mature technology, there are still various failure cases, and research in this field is ongoing. For e.g., the signature obtained from two different fingerprint sensors, can be different [9]. There are various reasons for this, e.g. change in the sensor used for acquiring the raw data (e.g., optical versus solid-state sensors in a fingerprint system), even variations in environment (e.g. humidity) [9]. Thus, in the case of pilot seat pressure biometry, due to environmental variability, or variations in a person's own features (image, pressure etc) the main biometric signature will change. This necessitates the need for adaptive biometrics, and is indeed an interesting research trend [10]. In the current paper we do not aim to develop an adaptive biometric system, however this is clearly a requirement in our work; as various features in a person's body (such as weight, bone mass distribution etc) will vary with time.

In [9] a detailed comparison of many biometric systems has been described; in the open literature there has been no attempt at developing a biometric device for using pressure signatures from seating positions. The attempts made in this paper are a novel approach for the design and

development of a pressure based biometric system.

II. PROPOSED METHOD

The biometry based identification may be stated as follows. Suppose we have a biometric system capturing some input data, from which certain features of interest are extracted. Let these features be denoted by X_{bio} . The goal would, then, be to determine which of the identities (in a database), $I_k, k \in \{1,2, \dots\}$ matches with the feature X_{bio} . The match itself would be obtained by a comparison with a suitably defined threshold,

i.e.

$$X_{bio} = I_k, X_{bio} = I_k \text{ if } \min_k \{S(X_{bio}, I_k)\} < \text{thresh}$$

Where $S(X_{bio}, I_k)$ can be thought of as a difference operator such that it searches for that feature in the entire database which minimizes the difference between the current feature and itself [9].

As shown in Fig. 1, the smaller circles indicate the higher pressure points. These points are in proximity to "Ischial tuberosity" [11] which is a bone protrusion and is observed that, this is the point where maximum weight is concentrated. The pressure magnitude decreases radially outward. These pressure signatures are unique for each person. Hence we need a pattern recognition technique to discriminate between signatures. In this paper, PCA is chosen for the task of authentication.

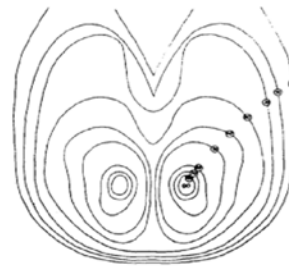


Fig. 1. Pressure distribution of a person sitting in chair

A. Why PCA?

While there exist many techniques to extract and compare patterns, in machine learning, we are focusing exclusively on the PCA technique mainly because it reduces the dimension of the data, which is critical in our application where we can have some 10000 cells (thus 10000 dimensions!) each capturing data at 100Hz or faster. The volume of the data will be large and

thus it requires the use of dimensionality reducing techniques, such as PCA. Furthermore, PCA is computationally a powerful algorithm and is highly relevant in such real time applications. For example, while standard PCA algorithms have a computational complexity of $O(d^3 + d^2n)$ (where 'n' is the number of features), some modifications result in a complexity of $O(d^3)$, and then there is the Fast PCA where matrix inversions (which results in $O(d^3)$ type complexity in other approaches) is not even required, and the algorithm converges in a few iterations[9]. Thus PCA is a well suited technique for the present application of pressure and vibration based biometry.

B. Procedure for PCA Analysis

Principle component Analysis is a statistical procedure, majorly used in face recognition. Eigen values or the prime components which accounts the best distribution of variation in the image are the basis of this procedure, which is successfully employed for authentication and identification of the pressure signatures in a controlled condition. The pressure signature matrix of a person is captured by the FSR 402 (Force sensitive resistor) sensors. Because of the force repeatability error, the data got from sensors will vary $\pm 2\%$ each time, hence the pressure signature matrix is captured for a sequence of different time intervals and an average matrix is calculated before PCA computation. Firstly, this averaged matrix is converted into column vector by concatenating each column one after other. This vector is mean subtracted, followed by the computation of covariance matrix. From this covariance matrix, Eigen values and Eigen vectors are calculated which forms principle components. These principle components depict the amount of variation in the pattern and uniqueness of each pressure signature. Identification of new signature is done by comparing the new signature with the previously stored data set based on threshold, but the new signature has to be processed in the same manner as the stored signature. Threshold plays a vital role in recognition. Threshold is taken as some factor of maximum of Euclidean distance where the factor is chosen arbitrarily. Threshold is computed by Euclidean distance classifier method. Minimum of the Euclidean distance $\epsilon(i)$ between all the person's principle components is computed, and maximum of $\epsilon(i)$ i.e. Θ is calculated. When a new pressure signature is

encountered, principle components are computed. It is compared with each of the principal components in the data base by calculating the maximum difference of the principle components $\Psi(i)$ of the new signature and each of the stored signature in the data base. $\epsilon(i)$ is compared against the threshold. If the value is less than or equal to the threshold value then the person is classified as the known person or else as unknown person.

C. Steps involved in signature discrimination

The following outlines the procedure for computing the principal components and the threshold for discriminating between pressure signatures.

Step 1: A pressure signature matrix of $N \times N$ is taken, where each pixel represents the pressure value.

$$A = \begin{bmatrix} A_{11} & A_{12} & \dots & A_{1N} \\ A_{21} & A_{22} & \dots & A_{2N} \\ \vdots & \vdots & \ddots & \vdots \\ A_{N1} & A_{N2} & \dots & A_{NN} \end{bmatrix}_{N \times N}$$

Step 2: Each of the matrixes is converted into column vector, V . Mean adjusted data is computed by subtracting the mean from the column vector, Covariance(X) of the mean adjusted value is calculated, Eigen value from the covariance matrix is calculated and finally the principal components, $\Psi(i)$, are computed

$$\Psi(i) = \lambda(i) * V[i]$$

Step 3: When a new pressure signature is encountered, the new principal component (Ψ) is computed and Euclidean distance between the principle component of new signature and existing signatures is calculated using,

$$[\epsilon(i)]^2 = \|\Psi - \Psi(i)\|^2 \text{ for } i = 1 \dots M \quad (6)$$

If $\epsilon(i)$ exceeds a pre-defined threshold value, then we conclude that the new principal component Ψ belongs to a different person. **Choice of the threshold:**

An arbitrary threshold value is initially computed as follows

$$\Theta = x * \max \{ \|\Psi(i) - \Psi(j)\|^2 \} \text{ where } i, j = 1 \dots M \quad (7)$$

Where x is the arbitrary constant

If $\epsilon(i) < \Theta$, then pressure signature is identified
 If $\epsilon(i) > \Theta$, then pressure signature is unidentified

D. Experimental results

To quantify the effect of threshold, an experiment was conducted in MATLAB with a

database of twenty different pressure signatures. Each pressure signature is a 100x100 matrix, where each element of the matrix depicts the pressure value. For the ideal case, we have assumed that the pressure signature of a person radially decreases outwards. For illustration, Fig. 2 shows the data base of twenty different ideal matrices. Each one is different from other by radius, or by angle, or the distance between the two pressure distributions (i.e. circles). Principal components are computed for 20 different pressure signatures. From the observation and graph (as shown in Fig. 2) the principal components computed is found to be unique for each signature. Hence PCA was able to discriminate between different pressure signatures. Since the choice of threshold is arbitrary, in this paper, experiments are conducted for threshold varying from 0.1 to 1 times of the maximum value of minimum Euclidian distances. From the observations and experiments (as shown in Fig 3) a threshold of 0.1 is able to recognize 18 signatures whereas a threshold of

1 is able to recognize only 15 signatures. Hence 0.1 times of the maximum value of minimum Euclidian distances is chosen to be the best for distinguishing two pressure signatures.

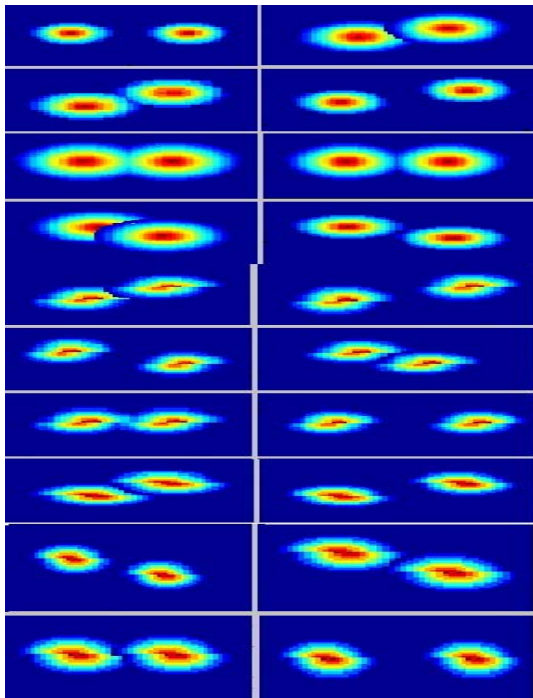


Fig. 2. Database of twenty different ideal pressure signatures

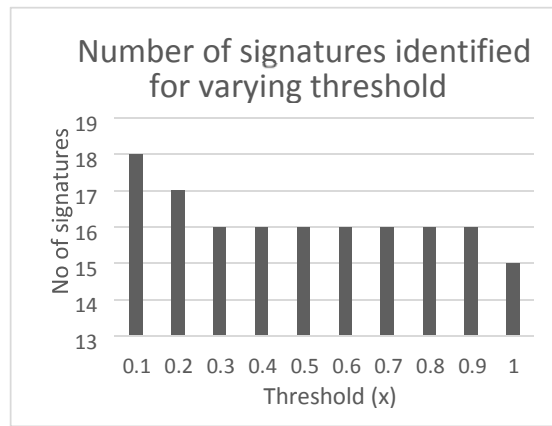


Fig. 3. Graph of number of signatures identified for varying threshold(x)

III. HARDWARE IMPLEMENTATION

The hardware implementation of the model proposed utilizes a pressure sensor testbed which outputs the required data in the matrix form, which is fed into the data base. Fig 4. shows the proposed hardware model which takes the matrix from pressure, compares with the database and identifies the pilot. Fig 5. shows the implemented hardware model which consists a testbed of FSR402 pressure sensors which has force sensitivity range between 0.1 to 10.0²Newton , arranged in a 3x3 matrix placed on a rectangular plastic sheet of area 30x42cm². The testbed is connected to grounding circuit which is then interfaced to Arduino mega microcontroller for the extraction of the signals from the sensors. The FSR402 sensors are robust polymer thick film devices that exhibit a decrease in resistance with increase in force applied to surface of the sensor. One lead of the sensor is pulled up to 5 Volts and the other lead is pulled down to ground by the grounding circuit. The signals from the sensors are transmitted through serial communication to Arduino microcontroller. The Arduino microcontroller converts these analog signals into digital signals through its inbuilt ADC (Analog to digital converter).

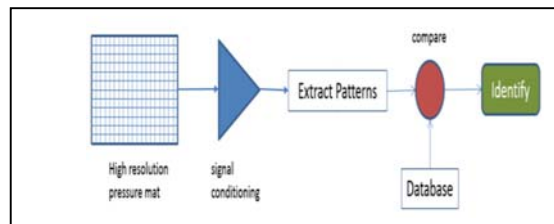


Fig. 4. Proposed hardware model

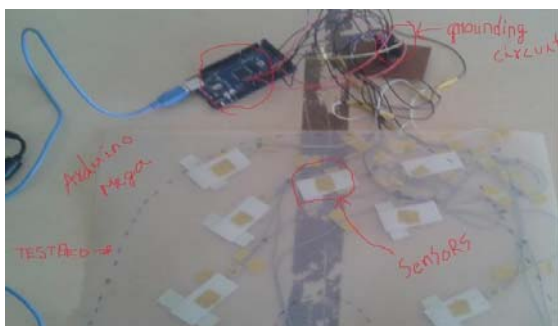


Fig .5.Implemented hardware model
CONCLUSION

This paper focuses on the development of a biometric system based on the whole body pressure signature, when a person is sitting in the pilot chair of an airplane cockpit. The hypothesis is that every individual has a unique pressure signature. Detailed simulation studies are presented in the paper, using the PCA machine learning technique, to discriminate between multiple signatures. A threshold of 0.1 is found to be having the highest recognition as per the experiments. Further work in simulation will focus on incorporating sensor noise, and the subsequent analysis of the person identification.

ACKNOWLEDGMENT

A part of this project was funded by the Aerospace Network Research Consortium (ANRC).

REFERENCES

[1] Douglas Snyder, Pilot authentication using voice biometric, US Patent WO2003029048 A2, 2003

[2] Bart Elias, Securing General Aviation, Congressional Research Service, March 2009

[3] Michael Arnouse, Aircraft security system based on biometric data, US Patent EP1494164 B1 2009

[4] Shiqi Yu et. al., First IEEE Symposium on Multi-Agent Security and Survivability, 2004

[5] Gene Grenaker, Very low cost stand-off suicide bomber detection system using human gait analysis to screen potential bomb carrying individuals, *Proc. SPIE 5788*, Radar Sensor Technology IX, 46 (August 05, 2005)

[6] J.M Fisher et. al., Objective Assessment Of Motor Symptoms In Parkinson's Disease Using Body-Worn Sensors, MDS 18th

International Congress of Parkinson's Disease and Movement Disorders, Volume 29, 2014

[7] Robert LeMoyne, Wearable and wireless accelerometer systems for monitoring Parkinson's disease patients—A perspective review, *Advances in Parkinsons Disease*, Vol 2 No 4, 113-115, 2013

[8] Wining, Michael, Nam-Hun Kim, and William Craelius. "Pressure signature of the forearm as a predictor of grip force." *Journal of rehabilitation research and development*, 45.6 (2008): 883-892.

[9] Arun Ross, Anil Jain, Biometric Sensor Interoperability: A Case Study In Fingerprints, Appeared in Proc. Of International ECCV Workshop on Biometric Authentication (BioAW), (Prague, Czech Republic), LNCS Vol. 3087, pp. 134-145, Springer Publishers, May 2004

[10] N Poh, Rattani A, Roli F, Critical analysis of adaptive biometric systems, *Biometrics*, IET (Volume:1 , Issue: 4), December 2012

[11] Reed and Grant (1993), "Development of a Measurement Protocol and Analysis Techniques for Assessment of Body Pressure Distributions on Office Chairs," technical report, University of Michigan Center for Ergonomics.



APPLICATION OF EXTENDED NERNST PLANCK MODEL IN NF200 MODELING FOR CHROMIUM REMOVAL

¹Manoj Kumaran, ²S. Bajpai

^{1,2}Department of Chemical Engineering, Dr. B.R.Ambedkar National Institute of Technology, Jalandhar, Punjab,

Email: ¹manojkntj@gmail.com, ²bajpais@nitj.ac.in

Abstract: Hexavalent Chromium is widely used in various industries including electroplating, mining, painting etc. Its effective reuse and disposal before discharge is a challenging work. Various methods such as Ion exchange, Solvent extraction, Adsorption, Membrane separation processes have been studied earlier. In this study, Chromium removal is done by polyamide thin film composite Nanofiltration membrane (TFC NF 200) system since it proved to be a very efficient in cross flow mode.

Extended Nernst Planck (ENP) model is essentially used membrane transport model for analysis of NF membrane performance. It is generally used to describe the flux of the ions through charged membrane. ENP equation includes ionic diffusive flow, electro-migration, and convective flow. However in this study, ENP equation depends mainly on Volume flux (J_v), Diffusive (f') and Convective (R') flow components which were estimated from the experimental data for both % rejection and permeate flux separately. Diffusive transport ($-f'\Delta C_i$) and convective transport ($J_v C_{i,0}(1-R')$) contributions were successfully determined by fitting the model to the experimental data. It was found that diffusive transport was more predominant over the Convective transport. Therefore in order to make the flow to be convective the pressure should be increased with decrease in temperature.

Key words: *Hexavalent Chromium, Nanofiltration, Extended Nernst Planck Model. Diffusive and Convective flow.*

1. INTRODUCTION

Heavy metals pollution is a threatening environmental issue as they are highly toxic, environmentally persistent, and accumulate in body tissues[1]. Because of this, the strict environmental regulations insists various industries such as tanneries, metal plating, mining, painting, car radiator manufacturing, battery manufacturing etc., to reduce the concentration of heavy metals in their effluent waste water within safe levels[2]. The effluents from these industries contain chromium either as hexavalent Cr (VI) or trivalent Cr (III) of which hexavalent form is highly toxic and the tolerated concentrations are controlled by strict norms[1][3]. Hexavalent chromium is a potential carcinogen as it breaks the DNA strand, DNA-protein crosslink, modifies DNA transcription process leading to chromosomal damage. Long term exposure of this metal to workers has proven to be harmful and may lead to diseases such as cancer of digestive tract and lungs, stomach ulcers, nausea, diarrhoea, liver and kidney damage, dermatitis, etc[4]. The recovery of the chromium is interesting from both environmental and economic points of view and has to be strictly maintained within the permissible limits.

Even though various methods such as Ion exchange, solvent extraction, precipitation, coagulation and adsorption were conventionally used Nanofiltration (NF) proved to more efficient in cross flow mode for Cr (VI) removal. Nanofiltration is generally a pressure driven membrane separation process that is performed in the range of 3-15 bar. Membrane used for NF process is generally charged membrane. NF is used for separation of sugars and divalent ions where particle size ranges from 0.5-5 nm. It can achieve very good separation of mono-valent salts with moderate pressure requirement[5].

The study mainly investigates the transport phenomena through the high-performance composite nanofiltration polyamide membrane. The rejection and flux of Cr (VI) solution were reported for different reaction time and concentration. The transport mechanisms of the ions through the membranes under different preparation conditions were investigated using a two-parameter model of Extended Nernst–Planck Equation to determine which mechanism (diffusive or convective) is the controlling factor for Cr(VI) removal [6]. The transport equations of ions through the membrane were discussed based on the Extended Nernst–Planck Equation, which includes three components such as ionic diffusion, electro migration and convective flow. Reflection coefficient for the solute avails the neglectance of the ionic portioning at membrane and external phase interface to study the transport mechanism[7].

2. MATERIALS AND METHODS

2.1 Membranes and Set up

A polyamide thin film composite nanofiltration membrane (NF TFC 200) in size 2540 with molecular weight cut off 200 was used in spiral wound configuration. The membrane was obtained from Permionics Pvt.Ltd., India. The operating limit of this membrane is provided in Table. The photograph of NF system used for this study. The NF pilot plant comprising feed tank, feed pump (low pressure), pressure sand filter, activated carbon filter, micron filter (5μ), intermittent tank, NF and RO membranes, high

pressure pump, etc., was obtained from Permionics pvt. Ltd., India

Table1. Membrane Characteristics

S.No.	Characteristics	NF	TFC
		200	membrane
1.	Maximum Operating Pressure	600	psig
2.	Maximum Operating Temperature	40	°C
3.	Free Chlorine Tolerance	< 0.1	ppm
4.	pH Range	3-10	
5.	Maximum Feed Flow	1.4	m ³ /h
6.	Surface area	2.6	m ²

The membrane housing cell was made of stainless steel with two halves fastened together with bolts. Prior to the start of the experiments, the membrane was stabilized with a pressure of 5 bars for 1 hour at 25°C. Both concentrate and permeate were returned to the feed vessel in order to maintain the constant concentration in the intermittent tank. Samples of the Permeate were collected to measure the observed Cr (VI) rejection,[2]

$$\% \text{ Rejection} = \left[\left(1 - \frac{C_p}{C_f} \right) \right] \times 100$$

(1)

Where C_f is the bulk feed solute concentration and C_p is the Permeate solute concentration. Further the chromium concentration was estimated by following standard APHA method (1992). The corresponding permeating flux (J_v) from the



FIG 1. Photograph of NF system

membrane was calculated as the volume of Permeate passing through the membrane per unit effective membrane area, per unit time in $Lm^{-2}h^{-1}$. Permeate flux is an important parameter to design and estimate the economic feasibility of the membrane separation process. After each experiment, the setup was rinsed with deionized water for 20min with 5 bar pressure to clean the system.[8]

2.2 Kinetic Modeling

The Extended Nernst–Planck Equation is one of the membrane transport model, which accounts for ionic diffusion, electro migration and convective flow through the membrane without considering morphology of the membrane. Besides considering the ionic and steric partitioning between the membrane and the external phases interface, reflection coefficient for solute sample was accounted to determine the transport mechanism of diffusive and convective flow. It depends on volume flux (J_v), Diffusive(f') and Convective(R') flow where the reflection coefficient of the samples was considered. The following equation is derived from the series of equation[6].

equation in terms of R' And f' . Substituting those R' and f' in equation (2). The solute flux(J_i) is given by the following equation.

$$J_i = B(C_m - C_p)$$

Where B is permeability coefficient and C_m is Concentration of solute at the membrane side and C_p is the concentration of solute in permeate.

3. RESULTS AND DISCUSSIONS

3.1 Permeate Characteristics studies

The permeate characteristics (Q_p and C_p) for spiral wound nanofiltration module were solved using the Finite difference method in our previous study. From this study we predicted the solute permeability (B) as $1.75 \times 10^{-7} m/s$, reflection coefficient as 0.9833 and mass transfer coefficient as $1.1 \times 10^{-4} m/s$. The maximum error between experimental and predicted values of C_p was below 3.1 %. However, the maximum error between experimental and predicted values of Q_p was below 13.1 %.. It was found

$$J_i = -f' \Delta C_i + J_v C_{i,o} (1 - R')$$

(2)

Where ΔC_i is the concentration of ion-I and $C_{i,0}$ is the concentration of ion-I at the concentrate side. The variables such as Volume Flux (J_v) and Solute Flux (J_i) were found from the previous work. The values of f' and R' can be calculated using Eq.3

$$R_r = \frac{R_p(J_v)J_v}{J_v + B_p(J_v)} \quad (3)$$

Where R_r is observed rejection. R_p and B_p are the constants which can be calculated using the following equations[6]

$$R_p = \frac{R'}{1 + (1 - R')(\exp(J_v/K) - 1)} \quad (4)$$

$$B_p = \frac{f' \exp(J_v/K)}{1 + (1 - R')(\exp(J_v/K) - 1)} \quad (5)$$

K is the mass transfer coefficient in m/s and By substituting equations (4) and (5) in (3) we get the [8]

that maximum error between experimental and predicted values of C_p and Q_p were below 10%. The permeate characteristics are given in the table

3.2 Extended Nernst Planck Modeling

Kinetic modeling based on ENP equation was used to describe the transport of hexavalent Chromium across the TFC NF200, including all the three components such as ionic diffusion, electromigration and convective flow. [7]

$$j_i = D_{i,p} \frac{dc_i}{dx} - \frac{z_i c_i D_{i,p}}{RT} F \frac{d\psi}{dx} + K_{i,x} c_i J_v$$

Since we consider only diffusive and convective flow, we use Eq.(2).from which value of f' an R' were predicted by Polymath Fogler Version 6.1 based on the experimental data in Table 2. These f' and R' values were tabulated in table 3.by solving using equation 3-5 and best fit of Extended Nernst Planck equation(Eq.2)was found by substituting in it. Thus by using the ENP equation, the transport of Cr(VI) across the membrane either by diffusive transport or

convective transport can be determined by calculating their ratio following Eq. (7):

$$\Gamma = \frac{-f'\Delta c_i}{J_v c_{i,0}(1-R')} \quad [7]$$

If the value of Γ is increases it signifies the flow is considered to be diffusive or else it is convective.

Table2. Permeate Characteristics for the Chromium (Cr VI) removal*

S.No.	P _f (Pa)	Q _f x10 ⁻⁴ (m ³ /s)	C _f (kg/m ³)	Q _{pExp.} x10 ⁻⁵ (m ³ /s)	Q _{pPredic.} x10 ⁻⁵ (m ³ /s)	% error Q _p	C _{pexp.} x10 ⁻² (kg/m ³)	C _{pPredic.} x10 ⁻² (kg/m ³)	% error C _p
1.	413685	1.96	0.06	1.66	1.6512	0.529	2.2045	22.238	-1.74
2.	482632	1.93	0.06	2.25	2.0211	10.174	2.0601	2.043	0.82
3.	551580	1.84	0.06	2.75	2.3906	13.065	1.9746	1.935	1.76
4.	620528	1.78	0.06	3.08	4.08	10.381	1.9140	1.874	1.86
5.	689475	1.74	0.06	4.08	3.5323	13.422	1.7926	1.845	-3.07

*-data obtained from the previous work

Table 3. Values of R'and f' for NF200 Membrane

S.No.	P _f (Pa)	F'	R'
1.	413685	5.197 E-07	0.9447748
2.	482632	4.94 E-07	0.921685
3.	551580	3.92 E-07	0.913819
4.	620528	9.12 E-06	0.892431
5.	689475	7.48 E-06	0.881429

4.CONCLUSION

Solute flux was found to be slightly higher than the diffusive and convective flow transport components. This signifies the error of about 6% - 13% in range of different pressure samples. It was found that at lower pressure there is minimal error as compared to maximum pressure. Based on the kinetic model performed with the extended Nernst Planck equation to understand the Chromium transport through the membrane it showed that the diffusive transport is dominant over the convective transport. Therefore to convert the flow to be convective the pressure should be increased with decrease in temperature.

REFERENCES:

- [1] Wahab Mohammad, R. Othaman, N. Hilal, "Potential use of nanofiltration membranes in treatment of industrial wastewater from Ni-P electroless plating" Desalination, vol ED.168 pp.241–252,2004.
- [2] S. Bajpai, A. Dey, M. K. Jha, S. K.Gupta, A. Gupta, "Removal of hazardous hexavalent chromium from aqueous solution using divinylbenzene copolymer resin". International Journal of Environmental Science and Technology, vol9 ED.4, pp.683-690, 2012.
- [3] Al-Rashdi, C. Somerfield, N. Hilal, "Heavy metals removal using adsorption and nanofiltration techniques", Separation and Purification Technology, vol ED.40, pp.209–259,2011.
- [4] N. M Gatto, M. A. Kelsh, D. Mai, M. Suh, D.M. Proctor, "Occupational exposure to hexavalent chromium and cancers of the gastrointestinal tract: A metaanalysis", Cancer Epidemiology, vol. ED 34, pp.388–399,2010.
- [5] F. J. Alguacil, M. Alonso, F. A. Lopez, A. Lopez-Delgado, I. Padilla, "Dispersion-free solvent extraction of Cr (VI) from acidic solutions using hollow fiber contactor"

Environmental science & technology, vol43 ED.20, pp.7718-7722,2009.

[6] W.P.Cathie Lee, Shee-Keat Maha C.P. Leo, Ta Yeong Wua, Siang-Piao Chai, "Phosphorus removal by NF90 membrane: Optimisation using central composite design" Journal of the Taiwan Institute of Chemical Engineers, ED.45, pp.1260–1269, 2014.

[7] A.L. Ahmad, B.S. Ooi, "Characterization of composite nanofiltration membrane using two-

parameters model of Extended Nernst–Planck Equation' Separation and Purification Technology, vol. ED 50, pp.300–309,2006

[8] Astrid Gjelstad, Knut Einar Rasmussen, Stig Pedersen-Bjergaard, "Simulation of flux during electro-membrane extraction based on the Nernst–Planck equation" Journal of Chromatography, 1174,pp.104–111,2007.



SEISMIC PERFORMANCE EVALUATION AND RETROFITTING OF RC MEMEBERS AND JOINTS

¹Dr. G.S Suresh, ²Mr. Sachin V

¹Professor, National Institute of Engineering, Mysore, Karnataka, India

² Post Graduate Student, National Institute of Engineering, Mysore, Karnataka, India

ABSTRACT: In the present work, structure designed and constructed for only gravity loads is considered for evaluation and retrofitting work. Finite element software ETABS is used to determine the seismic demand of each element. Retrofitting to increase the capacity of elements is suggested for the elements having ratio of Demand to Capacity more than 1. Pushover analysis is used to determine the performance of the structure before and after retrofitting. In the present work, deficient columns are retrofitted and re-analyzed to check performance of the structure in non-linear analysis. Performance of this retrofitted structure is then compared with the existing reinforcement structure and it is found that structure after retrofit have more base shear capacity and displacement capacity, storey drift of the retrofitted structure has decreased thereby ensuring a maximum safety of the structure even to the zone3 level of seismic intensity. From the present study it is brought out that structural elements designed only for gravity loads have less vulnerability to collapse in zone 2 level of seismic intensity, and for zone 3 level of seismic intensity itself structural elements fails to perform both serviceability limit state as well as ultimate-strength limit state.

KEY WORDS: Evaluation, Performance evaluation, Pushover analysis, RC joints,

Demand Capacity Ratio, Retrofitting, Non-linear analysis, Performance point,

1. INTRODUCTION

In the conventional limit state design approach, the designer normally takes into account the self-weight of the structure (dead load), imposed loads (live load), and depending on the location of the building, seismic, and climate related loads (wind and snow loads) are considered. While the vast proportion of the existing buildings experience only the types of loads mentioned above during their lifetimes, but building has to be designed to resist seismic load or lateral load which is assumed to occur once its life-time. In these conventional design method only two levels of design is considered, that is, ultimate-strength limit state and service-operational limit state for a building. But performance based design can be viewed as multi level design approach which has definite concern on performance of a building at intermediate limit states related to such issues as occupancy and life-safety standards. Hence we need to adopt a convenient analysis tool to analyze and design for performance-based approach. A structural analysis tool gives a number of analysis methods. For performance based analysis of structures a hierarchy of

structural analysis may be made. In which higher level procedure gives more accurate method of the actual performance of building subjected to earthquake loads, but interpretation of the results requires greater efforts and time consuming.

However in this work, existing reinforcement of the building is compared with linear static analysis result obtained as per the IS1893:2002(PART-1), structural elements which ever found deficient will be identified in this process and retrofitting methods are suggested. The performance of the building is checked using Non-Linear static procedure. Pushover analysis is a simplified, static, non linear procedure where a predefined pattern of earthquake loads is applied incrementally to the structure until a collapse mechanism is reached. The use of inelastic analysis procedure is an attempt to understand how structures will behave when subjected to earthquake load; it is assumed that the elastic capacity of the structure will be exceeded.

2. LITREATURE REVIEW

A detailed review has been carried out on the past research work on the behavior of joints both on experimental and analytical sides to focus on recent and past efforts related on seismic evaluation. A few research work done on the above mentioned area's are summarized below.

- ❖ **Pradip Sarkar, Rajesh Agarwal, and Devdas Menon (2007) [17]**, revised the relevant features of shear design of joints under seismic loads given in international codes of practice (ACI, NZS, EN) highlighting requirements of the various parameters. According to this paper shear transfer mechanism categorized into 2 mechanism viz. diagonal strut mechanism and truss mechanism. Assessment of shear strength, design and detailing of shear reinforcement has been covered. It is seen NZS is very conservative recommendation followed by Euro code and ACI give many practical recommendations. Whereas IS 13920:1993 is silent on many issues related to the design of RC beam column joints under seismic loading. Hence it is necessary to upgrade IS 13920 keeping with international trends.
- ❖ **G.Appa Rao, M.Mahajan, M.Gangaram, and Rolf Eligehausen (2008) [19]**, dealt with the method of strengthening non-seismically designed RC beam-column joints to seismic loading. Typical reinforcement details of joints in pre-seismic design have been explained. Review of strengthening method and features, advantages and test results of FRP in rehabilitation of RC structures have been discussed. Hence in this paper merits and demerits of the strengthening of joints have been highlighted.
- ❖ **S. R. Uma, and Sudhir K. Jain. (2006) [21]**, presented critical review of recommendations of well established codes regarding design and detailing aspects of beam column joints. The codes of practice considered are ACI 318M-02, NZS 3101: Part 1:1995 and the Euro code 8 of EN 1998-1:2003. All three codes aim to satisfy the bond and shear requirements within the joint. It is observed that ACI 318M-02 requires smaller column depth as compared to the other two codes based on the anchorage
- ❖ **Umesh Dhargalkar. (2002) [16]**, mainly dealt with the seismic assessment for the seismic retrofitting of the structures constructed with or without the seismic effect. The standard and comprehensive assessment involves data collection, compilation of data and assessing possible guidelines. Based on the data collected possible schemes of retrofitting can be checked by modelling an exact replica of the building. The best fit method is selected based on cost and convenience of implementation.

conditions. Significant factors influencing the design of beam-column joints are identified and the effect of their variations on design parameters is compared. The variation in the requirements of shear reinforcement is substantial among the three codes.

- ❖ **Sudhir K. Jain, and T. Srikant (2002) [22]**, discussed Pushover analysis for deficient buildings, new buildings or to make existing building perform well in future earthquake. In this work a four storey building with flat slab designed for wind load but not for seismic load is considered for the study. 2D frame of this building is modelled and Pushover analysis is performed in SNAP-2DX. Jacketing of column, providing additional beams and providing both columns jacketing and additional beams are the various retrofit schemes adopted. This scheme is studied at 4 different cases, i.e., at first storey only, first two storey, first three storey and all the four storeys. They found significant increase of strength and drift capacity when both jacketing of column and addition of beam.

3. PUSHOVER ANALYSIS

The Pushover analysis of a structure is a static non-linear analysis under permanent vertical loads and monotonically increasing lateral loads. The equivalent static loads approximately represent earthquake induced forces. A plot of total base shear versus top displacement in a structure is obtained by this analysis (Figure1) that would indicate any premature failure or weakness. The analysis is carried out up to failure, thus it enables determination of collapse load and ductility capacity. On a building frame, load/displacement is applied incrementally. The formation of plastic hinges, stiffness degradation and plastic rotation is monitored, and lateral inelastic force versus displacement response for the complete structure is analytically computed. This type of analysis enables weakness in the structure to be identified. There are different methods followed for pushover analysis. Basically it has been classified into two ways they are Force controlled and displacement

controlled. In force control, the structure is subjected to lateral forces and the displacements are calculated. In displacement control, the structure is subjected to a displacement profile and the lateral forces are calculated.

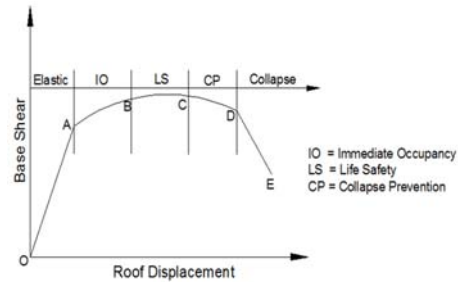


FIGURE.1. IDEALIZED PUSHOVER CURVE

4. PROBLEM STATEMENT

In the present work structural components of the building (Figure.2) are previously designed and constructed without considering the seismic effect. Structure is analyzed using ETABS by considering linear static analysis in x and y direction and Non linear static analysis along x direction only. ETABS design for seismic effect is compared with existing reinforcement and discussed. Capacity of each component with existing reinforcement in this building is compared with demand posed by the analysis results with consideration of lateral force for both Zone 2 and Zone 3 earthquake regions. This comparison is represented in the form of Demand and capacity ratios (DCR). Any structural elements found deficient in this DCR check will be retrofitted. For columns concrete jacketing and for beams Fiber Reinforced Polymer (FRP) wrapping is suggested. These analytical models (Zone2 and Zone3 ETABS designed models, existing reinforcement in Zone2 and Zone3 analysis, column retrofitted

models in Zone2 and Zone3) are subjected to PUSHOVER analysis, results obtained from this analysis are (Base shear versus Displacement curve, S_a versus S_d curve, Performance point and Hinge formation at performance point) discussed.

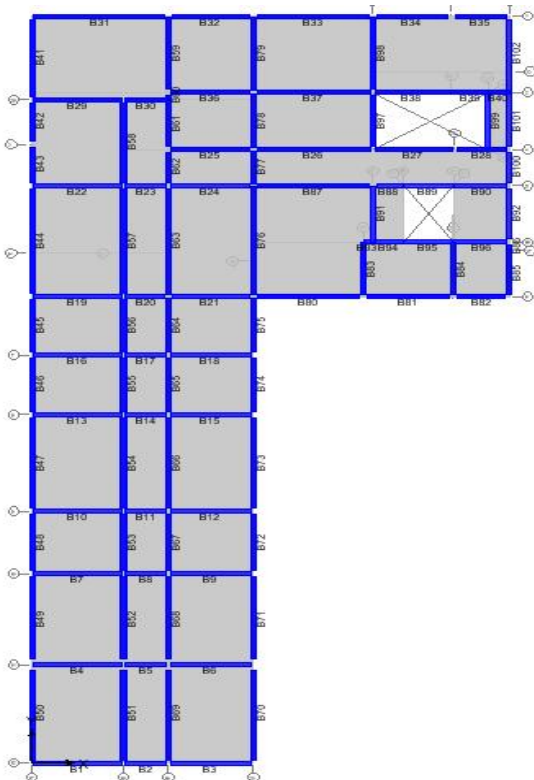


FIGURE.2 PLAN OF THE BUILDING CONSIDERED IN CASE STUDY5.

5. RESULTS AND DISCUSSION

I. EVALUATION OF BEAMS.

The capacity (flexural or shear) of the beam is obtained from the following derivation.

1. Moment of resistance of the beam (M_{ur}):

For a given cross section of the beam and for the existing reinforcement, Moment of resistance is calculated by finding Neutral axis (X_u) and determining stress and strain at the level of X_u . This is derived as follows.

STEP1: Stress at the level of neutral axis (X_u) is

$$\epsilon_{se} = \left(\frac{0.0035 \times (X_u - d')}{X_u} \right)$$

For the calculated stress, strain is obtained using stress-strain curve given in SP16.

STEP2: Based on the ideology, Compression (C) and Tension (T) are equal at X_u . Then C and T are calculated by;

$$C = (0.36 \times f_{ck} \times b \times X_u) + A_{sc} \times (f_{sc} - 0.45f_{ck}); \quad T = (f_{st} \times A_{st});$$

Where

b = breadth of the beam,

f_{ck} = flexural strength of concrete.

STEP3: After determining C & T moment of resistance is determined by

$$M_{ur} = (0.36f_{ck}bX_u) \times (d - 0.42X_u) + A_{sc}(d - d') \times (f_{sc} - 0.45f_{ck}).$$

STEP4: This Moment of resistance M_{ur} must be greater than Flexural demand M .

After determining the flexural capacity of the beam elements, it is compared with the demand obtained by ETABS linear static analysis with Zone2 and Zone3 seismic intensity and following results are obtained. And typical graphical representation is shown in Figure 3, 4 & 5.

1. 39 elements in left end of the beam, 82 elements in mid-span of the beam, 34 elements in right end of the beam have DCR value 1to2 in seismic Zone2. Where as in seismic zone 3 it is found that 83 elements in left end, 88 elements in mid-span, 89 elements in right end are deficient.
2. 12 elements in left end of the beam, 14 elements in mid-span of the beam, 6 elements in right end of the beam have DCR value 2to3 in seismic Zone2.

Where as in seismic zone 3 it is found that 27 elements in left end, 16 elements in mid-span, 17 elements in right end are deficient.

3. 2 elements in left end of the beam, 1 element in mid-span of the beam, 3 elements in right end of the beam have DCR value 3to4 in seismic Zone2. Where as in seismic zone 3 it is found that 7 elements in left end, 10 elements in right end are deficient.
4. 4 elements in left end of the beam, 4 elements in mid-span of the beam have DCR value above 4 in seismic Zone2. Where as in seismic zone 3 it is found that 5 elements in left end, 5 elements in mid-span, 5 elements in right end are deficient.

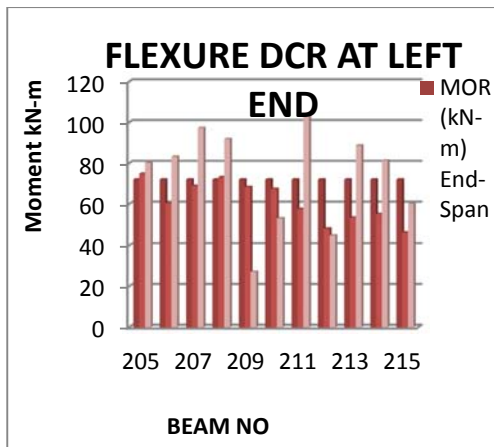


FIGURE.3. COMPARISON OF FLEXURAL DEMAND AND CAPACITY OF BEAM AT LEFT END

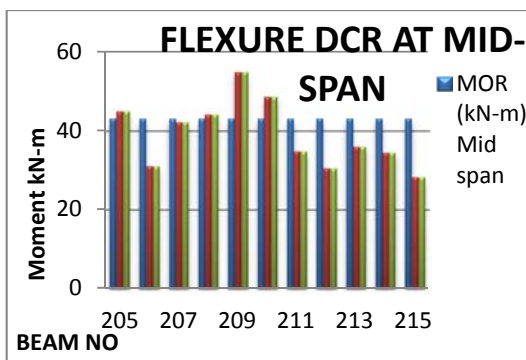


FIGURE.4. COMPARISON OF

FLEXURAL DEMAND AND CAPACITY OF BEAM AT MID-SPAN

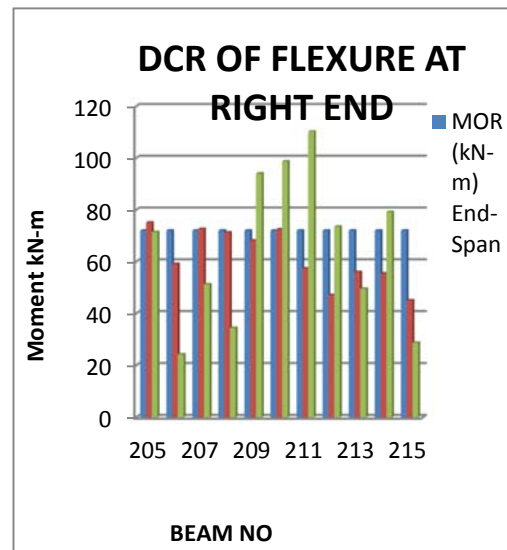


FIGURE.5 COMPARISON OF FLEXURAL DEMAND AND CAPACITY OF BEAM AT RIGHT END

From the above results it is observed that number of beam elements having DCR value greater than 1 are more in case of seismic zone3 and the structure is more vulnerable to seismic intensity zone3 itself.

2. Shear Capacity calculation (V_u): Shear strength concrete (V_{uc}) and Shear is strength of steel (V_{us}) is calculated and summation of this is compared with the Shear demand (V_u). The calculation of the shear demand is given by;

STEP1: For the existing A_{st} , Shear strength in concrete τ_c is found by utilizing IS456:2000 Table19. Where $\tau_c < \tau_{max}$.

STEP2: Shear resistance of concrete $V_{uc} = \tau_c b d$

STEP3: Shear resistance of the steel

$$V_{us} = \left(\frac{0.87 A_{sv} f_y d}{S_v} \right)$$

STEP4: Ultimate Shear resistance is given by

$$V_u = V_{us} + V_{uc},$$

where $V_u > \text{Shear demand (V)}$

STEP5: According to IS13920:1993, Shear force due to formation of plastic hinges at both ends of the beam plus the factored gravity load on the span.

For sway to right: $V_{u,a} = V_a^{D+L} -$

$$1.4 \left[\frac{M_{u,lim}^{As} + M_{u,lim}^{Bh}}{L_{AB}} \right]$$

And $V_{u,b} =$

$$V_b^{D+L} + 1.4 \left[\frac{M_{u,lim}^{As} + M_{u,lim}^{Bh}}{L_{AB}} \right]$$

Where

$M_{u,lim}^{As}$ & $M_{u,lim}^{Bh}$ are sagging and hogging moments of resistance of the beam section at ends A and B.

V_a^{D+L} and V_b^{D+L} are the shears at ends A and B due to vertical loads with 1.2 partial safety factor on loads.

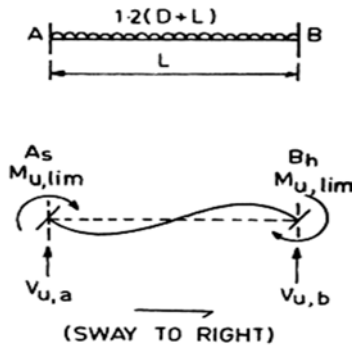


FIGURE.6. CALCULATION OF DESIGN SHEAR FORCE FOR BEAM

In determination of Shear demand of the beam we have taken only the gravity load

combination (i.e. DL+LL) hence we get only one shear demand and following results are obtained in terms of Demand Capacity Ratio DCR.

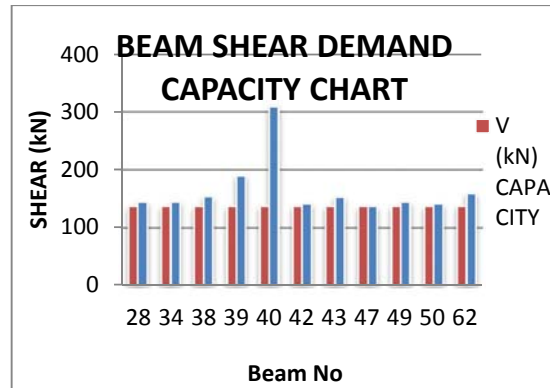


FIGURE.7.COMPARISON OF SHEAR DEMAND AND CAPACITY OF BEAM AT ENDS

1. 183 beam elements in the structure have DCR value 1 to 2.
2. 6 beam elements have DCR value 2 to 3.
3. 5 beam elements have DCR value 7 to 8 and
4. 5 beam elements have DCR value greater than 9.

II. EVALUATION OF COLUMN

In evaluation of the column the Factored axial load and moments (uni-axial or bi-axial) are compared with the ultimate moment carrying capacity of the column with the existing reinforcement and DCR is calculated. Similarly shear demand also calculated but compared with the capacity as given in IS13920:1993.given by

1. MOMENT CAPACITY OF THE COLUMN SECTION:

STEP1: For the given column section, existing reinforcement P_t , known d/D ration, p_t/f_{ck} is determined.

STEP2: By referring the interaction curve given in the SP16 for the actual $[P_u / f_{ck}bD]$, p_t/f_{ck} , determine $[M_u / f_{ck}bD^2]$ and calculate M_u , then compare it with the moment from the analysis.

STEP3: Determine the DCR of bending moment, member is safe if $DCR < 1$.

After determining the DCR of flexure following results are obtained.

1. 29 column elements have DCR value 1-2, 3 column elements have DCR value 2 to 3, 3 column elements have DCR value greater than 3 in zone2 seismic intensity. And
2. In zone 3 seismic intensity 46 column elements have DCR value 1 to 2, 8 elements have DCR 2 to 3, 3 elements have DCR 3 to 4 and 3 elements have DCR above 4.

In the case study structure 61 column elements were present out of which 60 columns have very less capacity in Zone 3 seismic intensity.

2. SHEAR CAPACITY OF THE COLUMN:

Calculation of shear capacity in column requires an assumption that one face of the steel reinforcement is completely in tension. Method of calculation of the shear capacity is explained with Figure.8.

STEP1: Area of reinforcement (A_s) of that face is calculated, for which τ_c is calculated from IS456:2000 Table 19.

STEP2: Since the shear reinforcement is known, Design shear strength is determined by;

$$V_{us} = \left(\frac{0.87 f_y A_{sv} d}{S_v} \right)$$

STEP3: Total shear strength (V_u) of the section is calculated by summing up the concrete shear strength (V_c) and shear strength of the stirrups (V_{us}), which is termed as shear capacity of the column.

STEP4: From the IS13920 the design shear force for column shall be the maximum of;

a) Calculated factored shear force from the analysis, and

b) A factored shear force given by $V_u = 1.4$

$$\left[\frac{M_{u,lim}^{bL} + M_{u,lim}^{bR}}{h_{st}} \right]$$

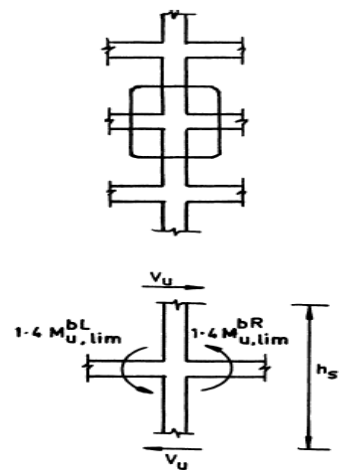


FIGURE.8. CALCULATION OF DESIGN SHEAR FORCE FOR COLUMN

Where,

$M_{u,Lim}^{bL} + M_{u,Lim}^{bR}$ Are moment of resistance, of opposite sign, of beams framing into the column from opposite faces and h_{st} is the storey height.

After a detailed evaluation of column it is found that all columns have higher shear strength capacity.

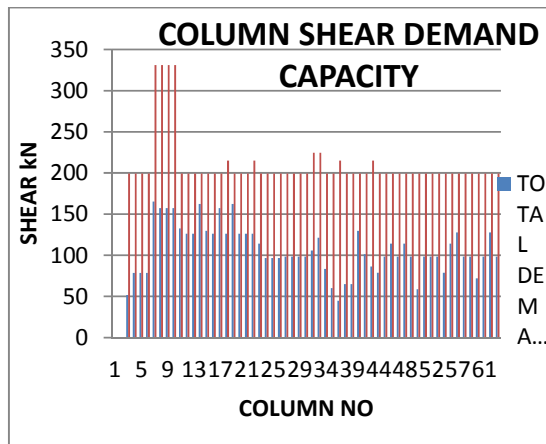


FIGURE.9.COMPARISON OF COLUMN SHEAR DEMAND AND CAPACITY

III.STRONG COLUMN WEAK BEAM

The current approach to the design of earthquake resistant RC rigid (i.e., moment resistant) frame is to have most of the significant inelastic action or plastic hinging occur in the beams rather than in columns. This is referred to as the “STRONG COLUMN-WEAK BEAM” concept and is intended to help ensure the stability of the frame while undergoing large lateral displacement under earthquake excitation. IS15988:2013 gives following equation to determine the strong column-weak beam

$$\sum M_c \geq 1.1 \sum M_B$$

Since interior column consists of beams running in two perpendicular direction, for the

simplification it is divided into Major and Minor axis. Number of Columns which do not holds good with Strong Column Weak Beam philosophy are tabulated in Table.1

TABLE.1. NUMBER OF COLUMNS WITH STRONG BEAM AND WEAK COLUMN

AXI S	STO REY 1	STO REY 2	STOR EY3	STO REY 4	STO REY 5
MAJ OR AXI S	37	48	38	34	39
MIN OR AXI S	25	20	11	9	12

Since too many columns in both major and minor axis are weak compared to its adjacent beams, retrofitting has to be adopted in all the storey level and performance is rechecked. Beam-Column joints of the case study 1 building are checked, and it is found that all joints are safe.

IV. RETROFITTING OF COLUMN

Evaluated columns after comparison with demand it is found that all columns are against the philosophy of “Strong Column Weak Beam”. Hence depending upon the DCR ration columns are categorized and retrofitted. A simplified analysis for the flexural strength of a retrofitted column can be done by the traditional method of interaction curves (SP 16: 1980, “Design Aids for Reinforced Concrete to IS 456: 1978,

published by the Bureau of Indian Standards). The retrofitted columns and dimension are shown in Table.2.

TABLE.2. Details Of Retrofitted Columns

SL.NO	Existing Column Size (mm)	Revised Section (mm)	Increased Ast mm ²	Total Columns
1	200X380	300X480	1561	40
2	200X685	300X785	3000	4
3	200X380	300X480	1273	3

V. STOREY DRIFT

TABLE.3. PERCENTAGE DECREASE IN STOREY DRIFTS OF THE RETROFITTED BUILDING

ZONES	DRIFT X	DRIFT Y
ZONE 2	45%	40%
ZONE 3	45%	42%

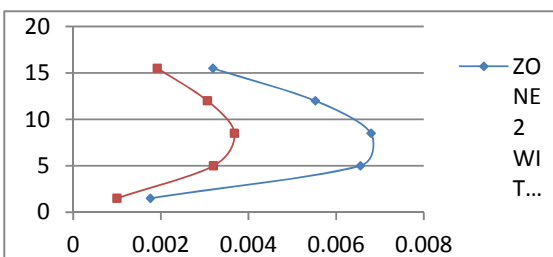


FIGURE.10.STOREY DRIFT X IN ZONE 2

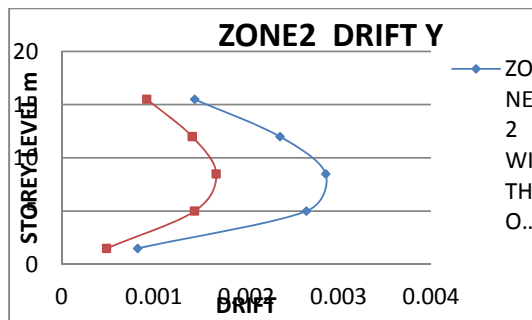


FIGURE.11.STOREY DRIFT Y IN ZONE3

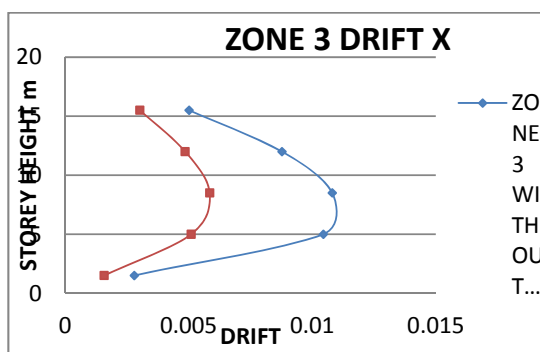


FIGURE.12.STOREY DRIFT X IN ZONE3

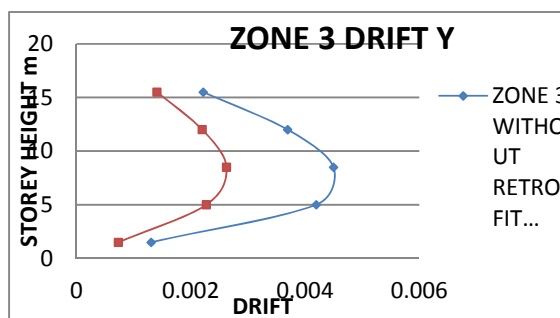


FIGURE.13.STOREY DRIFT Y IN ZONE 3

The actual storey drift of the case study building is displayed in Figure 10, 11, 12 and 13. In these figure's displacement of building in X and Y direction, with existing reinforcement and retrofitted members are compared and the percentage of decreased drift in the retrofitted model are shown in the Table.3. From the results of the storey drift we can conclude that, after retrofitting the building storey drift is reduced by 45% in X direction in both Zone2 and Zone3 seismic region and a 40% reduction in storey drift in Y direction in both Zone2 and Zone3

seismic region. Hence the building is safe after retrofitting under serviceability limit state.

6. RESULTS AND DISCUSSION OF PUSHOVER ANALYSIS

The result obtained from the Pushover analysis that is Base shear versus Displacement, Spectral acceleration versus Spectral Displacement and Hinge formation at performance point are discussed.

I. COMPARISON OF PUSHOVER CURVES

The case study building is designed in ETABS for ZONE 2 and ZONE 3 seismic loading. The same building is analyzed with the existing reinforcement without altering the member dimensions. During the evaluation part of the case study1 structure, it is observed that the columns are deficient in load carrying capacity. Hence retrofit is carried out to all columns. This retrofitted column is provided as such in ETABS and analyzed. Pushover analysis is carried out to all the above cases and 4 different PUHOVER curves are obtained and displayed in Figure.14.

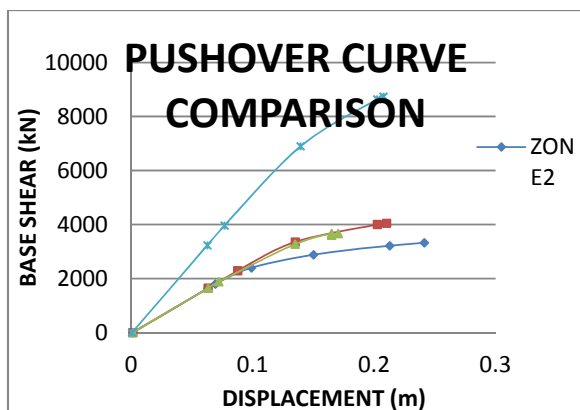


FIGURE.14. PUSHOVER CURVE COMPARISON

From the comparison of the PUSHOVER curves following conclusions are drawn

- i. Structure with existing reinforcement has lesser base shear capacity and displacement capacity compared to the

same structure designed for Zone2 and Zone3 level of earthquake. Hence, the structure with existing reinforcement is more vulnerable compared to those designed for earthquake loads.

- ii. Structure designed for Zone 2 has lesser base shear capacity compared to the structure designed for Zone3. Hence it can be concluded that structures designed for higher zones of earthquake have better seismic capacity.
- iii. The pushover curve for retrofitted building shows very high base shear capacity and displacement capacity compared to all other structure. Hence this structure is less vulnerable compared to all other building.
- iv. Retrofitting of the existing deficient buildings as detailed in the present study can be an efficient way of improving the seismic performance of vulnerable buildings.

II. COMPARISON OF PERFORMANCE POINT

TABLE.4. COMPARISION OF HINGES AT PERFORMANCE POINT

	D is p l a c e m e n t	B a s e	F o r c e	A-B	B - I O S O L S	I - O L C P	L - C C	C - C C	C - D E	D - E	> T O T A L
Z O N E 2	0. 0 9 9	2 3 8 3	1 3 8	134	1 1 8	0	0	0	0	0	16 10
Z O N E 3	0. 1 3 5 1	3 3 5 6	1 3 3 2	137	1 2 2	1 9	0	0	0	0	16 10

			. 4									
E X I S T I N G	0. 1 3 5	3 2 7 4 9	1 4 6 9	44		5 4	4 2	0	1	0	0	16 10
R E T R O F I T T E D	0. 7 6 8	3 9 6 5 4	1 5 4 2	56		1 2	0	0	0	0	0	16 10

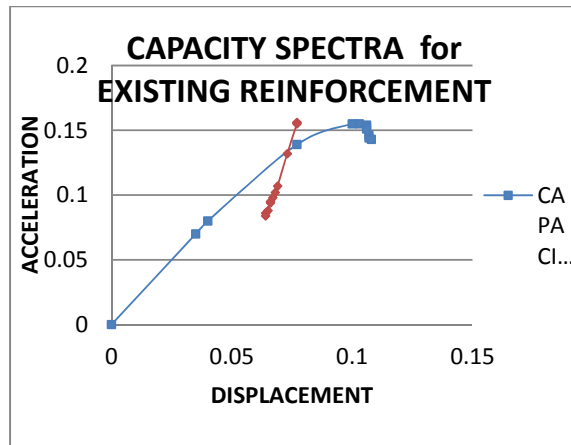


FIGURE.17.CAPACITY SPECTRA FOR STRUCTURE WITH EXIXTING REINFORCEMENT

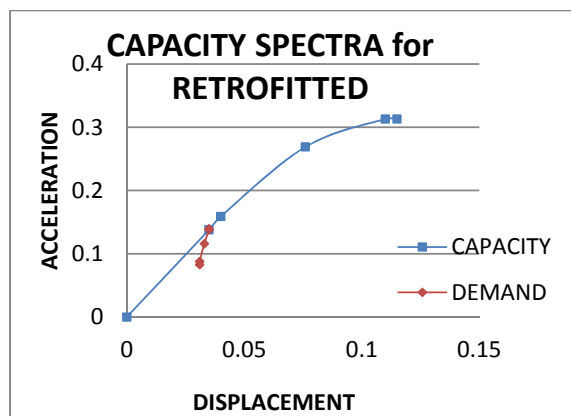


FIGURE.18.CAPACITY SPECTRA FOR STRUCTURE WITH ZONE2 DESIGN

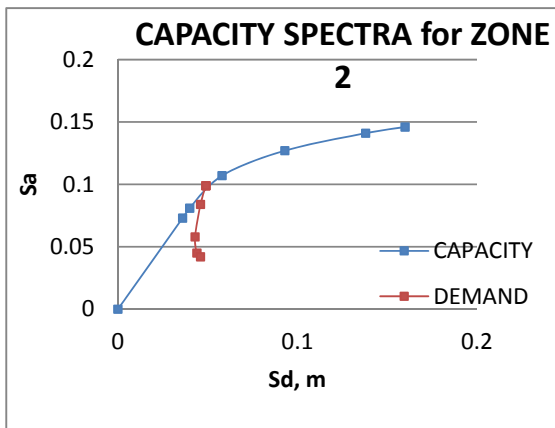


FIGURE.15.CAPACITY SPECTRA FOR STRUCTURE WITH ZONE2 DESIGN

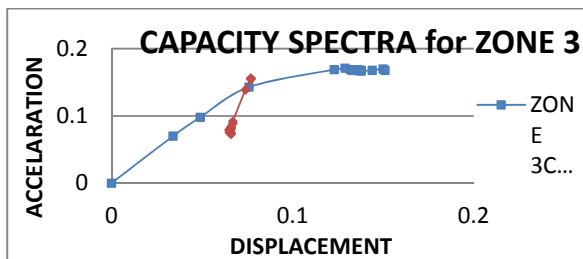


FIGURE.16.CAPACITY SPECTRA FOR STRUCTURE WITH ZONE3 DESIGN

The representation of the two curves in one graph is termed as the Acceleration versus Displacement Response Spectrum (ADRS) format as in Figure 15, 16, 17 and 18. The performance point is the point where the capacity spectrum crosses the demand spectrum. If the performance point exists and the damage state at this point is acceptable, then the building is considered to be adequate for the design earthquake. In the present case study, 4 different capacity spectrums are generated for the same structure (i.e., those designed for Zone2 and Zone3, existing reinforcement, retrofitted structural elements). Hence the capacity spectra of all the 4 models are represented and compared. The status of hinges formed at the performance point is depicted in Table.4. With

the performance point in all the 4 cases, we can conclude that in those designed for Zone2 and Zone3 cases, number of hinges in vulnerable damage states formed at performance point are more compared to the other two cases. In structure with existing reinforcement at performance point itself hinges have reached Collapse prevention level, where in other 3 cases no hinges are in collapse prevention level. Very few hinges are formed at immediate occupancy to life safety level in case of structure with Zone3 design and existing reinforcement cases, where no hinges formed in structure with Zone2 design and retrofitted case. In retrofitted structure very less hinges are formed and more hinges are there in elastic region itself. This concludes that retrofitted structure has very few elements that are vulnerable.

7. CONCLUDING REMARKS

- The data obtained in the form of results of analysis for structural elements (Beams and Column) by ETABS is huge. This has to be sorted out systematically so that evaluation of members becomes easier.
- Results of analysis for gravity and earthquake loading obtained in the ETABS are considered as Demand posed on the structure. This demand is compared with the capacity of the elements
- During the linear static analysis of the structure, it is observed that seismic demand of the structural elements increase with the change in the seismic zone and soil type. But the capacity remains unchanged. Hence this demand and capacity of the elements is compared.
- DCR of beam and column in flexure and shear in zone 2 exceeding 1 is less than that in seismic zone 3. This states that elements are more vulnerable to seismic zone3. Hence such column elements are identified and retrofitted using concrete jacketing.
- Before retrofitting almost all columns were failed in ETABS design check. But after retrofitting, all the column elements became safe to the ETABS design check.
- The pushover analysis is a relatively simple way to explore the non linear behavior of the buildings. The results obtained in terms of demand, capacity gave an insight into real behavior of the structure.
- Pushover analysis of casestudy1 building is carried out in 4 different cases. By the comparison of the pushover curve at all incidences we can say that existing structure, which was originally designed for gravity loads only, is more vulnerable to the lateral loads. Hence retrofit is recommended.
- Retrofitted structure is then analyzed using Pushover analysis. It is observed that with the increase in the column section and reinforcement, the base shear capacity and displacement capacity is increased tremendously.
- Pushover analysis also gives status of hinge formation at different level of displacement/base shear. After comparison of the hinge formation at the level of performance point in existing structure, it is found that more hinges have crossed elastic limit than the retrofitted structure. Also some hinges have been observed at collapse level in existing reinforcement structure.
- Comparison of Storey drift of the existing and retrofitted structure shows that structure after retrofit have about 50% less storey drift.
- Hence with all these information it can be concluded that structure after retrofitting the columns only, have shown increased

performance for both linear static and non linear static analysis.

- Performance based evaluation of structures gives true picture of element level and global level states of buildings. Pushover analysis can be effectively used in assessing the seismic performance evaluation of buildings.

REFERENCES

1. ACI-ASCE committee 352, American Concrete Institute, Detroit. "Recommendations for Design of Beam-Column joints in Monolithic Reinforced Concrete Structure". As a part of *Journal of Structural Engineering*, May-June 1985.
2. Daniel P Abrams. American Concrete Institute, Detroit. "Scale Relation for Reinforced Concrete Beam-Column joints". As a part of *Journal of Structural Engineering*, November-December 1987.
3. Bahjat Adbel Fattah and James.K.wight. "Study of Moving Beam Plastic Hinging Zones for Earthquake Resistant Design of RC building". American Concrete Institute, Detroit. As a part of *Journal of Structural Engineering*, January-February 1987.
4. A K Jain and R A Mir. The Indian Concrete Journal "Inelastic Response of Reinforced Concrete Frames Under Earthquake". April 1991.
5. V Kumar, B D Nautiyal and S Kumar. The Indian Concrete Journal. "A Study of Exterior Beam-Column Joints". As a part of *Journal of Structural Engineering*, January 1991.
6. A G Tsos, I A Tepos and G Gr Penelis. American Concrete Institute, Detroit. "Seismic Resistance of Type-2 Exterior Beam-Column Joints Reinforced with Inclined Bars". As a part of *Journal of Structural Engineering*, January-February 1992.
7. Moshe. A. Adin, David Z.Yankelevsky and Daniel N. Farhey. American Concrete Institute, Detroit. "Cyclic Behaviour of Epoxy-Repaired Reinforced Concrete Beam-Column Joint". As a part of *Journal of Structural Engineering*. March-April 1993.
8. Andre Filiatrault, Sylvain Pinear and Jules Houde. American Concrete Institute, Detroit. "Seismic Behavior of Steel Fiber Reinforced Concrete (SFRC) Interior Beam-Column Joint". As a part of *Journal of Structural Engineering*, September-October 1995.
9. Gregory.S.Raffelle and James.K.Wight. American Concrete Institute. "Reinforced Concrete Eccentric Beam-Column Connection Subjected to Earthquake Type of Loading". As a part of *Journal of Structural Engineering*. V.92, No1, January-February 1995.
10. Cheng-Cheng Chen and Gwang-Kai Chen. American Concrete Institute, Detroit. "Cyclic Behaviour of RC Eccentric Beam-Column Joints Connecting Spread-Ended Beams". As a part of *Journal of Structural Engineering*. V.96, No3, May-June 1999.
11. Shingeru Hakuto, Robert Park and Hitoshi Tanata. American Concrete Institute, Detroit. "Seismic Load Test on Interior and Exterior Beam-Column Joints with Sub-Standard Reinforcing Details". As a part of *Journal of Structural Engineering*. V.97, No1, January-February 2000.
12. N.Ganeshan and P.V.Indira. *The Indian Concrete Journal*. "Latex Modified SFRC Beam-Column Joints Subjected to Cyclic Loading". July 2000.
13. C.V.R.Murthy, Durgesh.C.Rai, K.K.bajpal, and Sudhir.K.Jain. *The Indian Concrete Journal*. "Anchorage Details and Joint Design in Seismic RC frames". April 2001.

14. Ziad Bayasi, and Michael Gebman. American Concrete Institute, Detroit. "Reduction of Lateral Reinforcement in Seismic Beam-Column connection via Application of Steel fibers". As a part of *Journal of Structural Engineering*. V.99, No6, November-December 2002.
15. Bing Li, Yiming Wu, and Tso-Chien Pan. American Concrete Institute, Detroit. "Seismic Behavior of Non-Seismically Detailed Interior Beam-Wide Column Joints". As a part of *Journal of Structural Engineering*. V.99, No6, November-December 2002
16. Umesh Dhargalkar. *The Indian Concrete Journal*. "Seismic Assessment of Buildings Methodology". August 2002
17. Pradip Sarkar, Rajesh Agarwal, and Devdas Menon. *Journal Structural Engineering*. "Design of RC Beam-Column Joints under Seismic Loading". Vol.33, No 6, February-March 2007.
18. Balthasar Novak, K.Ramanjaneyulu, Constanze Rohem and Saptharshisasmal. *Journal of Structural Engineering*. "Seismic Performance of D-region framed structure Designed according to Different code Requirement". Vol.35, No 1, April-May 2008.
19. G.Appa Rao, M.Mahajan, M.Gangaram, and Rolf Eligehausen. *Journal Structural Engineering*. "Performance of Non-Seismically designed RC Beam-Column joints strengthened by various schemes subjected to Seismic Load". Vol.35, No 1, April-May 2008
20. Akanshu Sharma, G.Genesio, and R.Eligehausen. *Journal of Structural Engineering*. "Non linear Dynamic analysis using Micro-plane model for concrete and Bond slip model for prediction of Behavior of Non-Seismically detailed RCC Beam-Column Joints". Vol.36, No 4, October-November 2009
21. S.R.Uma and Sudhir Kumar Jain, IIT-Kanpur March 2006.
22. Sudhir K.Jain and T.Srikant. *The Indian Concrete Journal*. "Analysis for seismic retrofitting of buildings". August 2002Seismic
23. IS -456-2000 -Code of Practice for Plain and Reinforced Concrete.
24. SP -16- Design Aids for Reinforced Concrete.
25. IS -875-1987 (Part-2) – Code of Practice for Live Loads Over Structures.
26. IS -1893-2002 (Part-1) –Code of Practice for Seismic Design
27. IS -15988 - 2013 - Seismic Evaluation and Strengthening of Existing Reinforced Concrete Buildings
28. IS -13920 -1993 - Ductile Detailing of Reinforced Concrete Structures Subjected to Seismic Forces



BUDGET MONITORING OF RESIDENTIAL BUILDING

¹Ingle Prachi Vinod

^{#1} Dept. of Civil Engineering, Bhivarabhai sawant college of Engg, Pune,

Email:¹prachi03ingle@gmail.com

Abstract

Financial planning is base for survival of any construction industry. It is essential as it identified as the common cause of business failure, and can lead to the failure of profitable and growing firms as well as those declining. As such, there is a need for adequate timing of fund availability in construction and deployment of excess fund to more productive use. Accurate cash flow projections are important to both an owner and a contractor. A corporation's business plan generally includes multi-year cash flow and expenditure forecasts and continuous budget monitoring should be done. Inaccurate cash flow projection of a large project can lead to take wrong decision which may not be in favor of company. Budget helps to aid the planning of actual operations by forcing managers to consider how the conditions might change and what steps should be taken now and by encouraging managers to consider problems before they arise.

Keywords *financial planning, cost control*

Introduction

As many of large scale project gets delay due to funds which is indirectly related to continuous budget monitoring. The project cash flow projection is derived from an execution plan and estimated expenditure. Many projects treat estimated expenditures as cash flow projections. A planned project cash flow is the baseline for comparison with the actual project expenditure. The purpose of budgeting is to

- 1) To provide forecast detail report on expenditure and revenues.
- 2) Whether actual budget and planned budget are implemented.

- 3) Establish cost constraint for project.

We consider the problems associated with resource utilization, accounting, monitoring and control during a project. Interpretation of project accounts is generally not straightforward until a project is completed, and then it is too late to influence project management. There are various problems associated with resource utilization, accounting, monitoring and control during a project. Even after completion of a project, the accounting results may be confusing. Hence, managers need to know how to interpret accounting information for the purpose of project management. A project typically goes through multiple phases till it gets final. Cost estimates, schedule and an execution plan are developed at each phase. Cash flow projection is also prepared to support funding decision at each stage. The time at which major cost savings can be achieved is during planning and design for the project. During the actual construction, changes are likely to delay the project and lead to inordinate cost increases. As a result, the focus of project control is on fulfilling the original design plans or indicating deviations from these plans, rather than on searching for significant improvements and cost savings. The detailed cost estimate provides a baseline for the assessment of financial performance during the project. Project budget is used as a guide for management. As a result, cost overruns or savings on particular items can be identified as due to changes in unit prices, labor productivity or in the amount of material consumer. Good managers should focus upon future revenues, future costs and technical problem.

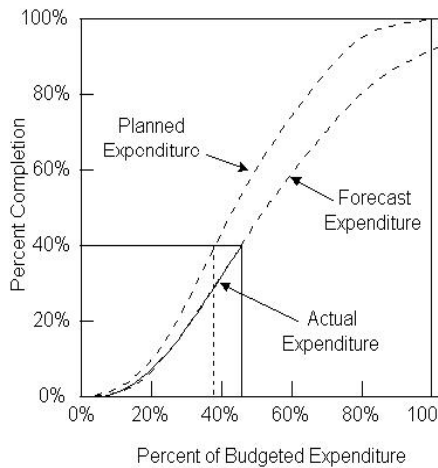


Fig 1. Graph Proportion Completion versus Expenditure for an Activity

Construction projects normally involve numerous activities which are closely related to the use of similar materials, equipment, workers or site characteristics. Without this updating, project schedules slip more and more as time progresses. To perform this type of updating, project managers need access to original estimates and estimating assumptions. In the traditional sense, the purpose of preparing budget is to understand and control costs. This concept of budget has therefore transformed into using budget proposal as an instrument for individual, public and private policy. It is useful to all parties involved in a project as a planning and control tool. Budget could be employed by the client to get priorities among projects competing for limited resources. Many start-up companies fail because of insufficient cash flow. Cash flow is where the project cost meets the schedule. Cash flow projections developed from credible project execution plans become the basis of project controls. Combining the cash flow and earned value technique, a project can track the real status of progress and detect any early cost deviation. Cash flow means the amount of cash being received and spent during a defined period of time.

Budget Monitoring Methodology:

A budget structure in construction projects is constituted of cost accounts such as bills, sections, items, and resources. Generally, a budget structure in construction projects includes into labor, material, equipment, subcontract, and indirect expenses

1. Budget Monitoring Process

In budget monitoring process we need to monitor each and every phase of project. There are various cost parameters and cost weight age which should be considered.

2. Evaluate the budget Process of residential building

when evaluating budget process all phases of budget are very important. Project initiation and development phase is very important activity for any budget monitoring. Other activity like estimation, construction and maintenance phases are also important in budget monitoring. Project Influence is highest or cost is negligible.

3. Analyze the budget process

Analyzing of budget process is very important. This stage is carried out continuous by while analyzing of budget we focus on procedure which is carried on site. Various techniques must be used for analyzing budget.

4. Develop Budget monitoring process

There are number of soft ware's available in market to work out cash flow and budgeting of any construction project

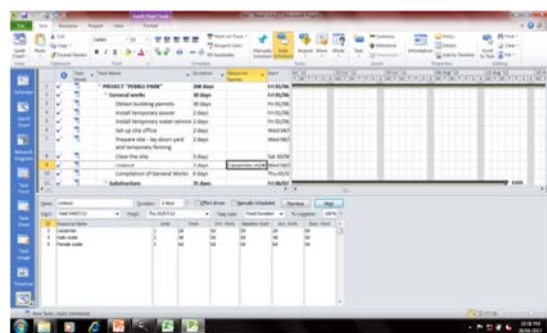
- 1) Primavera
- 2) Hit-office
- 3) Microsoft Project
- 4) Implementing using softwares.

Steps involved in Budgeting Process

1 linking of activity

2. Assigning Resources.

Such as material, labor, equipment. To monitor detail cost required for material used, equipments are hired or not rent bases. Which type of equipments is used.No. of labor used, wages being paid for them.



3. Make a comparative study of actual with the Resource sheet

plan

Using MSP we can Track the Gantt this gives comparison of actual duration and planned duration of project.

4. Develop s curve using MSP tool

S curve is the s shaped graph produced by the sigmoid formula which calculates the cumulative expenditure of certain parameters (man-hours, cost) against time and it is the representation of project path.

5. Applying the monitor tool to other project

There are various tools which we use in project. we find cash flow which is very important to monitor budget. Cash flow means the amount of cash being received and spent during a defined period of time.

In this Project Budget monitoring and various constraints are focused which are important.

Name of Site: Shriniwas Rainbow Developers

Location: Bavdhan Pune.

Type of Project: Residential Building

Slab area: 429392sqm

Salable built up: 317185sqm

The quantities required for man power study are calculated from the drawings

Estimation of quantity.

Sr No.	Item Of Work	Amount
1	Civil Cost	389305080.35
2	Development Cost	52283464.78
3	Podium Cost	59794169.09
4	Landscaping & Hardscaping & Lighting	8700000.00
5	Overheads	29800000.00
6	Other Expenses	40131788.67
	Total	580014502.89

Rate analysis

It is calculated with help of amount of quantity and rates for them.

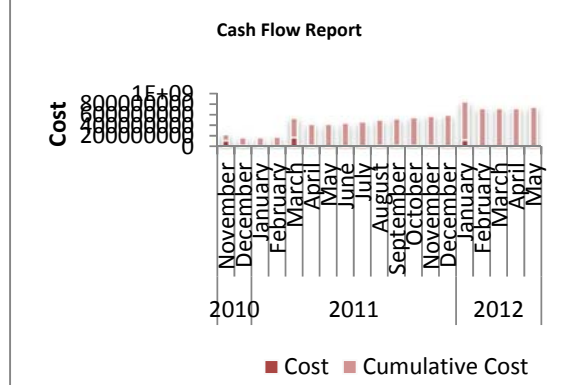
Linking in MSP

Linking is done for all activity. Critical path is determined so that we understand longest route. After preparing the schedule in MSP software the total project duration is estimated as 480 working days.

After linking activity we assign resources. Resource can be labor, material, and equipments. In resource sheet all standard rates are considered.

Comparison of actual and planned duration of projects.

Comparison of actual and planned duration of projects is done with help of tracking. Tracking means recording project details such as who did what work, when the work was done, at what cost. These details are often called as actual. Tracking is required to know the status of project, is too essential to track the project and to record the schedule of progress of work being performed. The total project cost is Rs 726964820.02 we have got cash flow. The total cost of the project has been divided into two types namely, direct cost and indirect cost. Direct project costs are those expenditures, which are directly chargeable to and can be identified specifically with the activities of the project. These include labor cost, equipment cost, transportation cost etc. cash outflow is not that more in the beginning later it goes on increasing and finally becomes very less. In initial stages of project the cash flow is not that much it constantly gets increased and later gets decreased. We also calculate resource cost summary. As we know 70 to 80 percent cost should be of material.



Scurve

The start up phase includes planning and mobilisation phase in which we need to take care about resource allocation. At start it picks up rapidly and towards end it decelerates again as multiple loose end. S curve is a virtual representation of progress path. S curve is the s shaped graph produced by the sigmoid formula which calculates the cumulative expenditure of certain parameter

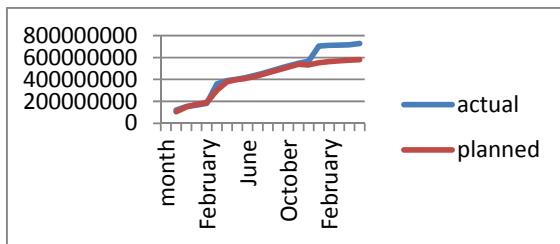


Fig 2. S Curve Analysis for Planned and Actual

Limitation Of study

The limited objective of budget monitoring is to control deserves emphasis. Budget control procedures are primarily intended to identify deviations from the project plan rather than to suggest possible areas for cost savings.

Conclusion

The total Budget cost estimates for project consists of actual cost of project increased by 153 million which was planned as 580 million and the actual cost of project is 73 million within period of 2012-2013. The Following parameters are responsible for increasing amount within one year.

Sr. No.	Parameter	Percent
1.	Internal plastering of 12 th floor	86%
2.	External painting(left side)	52%
3	External painting(front side)	15%
4.	External painting(right side)	47%
5.	Aluminum window grills	65%
6.	Internal painting 10 th floor	9%
7.	Building finishes	55%
8.	Garbage chute	1%
9.	Landscape	60%
10.	Sanitary fitting	75%

Sr. No	Delay	Duration(month)	Reason
1	Environment clearances	6	Due to no environment clearances all work got stop.
2	Permission	3	The permission was not sanctioned by town planning department up to G+12
3	Building Finishes	8	In proper planning

• **S curve analysis.**

The main highlights are in month of November, March and January due to which project got delayed. S curve is plotted in which we clearly get idea in month of November Rs119620313 was needed as it was initial stage of project so cost got increase. In month of March usage was Rs 35911873.19 at this time podium construction was there which requires huge investment and there was material shortage so money usage was more. In month of January investment was Rs703765331.9 the activities like external painting and external plastering was being there. Due to insufficient labor the cost got increase. From s curve it states that there is smooth flow of cash throughout the period with deviation in project.

- Excavation cost has provided with high rate by 15 to 20 Rs per cum rate as there was no space nearby to dump the material. The lead was not in region of 1km so they had to pay more for it.
- Cash inflow is calculated which came Rs. 2297018147.
- The profit margin was reduced by Rs. 153,022,021.

Future Scope:

The MSP software is the first source in conducting this study. This software will be used to develop a budget monitoring for the building construction project.

ACKNOWLEDGMENT

It's my pleasure to express my deep sense of gratitude to thank Prof S.v.Pataskar, PG co-coordinator civil department, for their valuable guidance, inspiration.

REFERENCES

- 1) Hyung K. Park¹, "Cash Flow Forecasting Model for General Contractors Using Moving Weights of Cost Categories"
- 2) Fagbenle Olabosipo "Developing a realistic budget for construction project" Department of building technology covenant university.

- 3) Tarek Zayed "Cash flow analysis of construction projects", Department of Building, Civil, and Environmental Engineering, Concordia University, Montreal, Canada.
- 4) Mark T. Chen "ABC of Cash Flow Projections".
- 5) Henry A. Odeyinka, "An evaluation of construction cash flow management approaches in contracting organizations", Nottingham Trent University, Nottingham School
- 6) Wenhua Hou, "Payment Problems, Cash Flow and Profitability of Construction Project", World Academy of Science, Engineering and Techno.
- 7) "Financial Management by," Prasanna candra.
- 8) www.sciencedirectory.com
- 9) www.asce.org



PRODUCTION OF BIOACTIVE COMPOUNDS USING MARINE ISOLATES IN CO-CULTURING SYSTEMS

¹Panjwani R, ²Deshpande A, ³Mahajani S, ⁴Joshi K

^{1,2,3,4} Sinhgad College of Engineering, Pune

Email: ¹richapanjwani@gmail.com, ²adabhishek260@gmail.com,

³smahajani.scoe@sinhgad.edu, ⁴joshikalpana@gmail.com

Abstract— Co-culture is the simultaneous cultivation of two or more species of microorganisms in the same medium. Routine laboratory procedures practice culture of a single microorganism wherein only a fraction of the total genes are expressed. Co-cultivation of two or more different microbes tries to resemble the natural environment in which these organisms originally grow. Competition between microbes is induced deliberately and stressful conditions arise leading to enhanced production of compounds produced in pure cultures or production of novel compounds that are not detected in pure cultures. Present study deals with the production of bioactive compounds in co-culture of marine microorganisms. These compounds were purified and further screened for antimicrobial activity against multiple drug-resistant micro-organisms.

Index Terms—Bioactive compounds, co-culture, marine, multiple drug-resistant micro-organisms.

I. INTRODUCTION

The marine environment covers almost 70% of the earth surface. Marine water bodies are a rich source of microorganisms which include a variety of fungus, bacteria, actinomycetes, etc.

and these organisms represent a novel source of new bioactive compounds. Marine organisms are a potent source for new biologically active secondary metabolites. Marine-derived fungi and bacteria from various coasts have been isolated, characterised and exploited for the production of various drugs.

Co-culture systems have been used to study the interactions between cell populations and are fundamental to cell-cell interaction studies of any kind. A co-culture is a cell cultivation set-up, in which two or more different populations of cells are grown with some degree of contact between them. These techniques find myriad applications in biology for studying natural or synthetic interactions between cell populations. The main reason for conducting co-culture experiments and motivation for using such a set-up include: (1) studying natural interactions between populations, (2) improving cultivation success for certain populations, (3) establishing synthetic interactions between populations [4]. The importance of this study is to compare the rate of antibiotic production by the bacteria solely and when it is co-inoculated with another bacterium. Quorum sensing forms the basis for cell induced antibiotic production. Bacterial cells have the ability to show cell to cell communication in presence of another bacteria with their autoinducers. This allows the bacteria to sense a critical cell mass and in response activate or repress target genes [5].

Marine microorganisms are a major source for Marine Microbial Natural Products (MMNP) discovery [3]. Co-cultivation is also one of the techniques used for activation of the silent genes for the production of new compounds. Growing or cultivating of two or more microorganisms in the same broth is called co-cultivation, also referred to as “mixed fermentation”. The present study deals with co-cultivation of marine microbial isolates. The extraction of bioactive compounds and further screening for antimicrobial activity was attempted against multiple drug-resistant micro-organisms isolated from clinical samples resistant against commonly used antibiotics.

II. MATERIALS AND METHODS

Marine microbial strains and media

The marine microbial strains used in this study are as follows: *Aspergillus fumigatus* (NCIM902), *Bacillus pumilus* (NCIM2327), *Candida albicans* (NCIM3100) and *Rhodococcus* sp. (NCIM5452). Strains were obtained from National Collection of Industrial Microorganisms (NCIM). *Bacillus* and *Rhodococcus* strains were cultured in nutrient broth (as suggested by NCIM) at 37°C while *Aspergillus* and *Candida* strains were cultured in yeast-malt extract broth at 37°C.

Test organisms

To test the antibiotic activity, clinical cultures of drug resistant strains, Methicillin resistant *Staphylococcus aureus* (MRSA), *Pseudomonas aeruginosa* (resistant to commonly used antibiotics) and MDR *E. coli*, isolated from clinical samples were used.

Pre-tests for microbial inhibition

To test the inhibition of one organism due to the bioactive compounds produced by another, cross streak method was used. Nutrient agar plates and yeast-malt extract agar plates were prepared. On these plates, one microorganism was streaked horizontally, while the other was streaked from the edge of the plate perpendicular to the first streak.

Combinations of organisms used for co-culture:

1. *Aspergillus fumigatus* – *Rhodococcus* sp. on nutrient broth agar plate

2. *Bacillus pumilus* - *Rhodococcus* sp. on nutrient broth agar plate

3. *Aspergillus fumigatus* - *Candida albicans* on yeast malt extract broth agar plate

Inhibition zones were observed at the intersection of two streaks.

Co-culture

The above mentioned combinations of microorganisms were grown in a medium to find out the production of antibiotic compound. Totally, three set of cultures of each combination were maintained as follows:

A. Live cells of 1st and 2nd strains

In this, 10ml of 24 hours old broth cultures of both strains were added to the 100 ml of respective broths.

B. Live cells of 2nd strain alone (control)

In culture system B, 10ml of 24 hours old culture of 1st strain alone was inoculated.

C. Live cells of 1st strain alone (control)

In culture system C, 10ml of 24 hours old 2nd strain alone was inoculated.

All the cultures were incubated at 37°C for 5 days. After the incubation period, the cultures were centrifuged at 2500 rpm for 20 minutes. The supernatant was collected and subjected to antibacterial assay with multiple drug resistant test strains.

Screening for antibiotic activity

Antibiotic activity was assayed using a standard agar well diffusion method [2]. Nine test tubes were prepared each containing 1ml of LB. After autoclaving, the pathogenic strains were inoculated in it. Nutrient agar plates were flooded with test strains. Wells were created using a cork borer on plates and the supernatants of co-culture experiments were introduced into the wells. The plates were then incubated for 24 hours and the inhibition zones were observed.

Totally, three sets of plates were maintained for each combination. Each plate in a set was flooded with different test strains. All plates contained three wells which included two supernatants from control flasks and one supernatant from co-culture flask.

Agar Well Diffusion:

Following groups were made and each group was tested against the test organisms:

Group I: In yeast-malt extract broth

1. *Aspergillus fumigatus* (control)
2. *Candida albicans* (control)
3. *Aspergillus* + *Rhodococcus* (Co-culture supernatant)

Group II: In nutrient broth

1. *Aspergillus fumigatus* (control)
2. *Candida albicans* (control)
3. *Aspergillus* + *Rhodococcus* (Co-culture supernatant)

Group III: In nutrient broth

1. *Bacillus pumilus* (control)
2. *Rhodococcus sp.* (control)
3. *Bacillus* + *Rhodococcus* (Co-culture supernatant)

These three groups were tested on the following organisms:

1. MDR *E. coli*
2. Methicillin resistant *Staphylococcus aureus* (MRSA)
3. *Pseudomonas aeruginosa* (resistant to commonly used antibiotics)

III. RESULTS

Pre-tests for microbial inhibition- Cross streak method

The tests showed that *C. albicans* completely inhibits *A. fumigatus* (Fig. 1{a}). Cross streak analysis for *B. pumilus* – *Rhodococcus sp.* combination showed that both organisms can grow together (Fig. 1{b}) while in *A. fumigatus* – *Rhodococcus sp.* combination, *Rhodococcus sp.* strongly (but not completely) inhibits *A. fumigatus* (Fig. 1{c}). Hence, the latter two combinations were selected for co-culture studies.

Screening for antibiotic activity

Antibiotic activity was studied using agar well diffusion method. In all cases, supernatants from co-culture showed higher antibiotic activity than those from individual controls which proved that co culturing would help bring out higher antibiotic activity (Fig. 2). Supernatant from *A. fumigatus* – *Rhodococcus sp.* co-culture maximally inhibited MDR *E.coli* while supernatant from *B. pumilus* – *Rhodococcus sp.* co-culture maximally inhibited

MDR *E.coli* and methicillin resistant *Staphylococcus aureus* (Fig. 3).

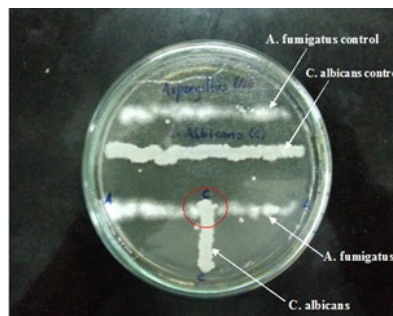
IV. CONCLUSION

Co-cultivation is one of the techniques used for activation of the silent genes for the production of new compounds [1].

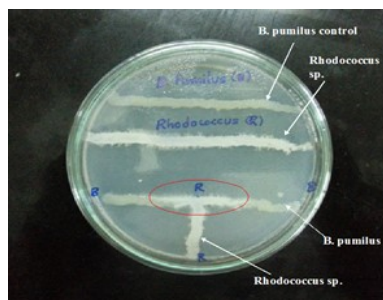
An effort was made to co-cultivate marine derived fungi and bacteria and isolation of crude bioactive compounds capable of acting on clinically resistant strains of infectious organisms.

Co-cultivation (also called mixed fermentation) of two or more different microorganisms tries to mimic the ecological situation where microorganisms always co-exist within complex microbial communities. The competition or antagonism experienced during co-cultivation is shown to lead to an enhanced production of constitutively present compounds and/or to an accumulation of cryptic compounds.

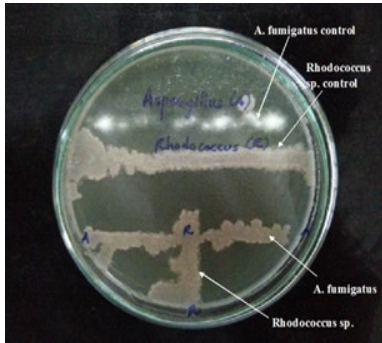
The present study provides a platform for further studies of interaction between marine bacteria and the exploration of their antibiotic property towards MDR bacteria.



(a) *A.fumigatus* - *C.albicans*

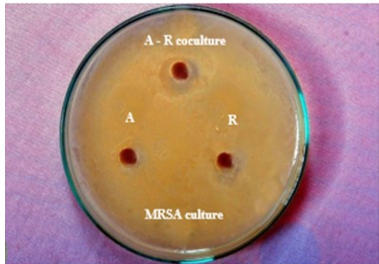


(b) *B.pumilus* – *Rhodococcus sp.*



(c) *A.fumigatus* – *Rhodococcus* sp.

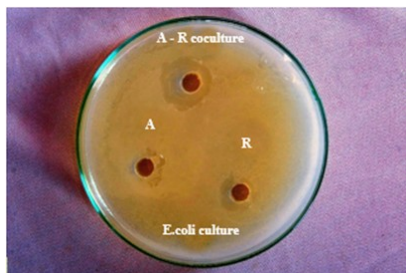
Fig. 1: Inhibition tests by cross streak method



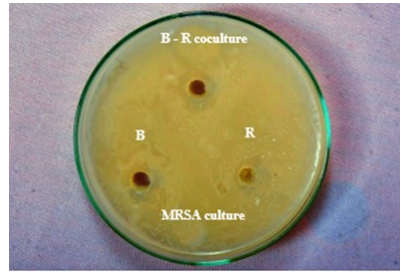
(a) A= 9 mm, R=8 mm, A-R co-culture= 14 mm



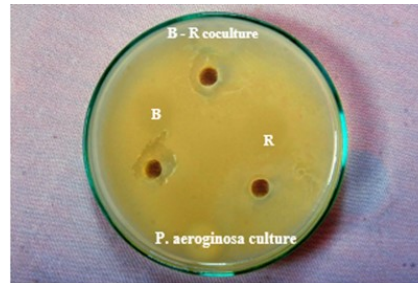
(b) A= 10 mm, R=9 mm, A-R co-culture= 14 mm



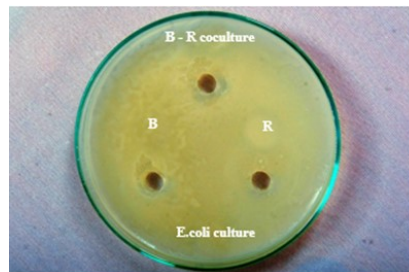
(c) A= 8 mm, R=13 mm, A-R co-culture= 20 mm



(d) B= 11 mm, R=8 mm, B-R co-culture= 15 mm

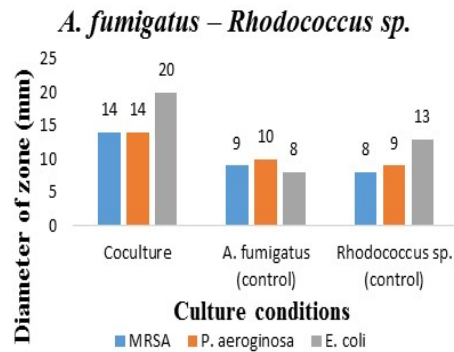


(e) B= 12 mm, R=8 mm, B-R co-culture= 14 mm



(f) B= 10 mm, R=0 mm, B-R co-culture= 15 mm

Fig. 2: Screening for antimicrobial activity using agar well diffusion method and the inhibition diameters (A- *A.fumigatus*, B- *B.pumilus*, R- *Rhodococcus* sp.)



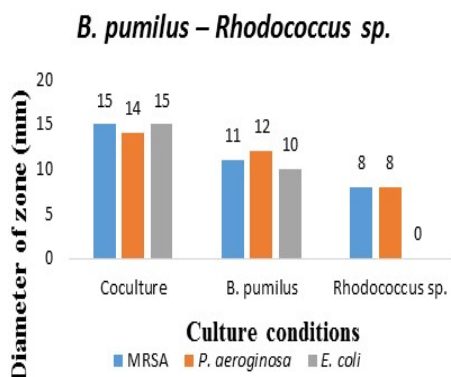


Fig. 3: Effect of culture conditions on production of antibiotic activity and tested against multiple drug resistant organisms.

REFERENCES:

- [1] Andreas Marmann, Amal H. Aly, Wenhan Lin, Bingui Wang and Peter Proksch, "Co-Cultivation—A Powerful Emerging Tool for Enhancing the Chemical Diversity of Microorganisms", *Mar. Drugs* 2014, 12, 1043-1065.
- [2] Cleidson Valgas, Simone Machado de Souza, Elza F A Smânia, Artur Smânia Jr, "Screening methods to determine antibacterial activity of natural products", *Brazilian Journal of Microbiology*, 2007, 38:369-380.
- [3] Delbarre-Ladrat C, Siquin C, Lebellenger L, Zykwinska A, Collic-Jouault S, "Exopolysaccharides produced by marine bacteria and their applications as glycosaminoglycan-like molecules", *Frontiers in Chemistry* 2014, 2.
- [4] Rateb ME, Hallyburton I, Housen W, Bull A, Goodfellow M, Santhanam R, "Induction of diverse secondary metabolites in *Aspergillus fumigatus* by microbial co-culture", *RSC Adv* 2013, 3: 14444-50.
- [5] Vasil ML, "NA Microarrays in Analysis of Quorum sensing: Strengths and Limitations", *J Bacteriol*, 2003, 185:2061–5



A HYBRID APPROACH FOR IPFC LOCATION AND PARAMETERS OPTIMIZATION FOR CONGESTION RELIEF IN COMPETITIVE ELECTRICITY MARKET ENVIRONMENT

¹Konduru VM ManoharVarma, ²J. Vara Prasad

^{1,2}Electrical and Electronics Engineering, Christ University Faculty of Engineering
Bengaluru, India

Email: ¹manohar.manu0219@gmail.com, ²Varaprasad.janamala@christuniversity.in

Abstract— The deregulated power system operation with competitive electricity market environment has been created many challenging tasks to the system operator. The competition with strategic bidding has been resulted for randomness in generation schedule, load withdrawal and power flows across the network. The economic efficiency of electricity market is mainly dependent on network support. In the event of congestion, it is required to alter the base case market settlement and hence the economic inefficiency in terms of congestion cost can occur. In order to anticipate congestion and its consequences in operation, this paper has been considered Interline Power Flow Controller (IPFC). A strategic approach is proposed for optimal location and then its parameters in Decoupled Power Injection Modelling (DPIM) are optimized using a new heuristic algorithm Gravitational Search Algorithm (GSA). The case studies are performed on IEEE 30-bus test system and the results obtained are validating the proposed approach for practical implementations.

Keywords— *Deregulated power system, competitive electricity market, congestion management, IPFC, Gravitational Search Algorithm (GSA)*

I. INTRODUCTION

The recent blackouts around the world have provided a movement for creating improvement in the operational security of interconnected power systems. Operational security management is highly challenging task and even more so in the presence of strategic market players, with both load fluctuations and abnormalities. Since network and market operations strongly coupled, any change in system operational security impacts the market economics and vice-versa. While the nature of the interactions between system security and market operations is well understood qualitatively, the quantification of operational security impacts on the overall market economics is, typically, not performed. In this paper, we proposed an approach to quantify the dependence of the performance of electricity market on the operational security taking into an account the interactions of the electricity markets and the presence of strategic bidding and load variations. We illustrate the application of strategic bidding to the IEEE-30 bus system for the study of its impacts of changing load periodically in a day-ahead energy market.

We also planned to mitigate congestion by the integration of Flexible AC Transmission Systems (FACTS) devices in the network. The approach to mitigating system congestion is

technically through system reconfiguration and re-dispatch. This has not much before or after the deregulation and is proved a security constrained economic dispatch. The major difference between before and after deregulation lies in the financial settlement. Congestion is a major concern in the present competitive electricity market because it hinders free competition in electricity trade. The present trend in congestion management is to use pricing tools in the form of nodal and zonal pricing. Despite these tools, the congestion is still in the place and it is increasing alarmingly. Congestion management includes both the congestion relief actions and the associated pricing mechanisms [1]. Congestion relief by re-dispatch will causes to increase generation cost and hence by means of reconfiguration, erection of new transmission lines or integration of FACTS device can adopt. But due to Right of Way (RoW) and cost concerns, instead of erection of new transmission lines FACTS devices can be the better option. Since congestion is uneconomical and undesirable in market operation as well as system security, the validation of FACTS devices should address technical as well as economical benefits. Among all the FACTS devices Interline Power Flow Controller (IPFC) is a versatile device to control power flow in many transmission lines simultaneously. Several references in technical literature can be found on application of IPFC for congestion management. In [2], the IPFC is applied for congestion relief, power flow control and to minimize the transmission losses. In [3], the congestion relief has been achieved by the application of IPFC and GUPFC in strategic bidding environment. The impact of these FACTS devices as shown economically via reduction in transmission congestion cost.

This paper is organized as follows: After introduction, section II describes the market settlement mechanism in competitive electricity market. In section III, the power injection modeling (PIM) of IPFC, strategy for its location are explained. In section IV, the heuristic optimization technique GSA application for optimization of IPFC parameters is explained. In section V, the case studies and discussions are illustrated with IEEE-30 bus system network. After section V, the comprehensive conclusions are given.

II. COMPETITIVE ELECTRICITY MARKET

The strategic bidding is a process of change in bid functions to maximize GENCOs' profit. In a perfect competitive market, the supply curve created by aggregating generator offers should closely approximate the system marginal production cost of generation [4]. Hence the bidding cost function treated as a continuous function and is given by a power producer i (or supply curve) is:

$$C_{bi}(P_{gi}) = a_{bi}P_{gi}^2 + b_{bi}P_{gi} + c_{bi} \quad (1)$$

where $(a_{bi}, b_{bi}$ and $c_{bi})$ are the bid coefficients and related with the actual cost function coefficients $(a_i, b_i$ and $c_i)$ as follows:

$$\xi_i = \frac{a_{bi}}{a_i} = \frac{b_{bi}}{b_i} \text{ and } c_{bi} = c_i \quad (2)$$

where ξ_i is the bidding parameter and represents mark-up above or below the marginal cost that a generator i decide to set its marginal bid in competitive market. Now, the marginal cost function will become as:

$$C_{bi}(P_{gi}) = \xi_i a_i P_{gi}^2 + \xi_i b_i P_{gi} + c_i \quad (3)$$

Then the equations for P_{gi} and λ_{MCP} will change as follows and the rest of procedure is as economic dispatch problem.

$$\lambda_{MCP} = \frac{P_D + \sum_{i \in NG} \frac{b_i}{2\xi_i a_i}}{\sum_{i \in NG} \frac{1}{2\xi_i a_i}} \quad (4)$$

$$P_{gi} = \frac{\lambda_{MCP} - \xi_i b_i}{2\xi_i a_i} \quad (5)$$

Now considered the effect of generator limits given by the inequality constraint:

$$0 \leq P_{gi} \leq P_{gi}^{\max} \quad \forall i \in NG \quad (6)$$

If a particular generator loading P_{gi} reaches the maximum limit P_{gi}^{\max} , its loading is held fixed at

this value and the balance load is shared between the remaining generators on an equal incremental cost basis.

III. INTERLINE POWER FLOW CONTROLLER

Objective of Interline Power Flow Controller (IPFC) is to provide a comprehensive power flow control scheme for a multi-line transmission system, in which two or more lines employ a Static Synchronous Series Compensator (SSSC) for series compensation as shown in Fig. 1. The IPFC scheme has the capability to transfer real power between the compensated lines in addition to executing the independent and controllable reactive power compensation of each line. The capability of IPFC makes it possible to equalize both real power and reactive power flow between the lines, to transfer demand from overloaded to under-loaded lines to compensate against resistive line voltage drops and the corresponding reactive line power and to increase the effectiveness of the compensating system for dynamic disturbance like transient stability and power oscillation [5].

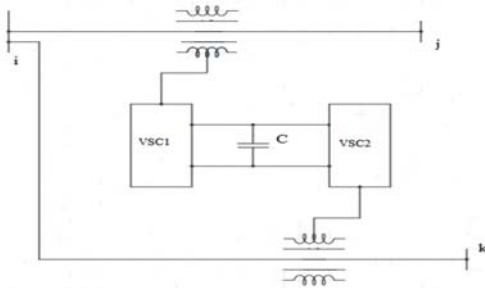


Fig.1 Schematic representation of IPFC

Fig.2 represents the equivalent circuit of the IPFC. This arrangement has two synchronous voltage sources with phasors V_{1pq} and V_{2pq} in series with transmission Lines 1 and 2, represent the two back to back dc to ac inverters. The common dc link is represented by a bidirectional link ($P_{12}=P_{1pq}=P_{2pq}$) for real power exchange between the two voltage sources. Transmission Line-1, represented by reactance X_1 , has a sending end bus with voltage phasor V_{1S} and a receiving end bus with voltage phasor V_{1R} . The sending end voltage phasor of Line- 2 represented by reactance X_2 is V_{2S} and the receiving end voltage phasor is V_{2R} .

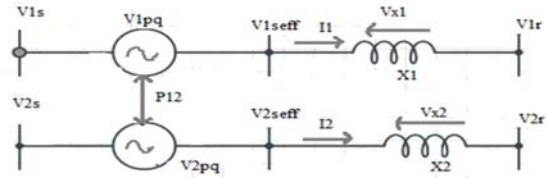


Fig.2 equivalent circuit of IPFC

A. Injection model of IPFC

Fig.3 shows the equivalent circuit of two converter IPFC. V_i , V_j and V_k are the complex bus voltages at the buses i , j and k respectively.

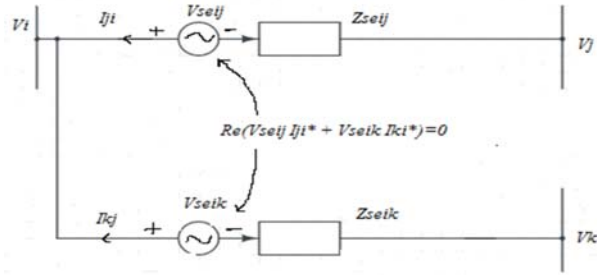


Fig.3 Equivalent circuit of two converter IPFC

The current source can be represented as follows

$$I_{se_n} = -jb_{se_n} V_{se_n} \quad (7)$$

Now, the current source can be modeled as injection powers at the buses i , j and k . the complex power injected at i^{th} bus is

$$S_{inj,i} = \sum_{n=j,k} V_i (-I_{se_n})^* \quad (8)$$

$$S_{inj,i} = \sum_{n=j,k} V_i (jb_{se_n} V_{se_n})^* \quad (9)$$

After simplification, the active power and reactive power injections at i^{th} bus are

$$P_{inj,i} = \text{Re}(S_{inj,i}) = \sum_{n=j,k} (V_i b_{se_n} V_{se_n} \sin(\theta_i - \theta_{se_n})) \quad (10)$$

$$Q_{inj,i} = \text{Im}(S_{inj,i}) = \sum_{n=j,k} (V_i b_{se_n} V_{se_n} \cos(\theta_i - \theta_{se_n})) \quad (11)$$

The complex power injected at n^{th} bus ($n=j,k$) is

$$S_{inj,n} = \sum_{n=j,k} V_n (-I_{se_n})^* \quad (12)$$

$$S_{inj,n} = \sum_{n=j,k} V_n (jb_{se_n} V_{se_n})^* \quad (13)$$

After simplification, the active power and reactive power injections at n^{th} bus are

$$P_{inj,n} = \text{Re}(S_{inj,n}) = \sum_{n=j,k} (V_n b_{se_n} V_{se_n} \sin(\theta_n - \theta_{se_n})) \quad (14)$$

$$Q_{inj,n} = \text{Im}(S_{inj,n}) = \sum_{n=j,k} (V_n b_{se_n} V_{se_n} \cos(\theta_n - \theta_{se_n})) \quad (15)$$

The placement of IPFC plays a vital role for congestion management. Placement of IPFC can be done with different optimization techniques, among all optimization techniques Particle Swarm Optimization gives precise and quick results. So, in this paper optimal location of IPFC is done by using PSO. After placement, parameters of IPFC are very important, optimal parameters can be chosen based on the location. In this paper for optimal parameters are done by using GSA.

IV. PROPOSED HYBRID APPROACH

The placement of IPFC plays a vital role for congestion management. Placement of IPFC can be done with different optimization techniques, among all optimization techniques Particle Swarm Optimization (PSO) gives precise and quick results. So, in this paper optimal location of IPFC is done by using PSO with an objective of voltage profile improvement. After placement, the IPFC parameters are optimized by using GSA technique.

A. PSO for voltage improvement

The aim of optimization is to determine the best suited to a problem under a given set of constraints. In computer science, particle swarm optimization (PSO) is a computational method that optimizes a problem by iteratively trying to improve a candidate solution with regard to a given measure of quality [13]. PSO optimizes a problem by having a population of candidate solutions, here dubbed particles, and moving these particles around in the search space according to simple mathematical formulae over the particle position and velocity.

Basic algorithm is proposed by Kennedy and Eberhart

x_i^k - Particle position

v_i^k - Particle velocity

p_i^k - Best remembered individual particle position

p_k^g - Best remembered swarm position

C_1, C_2 - cognitive and social parameters
 r_1, r_2 - random numbers between 0 and 1
 Position of individual particles updated as follows

$$x_i^{k+1} = x_i^k + v_i^{k+1} \quad (16)$$

With the velocity calculated as follows

$$v_i^{k+1} = v_i^k + c_1 r_1 (p_i^k - x_i^k) + c_2 r_2 (p_k^g - x_i^k) \quad (17)$$

Algorithm of particle swarm optimization

Step by step algorithms as follows:

1. Initialize
 - a. Set constants k_{max}, c_1, c_2 .
 - b. Randomly initialize particle positions $x_i^i \in D$ in IR^n for $i = 1, \dots, p$.
 - c. Randomly initialize particle velocities $0 \leq v_0^i \leq v_0^{max} \in D$ in IR^n for $i = 1, \dots, p$.
 - d. Set $k = 1$.
2. Optimize
 - a. Evaluate function value f_k^i using design space coordinates x_k^i .
 - b. If $f_k^i \leq f_{best}^i$ then $f_{best}^i = f_k^i, p_k^i = x_k^i$
 - c. If $f_k^i \leq f_{best}^g$ then $f_{best}^g = f_k^i, p_k^g = x_k^i$
 - d. If stopping condition is satisfied then go to 3.
 - e. Update particle velocities v_k^i for $i = 1, \dots, p$.
 - f. Update particle positions x_k^i for $i = 1, \dots, p$.
 - g. Increment k .
 - h. go to 2(a).
3. Terminate.

B. GSA for optimizing parameters of IPFC

In the proposed algorithm, agents are contemplated as objects and their performance is measured by their masses. All these agents attract each other by the gravity force, and this force occasions a global movement of all agents towards the agents with heavier masses. Hence, masses collaborate using a direct form of communication, through gravitational force. The ponderous masses, which correspond to best solutions, move more slowly than lighter ones, this assurance the exploitation step of the algorithm [11].

In GSA, each mass (agent) has four specifications: position, inertial mass, active

gravitational mass, and passive gravitational mass. The position of the mass correlate with panacea of the problem, and its gravitational and inertial masses are determined using a fitness function.

The GSA could be treated as a separate system of masses. It is like a small synthetic world of masses obeying the Newton laws of gravitation and motion.

Algorithm of gravitational search algorithms as follows

- Step1. Search space identification.
- Step2. Generate initial population between minimum and maximum values.
- Step3. Fitness evaluation of agents.
- Step4. Update $G(t)$, $best(t)$, $worst(t)$ and $M_i(t)$ for $i = 1, 2, \dots, m$.
- Step5. Calculation of the total force in different directions.
- Step6. Calculation of acceleration and velocity.
- Step7. Updating agent's position.
- Step8. Repeat step 3 to step 7 until the stop criteria is reached.
- Step9. Stop.

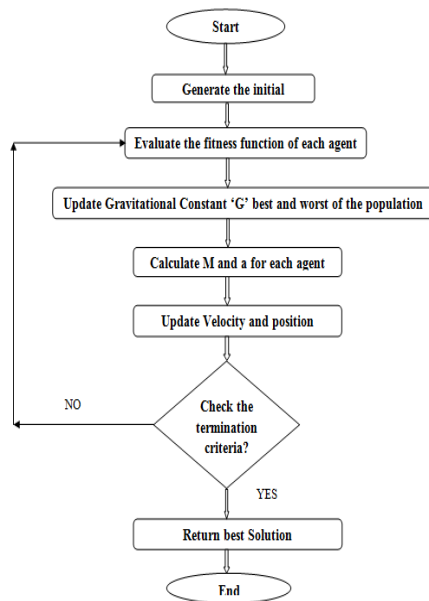


Fig.4 Gravitational search algorithm flow chart

V. CASE STUDIES

The proposed is approached is applied for IEEE-30 bus system. The cost coefficients are manipulated according to according to strategic

bidding parameter. The total system has been divided into two areas in which area1 has generator buses 1 and 2, area2 has generator buses 13, 22, 23 and 27. With normal bidding parameter and for base case load, the generation schedule has been determined as explained in section II. In area 1, The market is cleared at 3.5233 \$/MWh and the total cost is 243.2242 \$. Similarly, in area 2 the market is cleared at 3.9605 \$/MWh and the total cost is 396.4005 \$. In order to optimize economics in both areas simultaneously, the system is considered as one grid consisting of two areas. Under this consideration, the total load is 193.451 MW. For this load the market schedule is cleared at 3.8155 \$/MWh and total cost is 630.3476 \$. The market schedules for area1 and area2 when they are not interconnected are given in Table I and Table II respectively. When they are interconnected, the schedule is given in Table III. By observing market schedules in both cases, there is a economic benefit with MW interchange between two areas. Since area1 has producing more generation than its own load of 88.751 MW, area 2 importing power from area 1 about 17.5935 MW. If the network supports for this economic interchange, system operator can reduce a total operating cost of 9.277 \$. With this schedule the load flow is performed and we have observed the line 10 is overloaded. If a network subject to congestion, the IPFC has to control the power flow in such a way that all transmission lines are below their specified power ratings and so congestion impact on economic interchange can avoid. By placing IPFC in the lines connected between buses 10, 16 and 22. The congestion has been relieved and so market economic inefficiency situation is avoided. In addition to this the voltage profile has been improved and it can observe in Fig.5 and also the losses has been reduced from 9.7146 MW to 7.7402 MW.

TABLE I. AREA 1 GENERATION AND COST DETAILS

Load (MW)	PG1 (MW)	PG2 (MW)	MCP (\$/MWh)	Total Cost (\$)
88.751	33.3395	50.6672	3.5233	243.2242

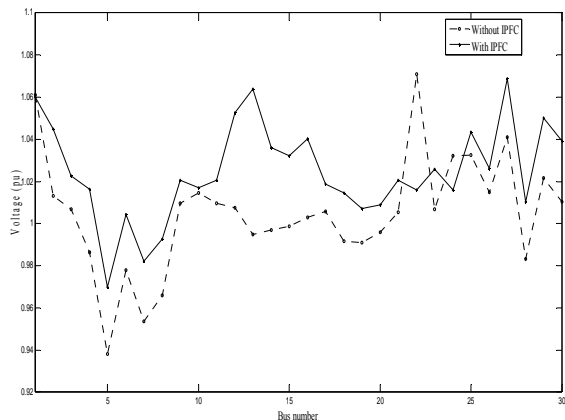
TABLE II. AREA 2 GENERATION AND COST DETAILS

Load (MW)	PG1 (MW)	PG2 (MW)	PG3 (MW)	PG4 (MW)	MCP (\$/MWh)	Total Cost (\$)
104.7	22.58	23.68	19.21	42.59	3.96	396.4

TABLE III. INTERCONNECTED SYSTEM DETAILS

Load MW	PG1 MW	PG2 MW	PG3 MW	PG4 MW	PG5 MW	PG6 MW	MCP \$/MWh	Total cost (\$)
193	48.58	59.01	16.31	22.52	16.31	33.9	3.81	630

Fig. 5 Changes in voltage profile at base case



The similar procedure is carried out for various loading level at various trading hours with different bidding parameters in different areas. The changes in load for 24 hours span in the form of a load curve are given in Fig.6.

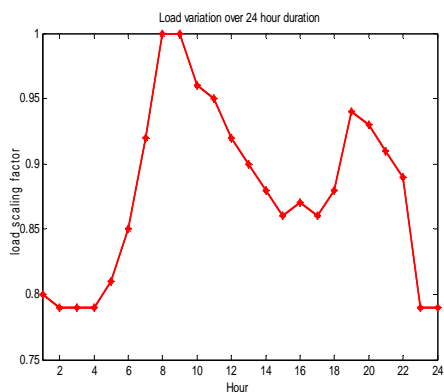


Fig.6 Load curve over 24 hours

The economic and power interchanges for different bidding parameters are shown in Fig.7 and Fig.8. Fig.7 shows when bidding parameters (Area1, Area2) = (0.5, 0.5) = (1, 1) = (2, 2). Fig.8 shows when bidding parameters (Area1, Area2) = (1, 0.5) = (2, 1).

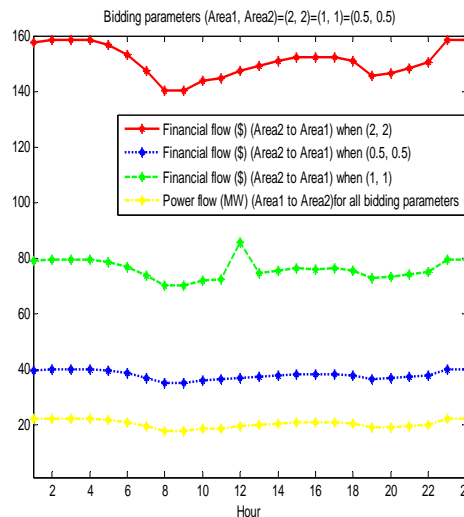


Fig.7 Financial and Power Interchanges

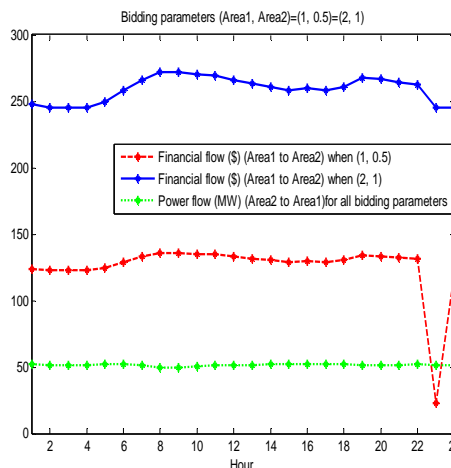


Fig.8 Financial and Power Interchanges

The congestion alleviation is occurred after connected the IPFC. These results are shown in Fig.9 and Fig.10

Fig.9 shows the congestion alleviation when bidding parameters (Area1, Area2) = (0.5, 0.5) = (1, 1) = (2, 2). During this strategic bidding congestion is occurred in 10th line, when the load at 8, 9 and 10th hours. This congestion is mitigated by installing IPFC

Fig.10 shows the congestion alleviation when bidding parameters (Area1, Area2) = (1, 0.5) = (2, 1). During this strategic bidding congestion is occurred in 30th line, except the load at 5th hour. This congestion is mitigated by installing IPFC.

In both Fig.9 and Fig.10 the difference of loading on the lines without and with IPFC are shown.

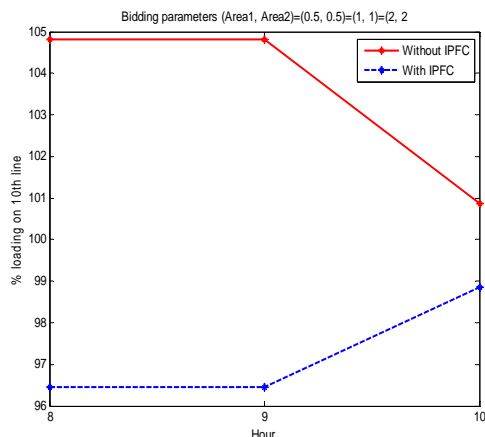


Fig.9 congestion relief in line 10 with IPFC

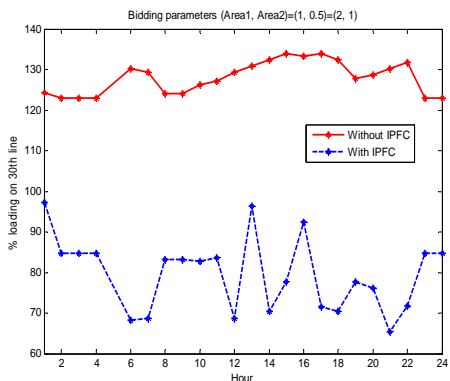


Fig.10 congestion relief in line 30 with IPFC

VI. CONCLUSIONS

This paper reviews the competition with strategic bidding in interconnected systems. In addition to this, the stress due to strategic bidding is increased; it leads to congestion in the system. This congestion is alleviated by installing IPFC in proposed IEEE 30-bus system. The case studies are performed on IEEE 30-bus test system and the results obtained are validated the proposed approach for practical implementation. This paper includes only generation side bidding,

it will be useful for further study on both generation side and distribution side biddings.

REFERENCES

- [1] Lommerdal, M. Soder, L., "simulation of congestion management Methods", IEEE Power Tech, Bologna, Volume 2, 23-26 June 2003.
- [2] Zhang, J., "Optimal Power Flow Control for Congestion Management by Interline Power Flow Controller (IPFC)," Power System Technology, 2006. PowerCon 2006. International Conference on , vol.,no., pp.1,6, 22-26 Oct. 2006.
- [3] Kumar, Ashwani, "Comparison of IPFC and GUPFC for congestion management in deregulated electricity markets," Industrial and Information Systems (ICIIS), 2014 9th International Conference on , vol., no., pp.1,7, 15-17 Dec. 2014.
- [4] J. Vara Prasad, K Chandra Sekhar, " Evaluation of available transfer capability in a competitive energy market", IEEE Trans.
- [5] Narain G. Hingorani, Laszlo Gyugyi, " Understanding FACTS: Concepts and Technology of Flexible AC Transmission Systems", IEEE press, New-York, 2000.
- [6] S.C.Srivastava, R.K.Verma, "Impact of FACTS devices on Transmission pricing in a de-regulated electricitymarket", IEEE Trans. 2000,pp. 642-648.
- [7] Gyugyi, L.Sen, K.K. and Schauder, C.D, " The interline power flow controller concept a new approach to power flow management in transmission systems", IEEE Trans. Power Del..14(3), pp. 1115-1123.
- [8] A. Karami, M. Rashidinejad and A.A. Gharaveisi, "Voltage security enhancement and congestion management via STATCOM & IPFC using artificial intelligence", Iranian Journal of Science & technology, Trans.B,Engineering, Vol.31, No.B3, PP 289-301.

- [9] Kennedy Mwanza, You Shi, “Congestion Management: Re-dispatch And application of FACTS”, Chalimers university of technology, Goteborg, Sweden, 2006.
- [10] Charles A. Gibson, Harold Zuniga, “ Interchange evaluation for electric power utilities”, IEEE Transc., session. 11D3, pp. 820-825. 1989.
- [11] I.Sai ram, J. Amarnath, “Optimal setting of IPFC for voltage stability improvement using (GA-GSA) hybrid algorithm”, IEEE Conference, 2013.
- [12] William W. Hogan, “Independent system operator (ISO) for a competitive electricity market”, Harvard University, June 1998.
- [13] James Kennedy, Russell Eberhart, “ Particle Swarm Optimization”, IEEE Transc., pp. 1942-1948, 1995.
- [14] A.R. Abhyankar, prof.S.A.Khaparde, “Introduction to deregulation in power industry”, IIT Bombay.